On the Design of Actuator and Control Systems in Early Development Stages

Amir Zare

Universität Bremen 2019

On the Design of Actuator and Control Systems in Early Development Stages

Vom Fachbereich für Physik und Elektrotechnik
der Universität Bremen

zur Erlangung des akademischen Grades

Doktor–Ingenieur (Dr.-Ing.)

genehmigte Dissertation

von

M.Sc. Amir ZAre

wohnhaft in München

Referent: Prof. Dr.-Ing. K. Michels
Korreferent: Prof. Dr. M. Zimmermann

Eingereicht am: 15.02.2019
Tag des Promotionskolloquiums: 29.03.2019

Preface

This thesis is based on the results obtained during my time as PhD student in the years from 2014 until 2017 at BMW Group and submitted for the degree of Doctor of Engineering (Dr. -Ing) at the University of Bremen. The research described herein was conducted under the supervision of Prof. Dr.-Ing. Kai Michels in the department of Information and Automation Engineering (IAT), University of Bremen.

This work is done by myself originally, except where acknowledgment and references are made to previous work. I confirm that neither this nor similar dissertation has been or is being submitted for any other qualification at any other university.

Part of this work has been presented in the following publications.

- A.Zare, K. Michels, M. Zimmermann, L. Rath-Maia, *On the Design of Actuator and Control Systems in Early Stages of Development*, In: chassis.tech plus 2017, Juni 20-21 2017, Munich, Germany.
- A. Zare, D. Odenthal, M. Zimmermann, M. Wahle, *Generische Vorsteuerung fuer Gesamtfahrzeug*, Invention Disclosure, registered, Nr. 3456, Application Date: 04.05.2017.

Acknowledgment

I would like to express my gratefulness to my thesis supervisor Prof. Dr.-Ing. Kai Michels for his continuous guidance and advice. His Support, patience, and precious inputs in our discussions are of utmost value to me. I am also very thankful to my supervisor Prof. Dr. Markus Zimmermann for initiating this research project in the first place, his guidance throughout the project and the encouragement and support he has given me. The time at BMW AG was really intriguing and rich in experiences. I would especially like to thank Dr. Martin Wahle for his generous support and counseling at the beginning of the project and his continuous valuable discussions about most of the topics in this research. I would like to extend my thanks and appreciation to Dr. Vena Gianpiero for willing to help me in mechanical topics.

I owe much to my colleagues and friends for their kind encouragement. A special acknowledgment goes to my friends Ali Shariati, Brahim Soltani, Ali Tuchi, Pegah Pezeshkan, and Nadia Parvizi who have been always there for me. I would also like to sincerely thank all my students, specially Lucas Rath-Maia, Sebastian Schoder, Yuran Liang and Julian Ruggaber. Their excellent contributions have significantly enhanced the quality of my research and its results.

Last but not least, I would like to say I am indebted to my parents Hassan Zare and Fariba Shadaei who have supported and guided me preciously and carefully throughout my education years. They all kept me going and have always been a source of inspiration to me.

Abstract

Vehicle development faces new challenges due to the increasing requirements on vehicle performance, e.g., on ride, comfort and safety. Adding mechatronic systems to the chassis helps to reach more ambitious design goals, however, it also adds to the complexity of the design process. The number of design variables increases significantly: in addition to the mechanical chassis, actuators of mechatronic systems and control logic parameters affect the overall vehicle performance. The complex interaction between many design variables poses a particular challenge. Engineers need to make important design decisions in early development stages, typically about the mechanical chassis, without knowing the final design, in particular the detail parameters of mechatronic systems.

The present dissertation illustrates the design variables of logics as well as actuators of lateral vehicle dynamics mechatronic systems by proposing appropriate principles of logic functions and functional models of actuators. The effects of logics as well as actuators on objective driving dynamics targets with respect to different driving maneuver will be pointed out. Besides, a so-called dependency graph of mechatronic-mechanical systems will be established, which helps engineers to control the complexity in the design procedure of mechatronic systems.

Moreover, the dissertation applies the theory of solution spaces for finding a robust solution space for the parametrization of control system logic parameters and a layout of actuators. In this way, solution intervals of mechatronic systems' design variables will be determined by setting quantitative requirements on the objective driving dynamics targets. For this purpose, mathematical surrogate models will be introduced which reduce the optimization time and describe correlations between design variables and driving dynamics targets. These surrogate models will be derived by machine learning methods such as artificial neural networks and support vector machines. In the end, the solution intervals of design variables will be converted into the solution verification variables for verifying end-products such as actuators.

A mechatronic rear steering system is considered as an application example. Requirements on the dynamics and overall performance of the actuator and the associated control logic parameters are derived by formulating requirements on the considered objective driving dynamics targets. The derived requirements

are ranges of permissible subsystem properties such as overshooting, steady state error, maximum rear angle of a rear steering actuator or damping factor of dynamic feedforward control, proportional term of feedback controller, etc.

Contents

Table of Symbols

Symbol	Description
$V_{X_i}(\cdot), E_{X_i}(\cdot)$	Variance or mean of argument (.) taken over X_i
$Sgn(.)$	Sign of argument (.)
$Vol(.)$	Volume of argument (.)
$n(.)$	Number of argument (.)
$max(.)$	Maximum of argument (.)
$Discrepancy(.)$	Discrepancy of argument (.)
ψ	Yaw angle
$\dot{\psi}$	Yaw angle velocity
$\ddot{\psi}$	Yaw acceleration
$\dot{\psi}_{ref}$	Reference yaw angle velocity
$\dot{\psi}_{act}$	Actual yaw angle velocity
$\dot{\psi}_{STM}$	Yaw angle velocity calculated from the single-track model
$\dot{\psi}_{ay}$	Lateral acceleration yaw angle velocity
ϕ	Roll angle
θ	Pitch angle
δ_H	Steering wheel angle
δ_f	Front wheel steering angle
δ_r	Rear wheel steering angle
$\delta_{r,stat}$	Output of the ARS static feedforward control
δ_{eff}	Effective wheel steering angle
c_f	Front total sideslip stiffness
$c_{f,mod}$	Modified front total sideslip stiffness
c_r	Rear total sideslip stiffness
$c_{r,mod}$	Modified rear total sideslip stiffness
β	Slip angle
$\dot{\beta}$	Slip angle velocity
m	Mass
v	Velocity
F_x	Force in direction of the x-axis (Vehicle longitudinal axis)
$F_{x,f}$	Longitudinal force acting on the tire of the front axle

Symbol	Description
$F_{x,r}$	Longitudinal force acting on the tire of the rear axle
F_y	Force in direction of the y-axis (Vehicle lateral axis)
$F_{y,f}$	Lateral force acting on the tire of the front axle
$F_{y,r}$	Lateral force acting on the tire of the rear axle
$F_{x,d}$	External force in direction of the x-axis (Vehicle longitudinal axis)
$F_{y,d}$	External force in direction of the y-axis (Vehicle lateral axis)
F_z	Force in direction of the z-axis (Vehicle vertical axis)
F_{total}	Total force
J_z	Vehicle inertia in direction of the z-axis (Vehicle vertical axis)
g	Gravitation constant
R	Path radius
α_f	Side slip angle on the front axle
α_r	Side slip angle on the rear axle
l	Wheel base
EG	Self-steering gradient
δ_A	Ackermann angle
r_{dyn}	Dynamic wheel radius
b_r	Track width of a vehicle
r_w	Wheel radius
A_{pistol}	Disk area
μ_{temp}	Friction coefficient caused by the disc temperature
a_y	Longitudinal acceleration
a_x	Lateral acceleration
h	Center of gravity hight
l_f	Distance of the center of gravity from the front axle
l_r	Distance of the center of gravity from the rear axle
δ_{fr}	Front steering angle of the right wheel
δ_{fl}	Front steering angle of the left wheel
$M_{br,stat}$	Output of the BR static feedforward control
$i_{M_{z,ff}}$	Translation factor of the static yaw moment
ω_{des}	Desired vehicle natural frequency
D_{des}	Desired vehicle damping ratio
T_{des}	Desired vehicle time constant

Symbol	Description
$a_{y,act,measured}$	Measured actual lateral acceleration
$\dot{\beta}_{STM}$	Side slip angle computed from the single-track model
$\dot{\beta}_{act}$	Actual side slip angle velocity of a vehicle
ϕ	Roll angle
K_p	Static gain
T_w	Time constant
$\dot{\delta}_{out}$	Output signal velocity
ϕ	Roll angle
T_w	Time constant
$\dot{\delta}_{out}$	Output signal velocity
$\dot{\delta}_{in}$	Output signal velocity
$\dot{\delta}_{cu}$	Upper bound of the model output velocity
$\dot{\delta}_{lu}$	Lower bound of the model output velocity
Ω_{ds}	Design space
C	Box constraint
ϵ	Slack variable
x_{act}	Design variable of an actuator
x_{log}	Design variable of a control system logic
I_{act}	Internal for a variable of an actuator
I_{log}	Interval for a variable of a control system logic
T_{ris}	Rising time
T_{st}	Stabilization time
SE	Static error
$M_{z,d}$	External disturbance moment in direction of the z-axis
$M_{z,FB}$	Yaw moment generated by feedback controller
LFD	Longitudinal force distribution
v_{ch}	Characteristic velocity
v_{crit}	Critical velocity
ω_0	Vehicle natural frequency
D	Vehicle damping ratio
T_z	Vehicle time constant
M_z	Yaw Moment
$M_{z,ff}$	Yaw Moment generated by feedforward control
$M_{z,stat}$	Yaw Moment generated by static feedforward control
$M_{z,dyn}$	Yaw Moment generated by dynamic feedforward control

Symbol	Description
$M_{z,dff}$	Yaw Moment generated by disturbance feedforward control
F_{br}	Brake force
r_w	Wheel radius
a_y	Lateral acceleration
$a_{y,max}$	Maximum lateral acceleration
SAF	Steering wheel angle factor
$freq$	Frequency
T_{eq}	Equivalent time delay
i_{ARS}	Translation ratio of active rear steering system
v_{trans}	Transient velocity
M_{br}	Brake moment
$a_{y,ack}$	Ackermann lateral acceleration
ω_f	Natural frequency factor
D_f	Damping ratio factor
T_f	Time constant factor
K_{os}	Indicator of oversteering
K_{cs}	Indicator of counter steering
g_{K_p}	Weighting factor of the feedback controller propotional term
F_c	Counter force
T_d	Time delay

List of Figures

List of Tables

Abbreviations

Abbreviation	Description
ESP	Electronic Stability Program
DSC	Dynamic Stability Control
CV	Characteristic Value
ECU	Electronic Control Unit
STM	Single-Track Model
ARS	Active Rear Steering Control System
DSI	Driving State Identification
ICM	Integrated Chassis Management
LTI	Linear Time Invariant System
LPV	Linear Parameter Varying System
FPEM	Frequency Domain Predicton Error Estimate
CAN	Controller Area Network
RSM	Response Service Machine
SVM	Support Vector Machine
NN	Neural Network
ms	Millisecond
FFT	Fast Fourier Transform
DSI	Driving Situation Identifier
YVA	Yaw Velocity Amplification
RWD	Rear Wheel Drive
FWD	Front Wheel Drive
AWD	All Wheel Drive
CG	Center of Gravity
LFD	Longitudinal Force Distribution
EG	Self-Steering Gradient
BS	Brake System
QSSC	Quasi Steady State Cornering
SWD	Sine With Dwell
BRWC	Brake While cornering
ABS	Anti lock Braking System
AI	Assessment Index

1 Introduction

1.1 Content and motivation

Vehicle dynamics are of great importance in vehicle development. The dynamic driving behavior of a vehicle is important for the safety of the vehicle passengers and the environment. In addition, it is an important purchase aspect for potential customers who value the driving experience. One of the aims of the vehicle dynamics development is to design vehicles optimally according to safety and customer requirements. BMW, as a premium manufacturer, is particularly well-known for its sporty vehicles. Therefore, a great deal of importance is attached to the dynamic design of the vehicle.

The design procedure of the vehicle dynamics is done in two phases: Early phase and late phase. In each phase, different parts of the chassis is designed and tested, figure 1.1.

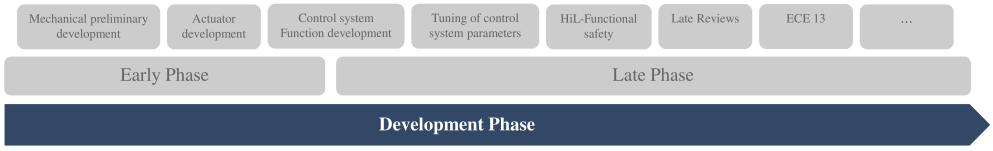

Figure 1.1: Development phases of the vehicle dynamics development

In order to achieve the optimal design of the chassis, mechanical variables influencing the driving dynamics are determined in the early phase of vehicle dynamics development. The potential of conventional mechanical components affecting the driving behavior in a constructive way is reaching its limits and is often associated with compromises when we are coping with many diverse customers requirements. However, modern chassis composed of a wide range of mechatronic systems offer the possibility of having more sheer pleasure and safety by influencing the driving behavior actively without meeting any concession. With the aid of chassis mechatronic systems, the vehicle can be adapted to meet individual safety and customer requirements. Yet, there are interactions between the different mechatronic systems, so that, for example, two separate control systems can change the driving behavior simultaneously with only one

controlled input. In this case, the accuracy of the regulations will be impaired. In the worst case, the driving behavior becomes worse than an unregulated or even unstable vehicle. Therefore, it is useful to determine, first, the control system and actuators parameters and the interaction between them and second, their impacts on the driving dynamics performance measures. As a result, the first goal of this work is to develop the principle model of such control systems and their associated actuators in the simulation environment and to explain the mathematical relations between them.

In the past, vehicle design was iterative. The departments submitted the system requirements one after the other until the designed components finally met the requirements, figure 1.2. Such an approach may lead to conflicts of goals regarding overall performances of a vehicle, since each department attempts to reach its specific component requirements instead of reaching the overall vehicle performance. Additionally, it cannot guarantee the reproducibility of the development for the next vehicle generations. Another disadvantage of iterative design is that it is highly time-consuming. Because, if all designed components, after assembling in a vehicle, do not achieve the overall vehicle performance, all design departments should start over the designing procedure.

Moreover, the designed components such as actuators and control systems must be able to cope with different variants of a vehicle with different weights and properties, which are not completely determined in early stages of the vehicle development. In other words, we are dealing with different kinds of uncertainties due to undefined properties, which cause the complexity in the design procedure. We also know that the actuators and their associated control systems have strong interactions. So, it would be more practical to design actuators and control systems together instead of designing each one separately.

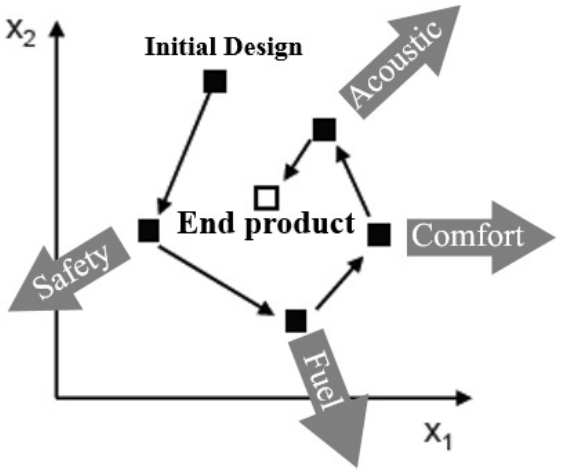

Figure 1.2: Multi-Objective Design with iterations

As a consequence, the second goal of the dissertation is to develop a method which confronts the complexity and ensures the robustness, transparency and reproducibility of the development of control systems and actuators. Besides, it is important to have a method which is able to consider all vehicle requirements formulated by different design departments at the same time, figure 1.3, in order to find the best design possibilities for each component. In this way, the time of the development is reduced drastically.

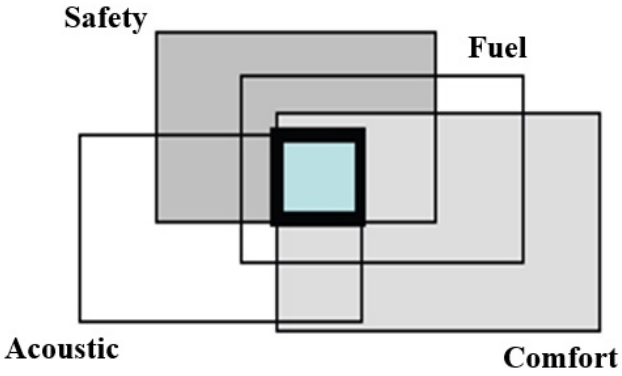

Figure 1.3: Multi-Objective Design based on solution spaces

The contribution of this dissertation can be summarized as follows:

- **New static feedforward control approaches for a rear steering and braking system:** Static feedforward controls are essential in the control engineering in order to accelerate the control loop and do not influence the stability of the system under investigation. Moreover, they regulate the vehicle in stationary rides before the feedback controller. As a consequence, we develop different characteristic curves as static feedforward control for different actuators assembled in a vehicle. The goal is to change the stationary response of the vehicle to the stationary steering.

- **A new centralized dynamic feedforward control approach for lateral vehicle dynamics control:** An open loop solution can fully take advantage of the potential of modern devices. A dynamic feedforward control can modify the dynamic behavior of the controlled input of a plant. As a result, we propose a new approach for a dynamic feedforward control in order to enhance the dynamic behavior of a vehicle in case of dynamic steering. The goal is to modify the transient response of the yaw velocity of a vehicle before the feedback controller acts over that.

- **A new simplified feedback control approach for lateral vehicle dynamics control:** As we know, the first and foremost task of a controller is to stabilize a system. So, we introduce a new approach for modeling such a controller based on the available ideas in the state of the art. Beside this goal, stabilizing the vehicle in critical situation, the developed controller should enhance the response of the vehicle in normal driving situations. Subsequently, the proposed approach considers also all other requirements in addition to stabilization.

- **A new approach for functional modeling of actuators, in particular a rear steering system, for the design procedure in the early stage of the development:** A new approach is presented how a functional model of an actuator can be built. This will be done based on the measurement data gathered from the test-rig. Such a functional model is adequate to cover the most important properties of an actuator and is of high interest in the early stage of the vehicle dynamics development for the design procedure. The model is identified with a few number of parameters and can be integrated in the simulation environment of the full vehicle model.

- **A new approach for data fusion for deriving mathematical surrogate models:** Using mathematical surrogate models instead of the fully physical vehicle and the control system models accelerates the opti-

mization time. A new approach for applying neural networks and support vector machine will be proposed for the data fusion.

- **A new approach for defining actuator test rig tests and verification variables:** Designing an actuator can be done by formulating requirements on its functional model parameters. However, these requirements cannot be transmitted in this form to suppliers for the construction. They must be converted into the requirements set down on the verification variables of test-rigs. The actuator constructed by suppliers has to fulfill these requirements. As a result, the verification tests and the associated variables are proposed in this dissertation. The way the requirements on the functional model are converted into the requirements on the verification variables is also clarified.

- **Application of system engineering theory to a robust actuator design and robust parametrization of a control system:** Finding a robust solution space for parameterizing the developed control system and constructing actuators, which copes with the variation of vehicle properties in the development of a vehicle, is getting of high interest in the last few years. We consider the theory of design of large scale systems subject to uncertainty, which has been being developed in the last three years in the system engineering, in order to find a robust solution space for the developed control system and functional actuator model parameters.

1.2 State of the art

For achieving the above-mentioned contributions, we first develop control system logic and functional actuator models for the vehicle lateral dynamics and second a method to parametrize the control system logic parameters and design an actuator robustly. Therefore, a brief review of the basics of the control theory will be given in this section. Afterwards, state of the art will be explained for lateral vehicle dynamics control systems, actuator modeling, a robust actuator design, and control systems.

Normally, a closed-loop control system consists of different subsystems. A feedforward control, a feedback controller, an actuator and a plant are examples of such subsystems, figure 1.4. Basically, a feedforward control can be divided into three groups, namely static, dynamic and disturbance feedforward control. Typically, a static feedforward control is a factor which accelerates the control loop and can be adjusted independently without consideration of the stability of a closed-loop system, as it is not included in the denominator of the closed-loop

transfer function of a plant and a feedback controller [47]. It can also reduce the static deviation of the error between the reference input and the close-loop system output, in case of using just proportional feedback controller [67]. Moreover, a dynamic feedforward control can modify the transient behavior of the controlled input, sent to the plant and partially relieve the feedback controller from regulating the transient phase of the error between the system output and the reference input. Mostly, the dynamic feedforward control is designed based on the desired dynamic behavior of an output of a closed-loop system.

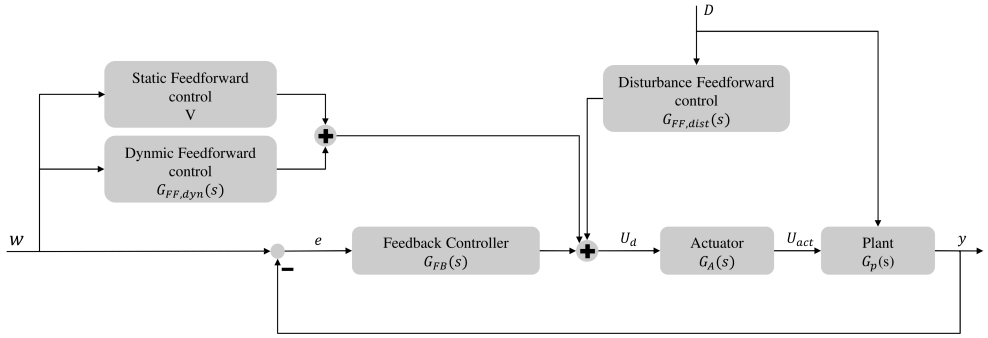

Figure 1.4: Block diagram of a closed-loop control system

If the disturbance (D) penetrating in the plant is measurable, a disturbance feedforward control can be designed based on the dynamic of the disturbance in order to compensate for its effect on the plant. The result of such regulation is that the feedback controller should not compensate for the effect caused by the disturbance which appears on the error and the control procedure will therefore be accelerated. If there is still an error between reference input and the closed-loop system output despite the regulation of all feedforward controls, it must then be regulated by a feedback controller. The calculated controlled input (U_d) has been then set into the plant through an actuator.

After this brief review of the basics of the control theory, we turn back to state of the art about the development of the lateral vehicle dynamics control systems. There are actually three different kinds of approaches for developing such control systems:

- Developing a specific control approach for each actuator available in chassis. Such approach is called decentralized control system.
- Developing decentralized control systems for various actuators and a coordinating system which coordinates the different control systems by pri-

oritizing the requirements of each control system. In this way, a better driving performance will be achieved. Such an approach is defined as *integrated vehicle dynamics control system* in the vehicle dynamics literatures.

- Developing a centralized control system which generates a global controlled input regarding to the driver input and independent from actuators.

[76] explains the difference between centralized and decentralized vehicle dynamics control systems. A centralized vehicle dynamics control system generates a generic controlled input (e.g. generic yaw moment) independent from implemented actuators in a vehicle. Subsequently, this controlled input will be distributed in different actuators (e.g. differential lock, brake, steering systems). A decentralized control system, however, includes control systems for each actuator. In the architecture of this kind of controller, a coordinator may be incorporated to manage the output of all functions to reach the optimal vehicle dynamics performance.

As pointed out, the decentralized control system can be with or without a coordinating system. In the last few decades, much research has been done about developing a decentralized control system for each actuator without implying any coordinating system. These control systems have been proposed just for one actuator. For instance, [51] proposes a new technique for developing a control system only for a rear steering actuator. There, an adaptive controller regarding the driving situation is introduced which is based on the phase plane method. [16] introduces an approach for designing a stationary value for the rear steering angle based on the optimization of the closed loop system, i.e. the single-track model (STM) of the vehicle with front and rear steering angles. The optimization is carried out with respect to an objective criterion formulated on the amplitude of the frequency response of the vehicle lateral acceleration. [34] introduces a new control concept for the torque vectoring based on quadratic gaussion theory to improve the lateral dynamics of the vehicle. This control approach considers the fact, that the only actuator implemented in the vehicle is a torque vectoring actuator. But, often there are more than one actuator implemented in a vehicle. If each actuator follows the command of its associated controller without consideration of what all other controllers are performing, the overall controlled performance of a vehicle can be impaired or sometimes unstable. Consequently, there has been much research in the last decade in finding a coordinating system for decentralized control systems of vehicle dynamics. [9] introduces the idea how to coordinate different control approaches

by introducing the urgency characteristic curve for coordinating between rear steering and brake system. A coordinating strategy between available control systems of various actuators in a vehicle is developed in [58] to achieve a better vehicle performance by avoiding the conflict scenarios between different control systems. A platform for functions, actuators, and electrical devices which connect these functions and actuators is presented in [70]. Moreover, it specifies how to integrate different control approaches of different actuators in only one platform.

The focus of this dissertation lies, however, on the development of centralized control approaches which consider the driver inputs and generate a global controlled input independent from actuators. As a result, state of the art of such control system approaches is explained. [8] uses two different control approaches for controlling brake and steering system to improve the lateral vehicle dynamics. The steering system controls the deviation between the reference and actual yaw velocity. Additionally, the braking system controls the velocity of the side slip angle to keep the stability of the vehicle under control. Both approaches generate a yaw moment as controlled input. This work also introduces an SI index to coordinate the generated yaw moments of these two different control strategies. [29] proposes an approach how to enhance the steerability of a vehicle by controlling the deviation between the reference yaw velocity and the output yaw velocity. It also clarifies how to enhance the stability of the vehicle by controlling the error between the reference and actual sideslip angle. The controlled input is a global yaw moment independent from implemented actuators. This work uses different rule bases for distributing the generated yaw moment between front and/or rear steering and braking system. The disadvantage is that the amount of the yaw moment for distributing should be predefined which increases the complexity of the design and parametrization of the controller parameters. Accordingly, if the amount of the yaw moment is small, then the front steering systems will be activated. If it is medium, then rear steering will be activated and if it is large, then braking system must be the only actuator to implement the requirement of the controller. [49] achieves a controlling approach which calculates a whole torque and force for a predefined trajectory. These yaw torque and longitudinal and lateral forces are independent from implemented actuators. Subsequently, an optimization method is developed in this work which distributes the yaw torque and forces optimally between actuators. Such an idea has been also investigated by [53] and [23].

In this dissertation, a new approach is proposed for functional modeling of an actuator. Thus, it is necessary to do a review of the available works in the field of actuator modeling. There are actually different kinds of methods for modeling of an actuator. Two of them are, for example, physical or empirical

modeling. [55] shows how a semi active damper can be modeled physically and functionally. Functionally, the actuator is modeled by dividing the system dynamics into electrical dynamics and mechanical ones. The electrical part is represented by a transfer function whose parameters are fitted, such that the best possible model output, as close as possible to the measurement output, is achieved. The proposed simplified model is derived, at the end, by just stimulating the actuator with different frequencies and getting the bode diagram and fitting a transfer function whose bode diagram fits to the one obtained from the measurement. [65] explains how to compute an idealized model of an actuator by defining a second-order transfer function whose damping ratio depends on the maximal bearable moment or force of the actuator under investigation. It, however, does not consider the nonlinearity existing in the actuator. [26] describes how to model a variable differential lock for the design procedure. It is just focused on the performance of the actuator in the time domain by stimulating the actuator with a step signal. Based on the step response of the actuator, the actuator is modeled by a first-order transfer function.

After developing control system logic as well as actuator models, a method is demanded for developing new actuators as well as parametrization of control system logics robustly, if we cope with the development of new vehicles. So far, many approaches have been established for designing new mechanical components in the vehicle dynamics development. Most of the researches focus on the development of virtual prototypes and virtual methods which firstly control the complexity of the development and secondly, decrease the time of development. [60] develops a tool for the vehicle dynamics development in order to control the complexity by keeping the tool user friendly, consistent, modular, scalable, and real-time executive. [63] also develops a simulation tool, in which an engineer can change the properties of mechanical components of a chassis and compare their effects on the driving dynamics very quickly. In this way, it can keep the complexity under control and reduce the time of the development process, since building up a virtual prototype is less time consuming than a real prototype. [43] develops a method for the virtual development of chassis components which influence the vehicle lateral dynamics. The method deals with the fact, how the properties of each chassis component affect the lateral vehicle dynamics. It is done by sensitivity analysis. However, the interaction of components is not considered. In addition, the surrogate models are developed in this work for different components, which define the main component properties. These surrogate models are then designed with respect to driving dynamics performance measures. The deficiency of of all these methods is that they can neither consider complex interactions of components under developing nor develop components regarding all driving dynamics performances, i.e.

ride, comfort and safety, at the same time. As a consequence, [78] proposes a new strategy based on the system engineering to keep the complexity under control regarding the products' properties qualitatively and quantitatively in the development process. In addition, it presents a new numerical method, the so-called solution spaces, for developing products quantitatively besides many design parameters and design goals. According to this method, a component with many design variables can be developed quantitatively with respect to all design goals. This method has been applied in many product developments of mechanical components in the last five years. For instance, [59] applies this theory for the virtual development of functional properties of axles. Moreover, the author compares the development of axles by this theory with the other available classic development methods and determines that a development based on this theory delivers a better accuracy and robustness with respect to the considered driving targets. Besides, this theory is applied in [75] to formulate requirements on design variables of functional models of tires and axles regarding all considered driving dynamics performance measures. It is also used by [22] to develop requirements on the design variables of the functional model of dampers. As we have seen, all the above-mentioned researches are done for the development of only mechanical component.

There are a few researches in the field of the parametrization of control systems or actuator designs. For example, [13] applies the parameter space method with respect to eta, beta and theta stability criteria in order to find solution spaces for control system parameters. The deficiency of this method refers to the number of parameters which can be considered in this method. Not more than a defined number of parameters can be considered by this method. Besides, the only considered requirement for the parametrization procedure is the stability criterion of the system. It also needs the linear transfer function of the open or closed loop system. It means a non-linear system must be linearized for this method. This method is also applied by [14] to find the solution space for the parametrization of the front steering system control parameters with respect to the unstructured uncertainties in the dynamic model of the vehicle such as mass, inertia and etc. [64] proposes a method based on the know-how management system. The author presents a quantitative method for parametrization of control systems based on driving dynamics performance measures. In this case, he considers different driving dynamics performance measures and sets quantitative requirements on them. Afterwards, he varies the parameters of the control systems a few times and looks which set of parameter configuration satisfies all driving dynamics performance measures. However, the problem of this method is, that it finds an optimum configuration and not a robust solution space and cannot take many different combinations of parameters into

account. The application of the method has just been done for stationary and dynamical feedforward control parameters and has not considered the effect of the feedback controller, reference input generator, and disturbance feedforward control on the driving dynamics performance measures. [20] develops a method based on a virtual platform, on which the parametrization of the control system parameters of brake interventions is determined, such that the goal conflict between vehicle safety and agility is denied. For this purpose, the author develops a new driving maneuver, which includes these two targets. There, a characteristic value with respect to this maneuver is developed for assessing whether the safety and agility are met. Just one optimum design for the parametrization is achieved without consideration of other driving targets.

1.3 Structure of the dissertation

In Chapter 2, the theory of vehicle lateral dynamics is explained, since we will develop control system logic and actuator models for the vehicle lateral dynamics. Also, the fundamental basics of active rear steering system and one-sided brake intervention will be rephrased in Chapter 2. Moreover, driving dynamics performance measures for ride and safety are explained and a review of the non-linear model of a chassis is given in Chapter 2.

In Chapter 3, control system logics for the lateral vehicle dynamics are developed. All the functions are developed based on the idea of a vehicle centralized control system. However, static feedforward controls are designed for each actuator assembled in a vehicle separately. Influences of each function on vehicle dynamics performance are thoroughly investigated.

In Chapter 4, a new approach is introduced to exploit the functional model of an actuator based on the measurement data from different tests carried out on the test-rig of an actuator. This approach analyzes the behavior of an actuator in the time and frequency domain. It also observes the non-linear behavior of the actuator and proposes a technique for modeling the non-linearity. The approach is then applied for modeling the rear steering actuator as example.

In Chapter 5, we introduce a method for the robust parametrization of a control system and design of an actuator, which is based on the so-called solution spaces existing in system engineering. The method demonstrates the demand of having verification tests and variables for the verification procedure of an actuator after formulating requirements on its design variables. These tests and variables are then explained in details and the method in system engineering is, hence, expanded.

In Chapter 6, the method introduced in Chapter 5 is applied for parame-

terizing the developed control system in Chapter 2 and designing a new rear steering actuator modeled in Chapter 4.

2 Vehicle Dynamics Theory

As a basic understanding of the vehicle is necessary for the modeling, design and evaluation of effects of a vehicle dynamics control system, the vehicle dynamics theory, in particular the lateral one, is described in more details in this chapter. In the beginning, the linear single-track model and its transfer function are described. The simulation environment, the two-track model and its special features are then explained. In addition, it is necessary to clarify the fundamentals of tire behavior in longitudinal and lateral directions, as they change the vehicle performance while cornering significantly. Different driving maneuvers with their objective targets are explained. They are then used for the investigation of the developed control system logics and the design procedure of an actuator and control system logic parameters.

2.1 Single-track model

Not only to investigate the vehicle behavior during cornering, but also to better describe the driving dynamics, mathematical surrogate models are used for modeling the driving dynamics. The single-track model is a simplified and linearized model for the mathematical representation of the lateral vehicle dynamics. Here, various simplifications are made in comparison to the real vehicle. The single-track model enables a fast and simple analysis of the lateral dynamic behavior of vehicles in the linear range. The degree of freedom of the system is significantly reduced by means of linearization, which makes the calculation and analysis of the driving behavior considerably easier. The most striking simplification is probably the merging of the wheel contact points on the front and rear axles. The simplified vehicle consists of a single front and a single rear wheel. Therefore, the vehicle shrinks into a single-track model (STM). In this way, the lateral force build-up of the wheels and the influences of kinematics and compliances are combined to form a linear sideslip stiffness. The vehicle's center of gravity is also set at the height of the road surface. Other simplifications are that rolling, i. e. turning around the x-axis of the vehicle, and pitching, i.e. the rotation of the vehicle around the y-axis, are prevented. The simplified and linearized single-track model is illustrated in the above-mentioned simplifications results in figure 2.1

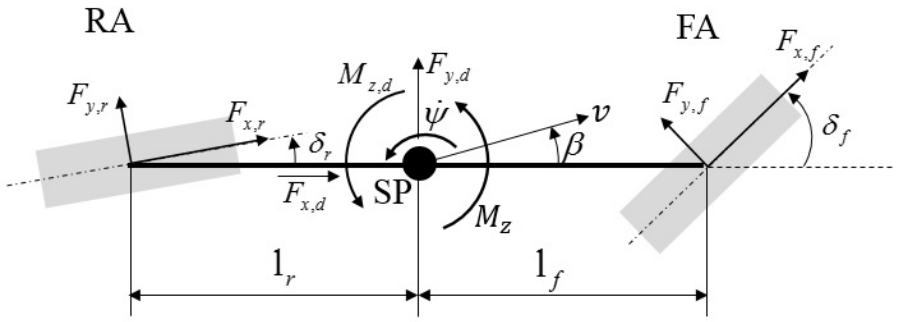

Figure 2.1: Single-track model

As a result, the model is reduced to the two degrees of freedom for the yaw movement around the z-axis in the center of gravity of the vehicle and the slip angle (β), which describes the deviation of the direction of the center of gravity speed from the longitudinal axis of the vehicle [48].

The motion equation of the vehicle can be derived from the kinematics of the single-track model. The force equilibrium in the vehicle longitudinal direction is as follows [52]:

$$m\dot{v} = F_{y,f}\sin(\beta-\delta_f)+F_{x,f}\cos(\beta-\delta_f)+F_{y,r}\sin(\beta-\delta_r)+F_{x,r}\cos(\beta-\delta_r)+F_{x,d} \tag{2.1}$$

The force equilibrium in the vehicle lateral direction is as follows:

$$mv(\dot{\beta}+\dot{\psi}) = F_{y,f}\cos(\beta-\delta_f)-F_{x,f}\sin(\beta-\delta_f)+F_{y,r}\cos(\beta-\delta_r)-F_{x,r}\sin(\beta-\delta_r)+F_{y,d} \tag{2.2}$$

The torque equilibrium at the center of gravity (CG) is as follows [52]:

$$J_z\ddot{\psi} = F_{y,f}l_f\cos\delta_f+F_{x,f}l_f\sin\delta_f-F_{y,r}l_r\cos\delta_r-F_{x,r}l_r\sin\delta_r+M_z+M_{z,d} \tag{2.3}$$

m, l_f and l_r express the vehicle mass, the distance of the center of gravity (CG) from the front axle and rear axle, respectively. $F_{x,d}$, $F_{y,d}$ are external forces in each direction and $M_{z,d}$ is a disturbance torque. M_z stands for the yaw moment generated by lateral vehicle control systems.

The longitudinal and lateral forces acting on tires are formulated from the vehicle properties as follows:

$$
\begin{aligned}
F_{total} &= ma_x \\
F_{x,f} &= (1 - LFD)F_{total} \\
F_{x,r} &= LFDF_{total} \\
F_{y,f} &= c_{f,mod}(\delta_f - \beta - \frac{l_f}{v}\dot{\psi}) \\
F_{y,r} &= c_{r,mod}(\delta_r - \beta + \frac{l_r}{v}\dot{\psi})
\end{aligned}
\tag{2.4}
$$

where

$$
\begin{aligned}
c_{f,mod} &= c_f(1 - \frac{a_x}{g}\frac{h}{l_r}) \\
c_{r,mod} &= c_r(1 + \frac{a_x}{g}\frac{h}{l_f})
\end{aligned}
\tag{2.5}
$$

Here, the longitudinal force distribution (LFD) is the proportion of the driving or braking force acting on the rear axle. In this dissertation, vehicles are considered as rear wheel drive, while The $LFD = 1$. Furthermore, we add an assumption to this STM model to later develop a function which compensates the influence of the longitudinal forces while cornering. The assumption is that the static pitch motion is considered proportional with longitudinal dynamics in the single-track model. Through braking or accelerating, a nick-angle arises, which induces a static change of wheel loads at the front and the rear axle. This changes the whole sideslip stiffness at the front and rear axle, which is dependent on the wheel loads [54]. The modified sideslip stiffnesses at the front and rear axle are represented as $c_{f,mod}$ and $c_{r,mod}$, respectively. c_f and c_r represent the total sideslip stiffness of the front and rear axle. a_x, h and g stand for the longitudinal acceleration, the center of gravity height and gravity value, respectively.

In the single-track model, the angles are assumed to be small [30]. Therefore, equation 2.2 and 2.3 can be linearized at the straight ahead drive with a constant velocity, longitudinal acceleration and longitudinal force distribution. Moreover, in order to explain mathematical formulations of the single-track model more easily, we consider no effects of disturbances, $M_{z,d} = 0$, $F_{x,d} = 0$ and $F_{y,d} = 0$. From the above-mentioned equations 2.1, 2.2, 2.3 and 2.4, the state space model is then defined as follows:

$$\begin{bmatrix}\dot{\beta}\\ \ddot{\psi}\end{bmatrix} = \begin{bmatrix}-\frac{c_{f,mod}+c_{r,mod}+F_{total}}{mv} & -1+\frac{c_{r,mod}l_r-c_{f,mod}l_f}{mv^2}\\ \frac{c_{r,mod}l_r-c_{f,mod}l_f}{J_z} & -\frac{c_{r,mod}l_r^2+c_{f,mod}l_f^2}{J_z v}\end{bmatrix}\begin{bmatrix}\beta\\ \dot{\psi}\end{bmatrix} + \begin{bmatrix}\frac{c_{f,mod}}{mv} & \frac{c_{r,mod}+F_{total}}{mv}\\ \frac{c_{f,mod}l_f}{J_z} & -\frac{(c_{r,mod}+F_{total})l_r}{J_z}\end{bmatrix}\begin{bmatrix}\delta_f\\ \delta_r\end{bmatrix} + \begin{bmatrix}0\\ \frac{1}{J_z}\end{bmatrix} M_z \tag{2.6}$$

Inserting 2.5 in equation 2.6 results in:

$$\begin{bmatrix}\dot{\beta}\\ \ddot{\psi}\end{bmatrix} = \begin{bmatrix}a_{11} & a_{12}\\ a_{21} & a_{22}\end{bmatrix}\begin{bmatrix}\beta\\ \dot{\psi}\end{bmatrix} + \begin{bmatrix}b_{11} & b_{12}\\ b_{21} & b_{22}\end{bmatrix}\begin{bmatrix}\delta_f\\ \delta_r\end{bmatrix} + \begin{bmatrix}0\\ \frac{1}{J_z}\end{bmatrix} M_z \tag{2.7}$$

where

$$\begin{aligned}
a_{11} &= -\frac{(c_r+c_f)gl_rl_f + a_x(h(c_rl_r-c_fl_f)+mgl_rl_f)}{mgl_rl_fv}\\
a_{12} &= -1+\frac{gl_rl_f(c_rl_r-c_fl_f)+a_xh(c_rl_r^2+c_fl_f^2)}{mgl_rl_fv^2}\\
a_{21} &= \frac{gl_fl_r\,(c_rl_r-c_fl_f)+a_xh(c_rl_r^2+c_fl_f^2)}{J_zgl_rl_f}\\
a_{22} &= \frac{a_xh(c_fl_f^3-c_rl_r^3)-gl_rl_f(c_rl_r^2+c_fl_f^2)}{J_zgl_rl_fv}\\
b_{11} &= \frac{c_fgl_r-a_xc_fh}{mgl_rv}\\
b_{12} &= \frac{c_rgl_f+a_x(c_rh+mgl_f)}{mgl_fv}\\
b_{21} &= \frac{l_f(c_fgl_r-a_xc_fh)}{gl_rJ_z}\\
b_{22} &= -\frac{l_r(c_rgl_f+a_x(c_rh+mgl_f))}{gl_fJ_z}
\end{aligned} \tag{2.8}$$

If we want to consider only the lateral vehicle dynamics without the static effect of the longitudinal forces on the cornering ($a_x = 0$), the state space model becomes as follows:

$$\begin{bmatrix}\dot{\beta}\\ \ddot{\psi}\end{bmatrix} = \underbrace{\begin{bmatrix}-\frac{c_r+c_f}{mv} & -1+\frac{c_r l_r - c_f l_f}{mv^2}\\ \frac{c_r l_r - c_f l_f}{J_z} & -\frac{c_r l_r^2 + c_f l_f^2}{J_z v}\end{bmatrix}}_{\mathbf{A}} \begin{bmatrix}\beta\\ \dot{\psi}\end{bmatrix} + \underbrace{\begin{bmatrix}\frac{c_f}{mv} & \frac{c_r}{mv} & 0\\ \frac{c_f l_f}{J_z} & -\frac{c_r l_r}{J_z} & \frac{1}{J_z}\end{bmatrix}}_{\mathbf{B}} \begin{bmatrix}\delta_f\\ \delta_r\\ M_z\end{bmatrix} \tag{2.9}$$

This model considers only the yaw motion of a vehicle while cornering and neglects all lifting, rolling and pitching motions. The eigenvalues of the matrix **A** are calculated from the characteristic polynomial as follows:

$$det(A - \lambda I) = 0 \tag{2.10}$$

$$\lambda^2 - (a_{11} + a_{22})\lambda + (a_{11}a_{22} - a_{12}a_{21}) \tag{2.11}$$

where

$$\begin{aligned} a_{11} &= -\frac{c_r + c_f}{mv} & a_{12} &= -1 + \frac{c_r l_r - c_f l_f}{mv^2}\\ a_{21} &= \frac{c_r l_r - c_f l_f}{J_z} & a_{22} &= -\frac{c_r l_r^2 + c_f l_f^2}{J_z v} \end{aligned} \tag{2.12}$$

The solution of the characteristic polynomial is

$$\lambda_{1,2} = \frac{a_{11} + a_{22}}{2} \pm \sqrt{\left(\frac{a_{11} + a_{22}}{2}\right)^2 - (a_{11}a_{22} - a_{12}a_{21})} \tag{2.13}$$

The stability criterion according to Hurwitz states that all coefficients of the polynomial must be positive. Only the constant term can be negative. From this follows:

$$(a_{11}a_{22} - a_{12}a_{21}) > 0 \tag{2.14}$$

which means

$$\frac{c_f c_r l}{m J_z v^2}\left(l + v^2 \frac{m(c_r l_r - c_f l_f)}{c_f c_r l}\right) \tag{2.15}$$

This model is then always stable, if the criterion below is met:

$$c_r l_r > c_f l_f \tag{2.16}$$

otherwise the stability only holds until the critical velocity of a vehicle be-

comes:

$$v_{crit}^2 < \frac{c_f c_r l^2}{m(c_f l_f - c_r l_r)} \tag{2.17}$$

where

$$l = l_f + l_r \tag{2.18}$$

Stationary steering

On the basis of the stationary steering behavior, various driving dynamics parameters can be obtained from the single-track model to assess the driving behavior. The characteristics of stationary steering behavior are the self-steering behavior and the resultant self-steering gradient as well as the characteristic or critical speed of the vehicle.

stationary steering behavior and gradient

Self-steering behavior is an important criterion for assessing the driving behavior of vehicles. In this case, the steering angle demand, independent of the driver's influence, is determined for a circular drive at a constant radius and an increasing driving speed. The centrifugal force affects the turning motion of the vehicle, resulting in sideslip angle on the tire. This results in a higher steering angle effort to cross the curve. During the stationary circular drive, the additional steering angle to the Ackermann angle [30] is investigated in relation to the lateral acceleration a_y. The conditions for the stationary cornering are as follows:

$$\begin{aligned} v &= const. \\ \dot{\psi} = const. &\Rightarrow \ddot{\psi} = 0 \\ \beta = const. &\Rightarrow \dot{\beta} = 0 \end{aligned} \tag{2.19}$$

Accordingly,

$$\begin{aligned} ma_y &= F_{y,f} + F_{y,r} = F_{y,f}\frac{l}{l_r} \\ ma_y\frac{l_r}{l} &= F_{y,f} = c_f \underbrace{\left(\delta_f - \beta - \frac{l_f}{v}\dot{\psi}\right)}_{\alpha_f} \end{aligned} \tag{2.20}$$

analogously,

$$ma_y \frac{l_f}{l} = F_{y,r} = c_r \underbrace{\left(-\beta + \frac{l_r}{v}\dot{\psi}\right)}_{\alpha_r} \tag{2.21}$$

Equations 2.20 and 2.21 deliver with $\dot{\psi} = \frac{v}{l}$ (small angle):

$$\begin{aligned} \underbrace{\alpha_f - \alpha_r}_{\Delta\alpha} &= \frac{m}{l}\left(\frac{l_r}{c_f} - \frac{l_f}{c_r}\right) a_y \\ &= \delta_f - \frac{l_f + l_r}{v}\dot{\psi} = \delta_f - \underbrace{\frac{l}{R}}_{\delta_A} \end{aligned} \tag{2.22}$$

Where, R and l stand for the path radius and the wheel base, respectively.

Based on the Ackermann angle (δ_A) and the simplifications resulting by the stationary circular drive, it is possible to derive the steering angle from the single-track model as in Equation 2.23. The equation shows that, in addition to the geometric steering angle, the driver must also provide the vehicle with an additional steering angle to compensate for the sideslip angle difference, $\Delta\alpha$.

$$\delta_f = \underbrace{\frac{l}{R}}_{\delta_A} + \underbrace{\underbrace{\frac{m}{l}\left(\frac{l_r}{c_f} - \frac{l_f}{c_r}\right)}_{\text{EG}} a_y}_{\Delta\alpha} \tag{2.23}$$

To characterize steering behavior, the terms understeer and oversteer as well as neutral driving behavior are introduced here. For the evaluation of the vehicle behavior according to Olley, the sideslip angle difference is used, Table 2.1.

Conditions	States
$\Delta\alpha = \alpha_f - \alpha_r < 0$	Oversteer
$\Delta\alpha = \alpha_f - \alpha_r = 0$	Neutral steer
$\Delta\alpha = \alpha_f - \alpha_r > 0$	Understeer

Table 2.1: Definition of vehicle states according to Olley

This definition considers the absolute steering angle. However, the steering angle gradient $d\delta_f/da_y$ is more important than the absolute steering angle while cornering. In the linear range of lateral vehicle dynamics ($a_y < 4m/s^2$), the

self-steering gradient (EG) is a vehicle parameter that depends on the vehicle mass, the position of the center of gravity and the total sideslip stiffness of the front and rear axles.

$$EG = \frac{m(c_r l_r - c_f l_f)}{l c_v c_r} \tag{2.24}$$

The self-steering gradient describes the self-steering behavior of the vehicle and indicates how much the lateral acceleration affects the steering angle requirement. Therefore, the front steering angle demand is expressed as follows:

$$\delta_f = \delta_A + EG \cdot a_y \tag{2.25}$$

The required steering angle for a stationary circular drive is composed of two parts: the Ackerman's angle defined by the vehicle geometry and the self-steering angle. The driving condition differentiates between neutral steer, understeer and oversteer, as defined in Table 2.2, based on the self-steering gradient. Neutral steering means, that the steering angle must remain constant at any speed or lateral acceleration [66].

Conditions	**States**
$EG < 0$	Oversteer
$EG = 0$	Neutral steer
$EG > 0$	Understeer

Table 2.2: Definition of the vehicle states with respect to the self-steering gradient

Figure 2.2 shows the steering angle above the lateral acceleration for a stationary circular motion in the linear and non-linear range.

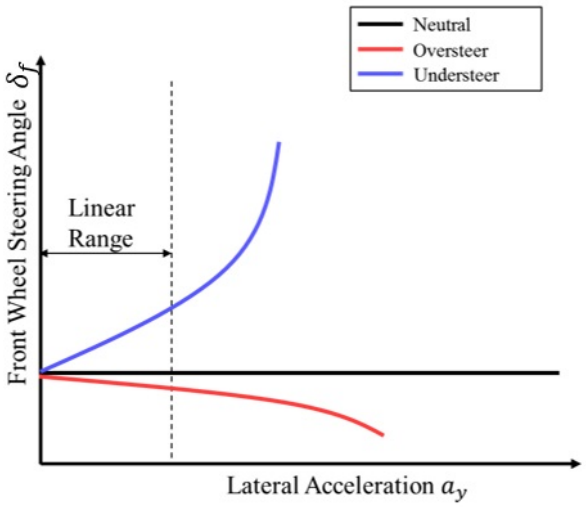

Figure 2.2: Steering behavior in stationary cornering while the road radius is constant

In this figure, the steering effort at a constant radius at different velocities is investigated. The steering angle demand remains unchanged, if the vehicle has a neutral property. For $EG > 0$, a steering effort has to be provided in addition to the Ackermann angle. Conversely, in the case of oversteering, the steering angle demand is reduced by a negative gradient. At a lateral acceleration of less than approx. $4m/s^2$, this gradient is quasi-constant. However, an increasing gradient occurs at high lateral acceleration because the properties of the tires are non-linear in terms of sideslip stiffness due to wheel load changes and increased lateral forces on the tires.

As already described, the yaw velocity $\dot{\psi}$ is one of the most important output variables in the driver-vehicle control loop. Therefore, it is necessary to examine the driving behavior with the help of the yaw velocity response to a steering angle input under stationary consideration. The stationary yaw velocity amplification, also known as the steering angle-related circular motion value, is introduced in this context. The mathematical relationship between the yaw velocity amplification and front axle steering angle can be derived from equations 2.9 and 2.19:

$$\delta_f s[mvl_f c_f] + \delta_f[c_f c_r l] = \dot{\psi} s^2[mJ_z v] + \dot{\psi} s[J_z(c_f + c_r) + m(c_f l_f^2 + c_r l_r^2)] + \dot{\psi}\frac{[c_f c_r l^2 - (c_f l_f - c_r l_r)mv^2]}{v} \tag{2.26}$$

$$\frac{\dot{\psi}(s)}{\delta_f(s)} = \frac{[mvl_f c_f]s + c_f c_r l}{[mJ_z v]s^2 + [J_z(c_f + c_r) + m(c_f l_f^2 + c_r l_r^2)]s + \frac{[c_f c_r l^2 - (c_f l_f - c_r l_r)mv^2]}{v}} \tag{2.27}$$

by reformulating:

$$\frac{\dot{\psi}(s)}{\delta_f(s)} = \underbrace{\underbrace{\frac{v}{l + \frac{m}{l}\left(\frac{l_r}{c_f} - \frac{l_f}{c_r}\right)v^2}}_{=\left(\frac{\dot{\psi}}{\delta_f}\right)_{stat}}}_{\text{Stationary}} \cdot \underbrace{\frac{1 + T_z s}{1 + \frac{2D}{\omega_0}s + \frac{1}{\omega_0^2}s^2}}_{\text{Transient}} \tag{2.28}$$

The stationary yaw velocity amplification, equation 2.29, depends significantly on the driving speed. Its schematic progression as a function of speed is shown in figure 2.3

$$\left(\frac{\dot{\psi}}{\delta_f}\right)_{stat} = \frac{v}{l + \frac{m}{l}\left(\frac{l_r}{c_f} - \frac{l_f}{c_r}\right)v^2} = \frac{v}{l + EG.v^2} \tag{2.29}$$

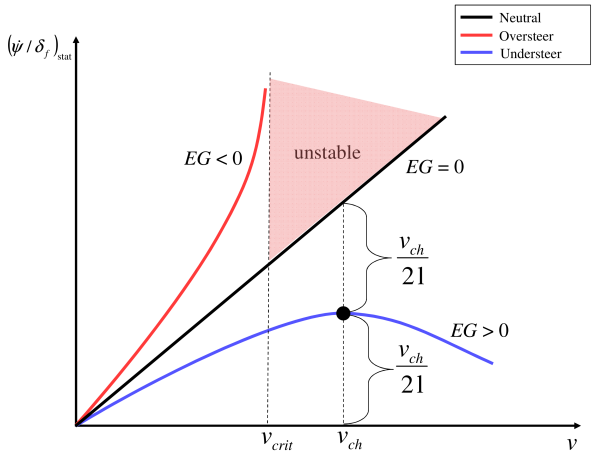

Figure 2.3: The behavior of stationary yaw velocity amplification regarding velocity

A vehicle with a tendency to understeer, nowadays a standard for production of vehicles, has a slowly increasing stationary yaw velocity amplification. At a certain speed v_{ch}, the yaw gain reaches its maximum value indicated by $\left(\frac{\dot{\psi}}{\delta_f}\right)_{stat,max}$ and goes down again with increasing speed. But, the yaw velocity amplification of an oversteer vehicle tends to infinity at the critical velocity v_{crit}, which is undesirable for a driver, as he/she cannot control the vehicle at this velocity. The critical and characteristic velocity are then calculated as follows:

1. For understeer vehicles ($EG > 0$):

$$\left(\frac{\dot{\psi}}{\delta_f}\right)_{stat} = \frac{v}{l + EG.v^2} \tag{2.30}$$

$$\frac{d}{d\delta_f}\left(\frac{\dot{\psi}}{\delta_f}\right)_{stat} = \frac{l - EG.v^2}{(l + EG.v^2)^2} = 0 \rightarrow v_{ch}^2 = \frac{l}{EG} \tag{2.31}$$

2. For oversteer vehicles ($EG < 0$):

$$\frac{d}{d\delta_f}\left(\frac{\dot{\psi}}{\delta_f}\right)_{stat} = \frac{l - EG.v^2}{(l + EG.v^2)^2} = 0 \rightarrow v_{ch}^2 = \infty \rightarrow v_{crit}^2 = -\frac{l}{EG} \tag{2.32}$$

Accordingly,

$$v_{ch}^2 = -v_{crit}^2 = \frac{l^2}{m} \frac{c_f c_r}{l_r c_r - l_f c_f} \tag{2.33}$$

And the stationary yaw velocity amplification can be converted as follows:

$$\left(\frac{\dot{\psi}}{\delta_f} \right)_{stat} = \frac{1}{l} \frac{v}{1 + \frac{v^2}{v_{ch}^2}} \tag{2.34}$$

The characteristic speed is clearly illustrated by the self-steering behavior. Equation 2.34 shows that the vehicle is controlled in a neutral manner when v_{ch} is equal to infinity. If v_{ch} is greater than zero, the vehicle has a tendency to understeer and can be controlled at any speed. However, if v_{ch} is imaginary or v_{crit} is real, the vehicle has an oversteering tendency. It can be controlled stable at speeds below v_{crit}. From v_{crit} on, however, the yaw amplification goes against infinity and therefore the vehicle becomes unstable and the controllability is lost. However, such an oversteering design for series-produced vehicles has not been put on the market for years due to safety reasons.

Transient steering

In order to assess the dynamic driving behavior and for the subsequent control design, it is also necessary to know the driving behavior regarding transient steering. In this case, yaw natural frequency and yaw damping are characteristic variables and are briefly explained below.

The transfer function of the vehicle can be derived from the state space model, equation 2.9, as follows:

$$\mathbf{G}(s) = (\mathbf{I}s - \mathbf{A})^{-1} \mathbf{B} \tag{2.35}$$

$$\begin{bmatrix} \beta \\ \dot{\psi} \end{bmatrix} = \begin{bmatrix} G_{\beta/\delta_f}(s) & G_{\beta/\delta_r}(s) & G_{\beta/M_z}(s) \\ G_{\dot{\psi}/\delta_f}(s) & G_{\dot{\psi}/\delta_r}(s) & G_{\dot{\psi}/M_z}(s) \end{bmatrix} \begin{bmatrix} \delta_f \\ \delta_r \\ M_z \end{bmatrix} \tag{2.36}$$

Among all these transfer functions, which can be easily derived, the transfer function $G_{\dot{\psi}/\delta_f}(s)$ is our point of interest, since we use it in the next chapter for developing lateral vehicle dynamics control systems. As a consequence, some features of this transfer function will be studied. The transfer function has the following form:

$$G_{\dot{\psi}/\delta_f}(s) = \left(\frac{\dot{\psi}}{\delta_f}\right) = \left(\frac{\dot{\psi}}{\delta_f}\right)_{stat} \cdot \frac{1 + T_z \cdot s}{1 + \frac{2 \cdot D}{w_0} \cdot s + \frac{1}{w_0^2} \cdot s^2} \tag{2.37}$$

Where, D stands for the damping ratio, w_0 for the undamped natural frequency and T_z for time constant. They are then defined as follows:

$$\begin{aligned} \omega_0 &= \sqrt{\frac{c_r \cdot l_r - c_f \cdot l_f}{J_z} + \frac{c_f \cdot c_r \cdot l^2}{J_z \cdot m \cdot v^2}} \\ D &= \frac{1}{2w_0} \cdot \left[\frac{c_f + c_r}{m \cdot v} + \frac{c_f \cdot l_f^2 + c_r \cdot l_r^2}{J_z \cdot v}\right] \\ T_z &= \frac{m \cdot v \cdot l_f}{c_r \cdot l} \end{aligned} \tag{2.38}$$

$\left(\frac{\dot{\psi}}{\delta_f}\right)_{stat}$ is also obtained from equation 2.29.

The transfer function of equation 2.37 has a $PDT2$ form [61]. The natural frequency and damping factor of the transfer function in equation 2.37 are often referred to as yaw natural frequency and yaw damping. The yaw natural frequency provides information about the transient yaw reaction of a vehicle with steering movements of different speeds. The smaller the yaw natural frequency, the longer the response time for rapid changes in the steering angle. The yaw damping influences the transient oscillation of the yaw velocity during steering excitation. It describes the stability of the system and the response to a steering input. figure 2.4 shows the dependence of the natural frequency and damping ratio on the driving speed for the vehicle used in this work. As can be observed here, the yaw damping ratio as well as the yaw natural frequency decrease with increasing driving speed. The vehicle is therefore less damped at high speeds. As the yaw natural frequency decreases, the response to changes in steering angle becomes faster [30].

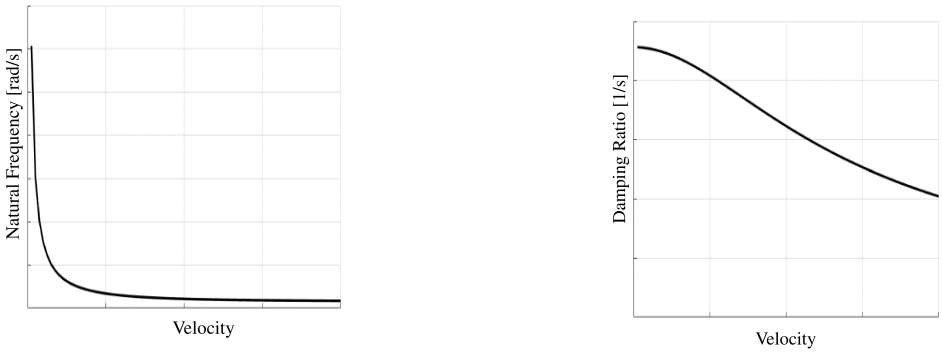

(a) (b)

Figure 2.4: (a): Natural frequency and (b) Damping ratio as a function of the vehicle velocity

2.2 Active Rear Steering

Active rear-wheel steering systems were designed in the early 1930s. The first application was the reduction of the vehicle turning circle. BMW, as a premium car manufacturer has long been seeking an integrated, active rear-wheel steering system with high performance and has introduced an electromechanical rear-wheel steering system with the new 7, 6 and 5 Series models to the market since 2008, figure 2.5.

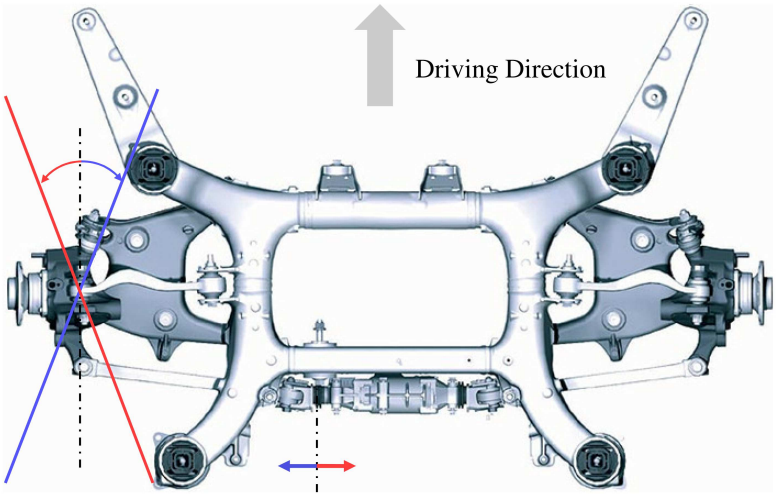

Figure 2.5: Rear steering system of BMW [56]

The rear wheel steering turns the rear wheels either in the opposite or the same direction of the front wheels. Opposite steering reduces the steering radius, allowing the vehicle to travel with the same steering wheel angle and the same driving speed through a smaller steering radius, making it more agile than an unregulated vehicle. However, the same steering makes the vehicle more stable and drive in a larger steering radius. Accordingly, the stability of the vehicle's dynamics response is improved. In addition, the same directional steering reduces the frequency and effort of controlling a vehicle by the Electronic Stability Program (ESP), abbreviated as DSC (Dynamic Stability Control) in BMW vehicles.

figure 2.6 shows the functional characteristics of active rear-wheel steering with opposite-directional and same-directional steering. When rear steering is opposite to the front wheels, the momentary pole is reduced due to the vehicle kinematics, which means that the vehicle can drive through the curve with a smaller radius. In contrast, rear-wheel steering with the same direction of rotation to the front wheels contributes to an increase of the steering radius and thus more stabilization.

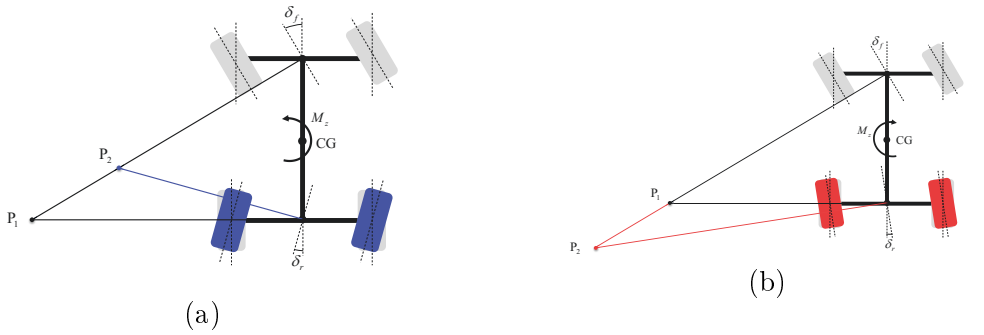

Figure 2.6: Functionality of active rear steering system (a): opposite steering (b) same directional steering

One of the most important points in the design software and function in vehicles is, that they have to be ensured with respect to the functional safety, meaning whether a vehicle can still be controlled by a driver, if the controller runs out of the performance, while giving out a controlled input wrongly. Accordingly, it is not desirable to let a controller set a rear steering angle arbitrarily. It must be then bounded. In this work, the maximum rear steering angle is set to 3°.

Conversion factor yaw torque to rear wheel steering angle

As we explained in the state of the art, we will develop a centralized controller, which generates a torque around the z-axis (yaw moment) of a vehicle independently of implemented actuators. But this generated torque is a signal and must be implemented by an actuator in form of forces or torques on the wheels. Accordingly, we compute a conversion factor which transforms the torque, i.e. the yaw torque, into a rear wheel steering angle. Then, this computed angle is the input of the rear steering actuator.

Based on equation 2.9, we would like to find out the static conversion factor transforming a yaw moment into a rear wheel steering angle. In this case we set the static part of the transfer function from the yaw velocity to the rear wheel steering equal to the static part of the transfer function from the yaw velocity to the yaw moment. According to equation 2.9 and 2.36, the transfer function from the yaw velocity to the rear wheel steering is as follows:

$$\frac{\dot{\psi}(s)}{\delta_r(s)} = \frac{a_{1r}s + a_{0r}}{b_{2r}s^2 + b_{1r}s + b_{0r}} \tag{2.39}$$

where

$$
\begin{aligned}
a_{1r} &= -c_r l_r m v^2 \qquad a_{0r} = -c_r c_f l v \\
b_{2r} &= J_z m v^2 \qquad b_{1r} = c_r m l_r^2 v + c_f m l_f^2 v + J_z c_r v + J_z c_f v \\
b_{0r} &= c_r c_f l_r^2 + 2 c_r c_f l_r l_f + c_r m l_r v^2 + c_r c_f l_f^2 - c_f m l_f v^2
\end{aligned} \tag{2.40}
$$

and

$$
\frac{\dot{\psi}(s)}{M_z(s)} = \frac{a_{1z} s + a_{0z}}{b_{2z} s^2 + b_{1z} s + b_{0z}} \tag{2.41}
$$

$$
\begin{aligned}
a_{1z} &= m v^2 \qquad a_{0z} = (c_r + c_f)\, v \\
b_{2z} &= J_z m v^2 \qquad b_{1z} = c_r m l_r^2 v + c_f m l_f^2 v + J_z c_r v + J_z c_f v \\
b_{0z} &= c_r c_f l_r^2 + 2 c_r c_f l_r l_f + c_r m l_r v^2 + c_r c_f l_f^2 - c_f m l_f v^2
\end{aligned} \tag{2.42}
$$

If we set $s = 0$ in equations 2.39 and 2.41, then we obtain the static terms of these transfer functions:

$$
\left(\frac{\dot{\psi}(s=0)}{\delta_r(s=0)} \right) = \left(\frac{\dot{\psi}(s)}{\delta_r(s)} \right)_{stat} = \frac{a_{0r}}{b_{0r}} \tag{2.43}
$$

$$
\left(\frac{\dot{\psi}(s=0)}{M_z(s=0)} \right) = \left(\frac{\dot{\psi}(s)}{M_z(s)} \right)_{stat} = \frac{a_{0z}}{b_{0z}} \tag{2.44}
$$

By setting equation 2.43 equal to 2.44

$$
\frac{a_{0r}}{b_{0r}} \cdot \delta_r = \frac{a_{0z}}{b_{0z}} \cdot M_z \tag{2.45}
$$

As we can see from equations 2.40 and 2.42, $b_{r0} = b_{z0}$ subsequently,

$$
\delta_r = \underbrace{-\frac{c_r + c_f}{c_r c_f l}}_{M_{z \to \delta_r}} M_z \tag{2.46}
$$

As a consequence, the conversion factor transforming a yaw moment into a rear wheel steering angle is as follows:

$$
\boxed{M_{z \to \delta_r} = -\frac{c_r + c_f}{c_r c_f l}}
$$

2.3 One-Sided Brake Intervention

In normal BMW vehicles, the DSC is able to stabilize the vehicle and restore its controllability by active braking on the individual wheels in instable driving conditions. The DSC is not activated during a normal driving situation, below a certain driving limit, since no stabilization task is required [12]. By integrating an agilising function, the driving performance of the vehicle can be improved in these driving situations. The dynamic braking action generates a desired yaw moment by braking on a wheel in a similar way to the DSC to improve driving behavior, especially while cornering. Setting up such a function is relatively inexpensive because dynamic braking can use a common actuator together with the DSC or ABS. figure 2.7 shows a schematic of the function of individual wheel braking. The control system calculates a desired braking moment for a brake action and distributes the moment to a corresponding wheel considering driving situations and direction of the set point. When cornering to the left, a turning yaw moment will be generated. When the rear left wheel is braked by the control system, a braking force is generated on the tire. This causes an additional agilisation yaw moment around the vehicle's z-axis, caused by the braking force with the lever arm of the track width. Additionally, the functional safety takes into account whether a vehicle can still be controlled by a driver if the controller runs out of the performance while giving out a controlled input wrongly. Accordingly, it is not desirable to let a controller set a brake moment arbitrarily. The brake moment must be bounded. In this work, the maximum brake moment is set to 900$[NM]$.

Conversion factor yaw moment to brake moment difference

As we can see from figure 2.7, a yaw moment (M_z) can be converted to a brake moment difference based on the vehicle kinematics as follows:

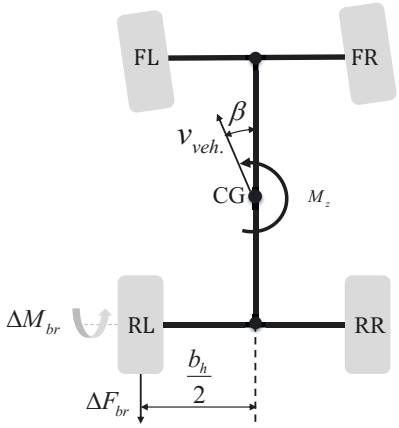

Figure 2.7: Basic functionality of the dynamic braking action

$$M_z = \Delta F_{br} \frac{b_r}{2} = \frac{\Delta M_{br}}{r_{dyn}} \frac{b_r}{2} \tag{2.47}$$

where ΔF_{br}, b_r, ΔM_{br} and r_{dyn} represent a brake force difference between the right and left rear wheel, the track width of a vehicle, a brake moment difference generated by the brake force difference, and dynamic wheel radius [48], respectively; hence, the conversion factor transforming a yaw moment to a brake moment difference is as

$$\boxed{M_{z \to \Delta M_{br}} = \frac{2 r_{dyn}}{b_r}}$$

As soon as the brake moment difference is computed, it can be converted to the brake pressure difference which the brake system has to implement. It is easily modeled as follows:

$$\Delta P_{brake} = \frac{\Delta M_{br}}{A_{pistol} \cdot r_w \cdot \mu_{temp}} \tag{2.48}$$

where, A_{pistol}, r_w and μ_{temp} are the disk area, the wheel radius, and the friction coefficient caused by the disc temperature.

In summary, it can be inferred that the active rear wheel steering and the individual wheel dynamic braking action can improve the driving characteristics of the entire vehicle not only in the linear range but also in the non-linear range of the vehicle dynamics.

2.4 Driving Maneuvers and the objective driving performances

In order to achieve desired static and dynamic steering performances of a vehicle, the vehicle properties are typically designed and tuned by simulations and driving experiences with respect to different driving maneuvers. Normally, these maneuvers are divided into two groups, Open-Loop and Closed-Loop maneuvers. The difference between these two groups refers to the driver, as shown in figure 2.8.

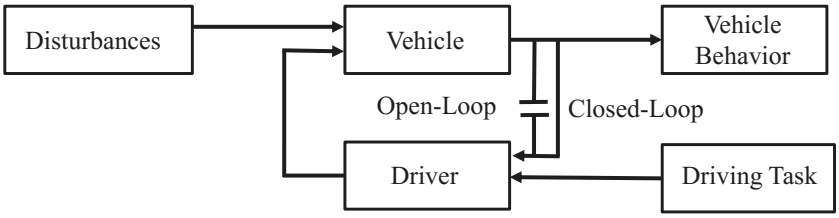

Figure 2.8: The influence of a drive in the Open-Loop and Closed-Loop Maneuvers

In open-loop maneuvers, the driver does not react on vehicle trajectories and responses but follows a predetermined task to accomplish planned maneuvers. Inversely, the driver affects the vehicle trajectories and responses in the closed-loop maneuvers. For designing vehicle properties in the early stages of the development, open-loop maneuvers are applied and the design is carried out based on the simulation, since they are reproducible and there is no need to model the human behavior which cannot be fully algorithmically described [43]. In this section, the open-looped driving maneuvers, which are relevant for this dissertation, as well as their associated objective targets are explained, which have to be achieved during the design of different components of the chassis. These maneuvers are as follows:

- **QSSC** - Quasi Steady State Cornering [4]
- **SWD** - Sine With Dwell [3]
- **BRWC** - Brake While Cornering [1]
- **WEAVE** - Sinus with constant frequency [2]
- **CSST** - Continuous Sine Steering [2]

QSSC - Quasi Steady State Cornering

The QSSC is a maneuver for evaluating the static vehicle performance. The vehicle can be driven either on curves with different radii but a constant velocity or on a curve with a defined radius but varying velocities [18].In this dissertation, a simulation scenario with a radius of $105m$ is defined, where the vehicle is accelerated on the curve with a slow initial acceleration of $0.5m/s^2$, figure 2.9. At the same time, the steering wheel angle is adapted and measured, such that the vehicle stays on the lane with the radius $R = 105m$. With increasing velocity, the lateral acceleration a_y rises. The simulation will be aborted, as soon as the vehicle leaves the defined trajectory due to increasing velocity or lateral acceleration. In order to evaluate driving performances during QSSC, some objective targets are defined. The first one is the maximum lateral acceleration, where the simulation ends up. The second one is the self-steering gradient in the linear range of the vehicle dynamics, i.e. between 0 and $4m/s^2$. The third one is the self-steering gradient in the non-linear range of vehicle dynamics which is defined as the gradient between 7 and 95% of the maximum lateral acceleration. It should be noticed that the self-steering gradient is defined with respect to the steering wheel angle, δ_H, and not the wheel steering angle, δ_f. The three above-mentioned criteria are listed in Table 2.3.

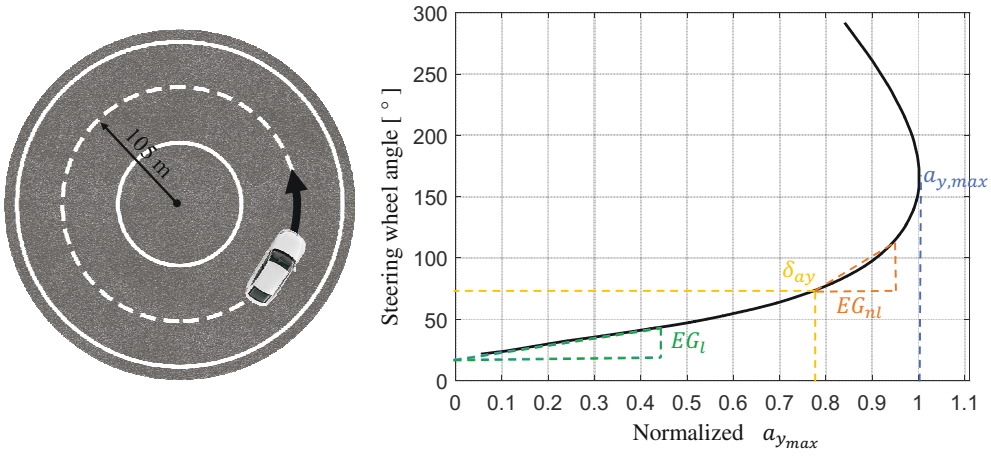

Figure 2.9: Quasi Steady State Cornering Maneuver and its associated objective targets

Objective driving dynamics performance measures for QSSC	
CV	**Description**
$a_{y,max}$	Maximum lateral acceleration
$EG_l = \left(\frac{d\delta_H}{da_y}\right)_{a_y=0-4}$	Self-steering gradient in linear domain from $a_y = 1 - 4m/s^2 y$
$EG_{nl} = \left(\frac{d\delta_H}{da_y}\right)_{a_y=7}$	Self-steering gradient in non-linear domain from $a_y = 7m/s^2$ until 95% of $a_{y,max}$

Table 2.3: Characteristic values for QSSC

SWD - Sine With Dwell

Sinus with dwell (SWD) is a very important maneuver for examining the driving safety and stability, in particular for the validation of the electronic stability program (ESP). This maneuver includes a single sinus period with holding time of 0.5s at the valley. It is executed with a defined amplitude, the defined frequency $f = 0.7Hz$ and the constant velocity $v = 80km/h$. After 3/4 of the sinus period, the steering input stays constant for 0.5s. The amplitude is made up of two parts: a steering wheel angle factor (SAF) and the characteristic steering wheel angle, determined by a pre-maneuver with a ramp steering wheel angle. It means, the ramp maneuver is first carried out at a constant velocity to reach the lateral acceleration of $a_y = 0.3g$. The steering angle at this acceleration is then $\delta_{H,0.3g}$, figure 2.10.

$$\delta_{H,amplitude} = SAF \cdot \delta_{H,0.3g} \tag{2.49}$$

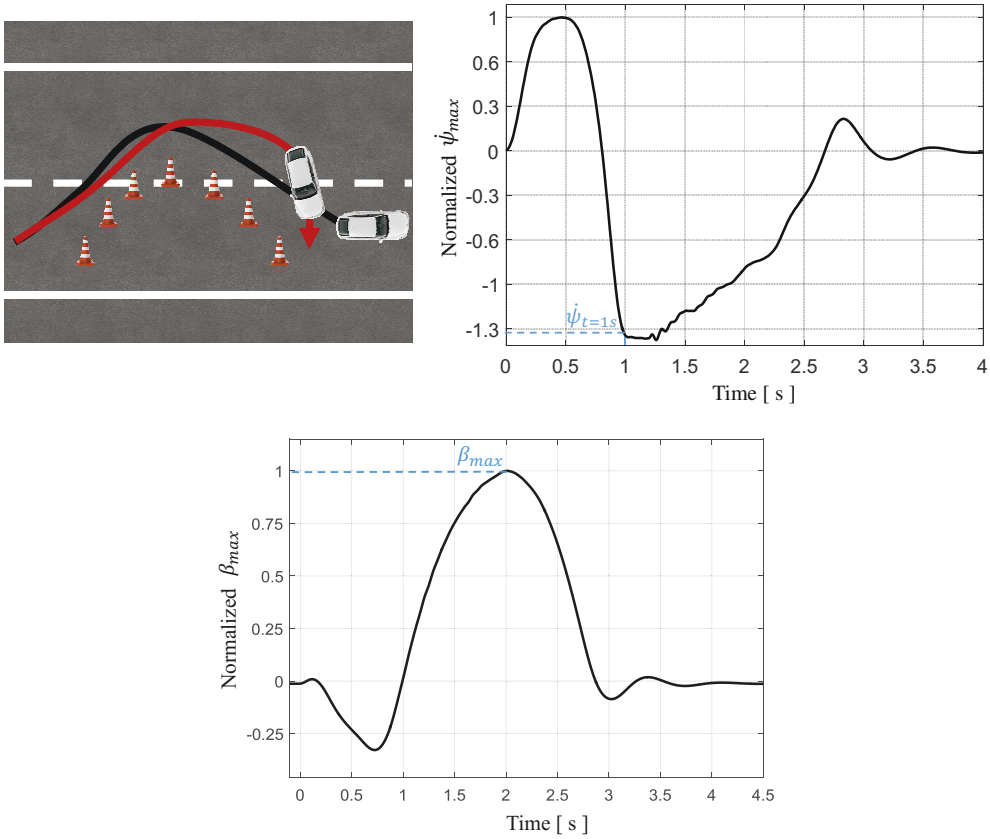

Figure 2.10: Sine With Dwell Maneuver and its associated objective targets

The main goal of this maneuver is that the vehicle must always maintain the stability and present a controlled behavior until a defined steering factor. Accordingly, the side slip angle of a vehicle has to be under a certain value (β_{max}). Furthermore, other driving targets must also be achieved during this maneuver. For example, the vertical contact force of inner tires during steering must always be more than a minimum value, $F_{z,min}$. All driving dynamics performance measures relevant to this maneuver are listed in table 2.4.

BRWC - Brake While Cornering

The maneuver brake while cornering is utilized to investigate the driving performance during the load change between the front and rear axle and the interaction between lateral, longitudinal and vertical vehicle dynamics. It is a static maneuver. A vehicle is braked with a constant longitudinal acceleration on a

Objective driving dynamics performance measures for SWD	
CV	**Description**
β_{max}	Maximal CG slip angle
$F_{z,min}$	Minimal vertical tyre force
$\dot{\psi}_{t=te+1.75s}/\dot{\psi}_{max}$	Yaw velocity reduction behavior

Table 2.4: Characteristic values for SWD

road curve with a constant radius. The steering wheel angle is kept unchanged thereby. In this dissertation, the considered radius is $R = 400m$ and the vehicle speed increases until the vehicle reaches a lateral acceleration of $a_y = 5m/s^2$, figure 2.11.

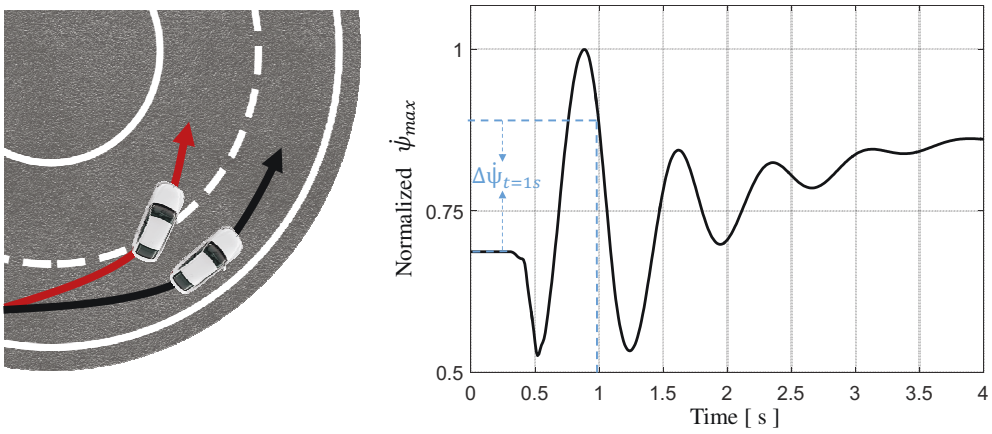

Figure 2.11: Brake While Cornering Maneuver and its associated objective targets

At this acceleration, the driver brakes with a constant longitudinal acceleration of $a_x = -5m/s^2$. While braking, the weight is shifted into the front axle. This fact increases the yaw velocity and the vehicle tends to oversteer. The associated driving target is shown in table 2.5.

WEAVE Test

Weave is a maneuver with a sinus input with the constant frequency of $f = 0.25Hz$ as steering wheel angle, figure 2.12, where steering characteristics are evaluated in terms of yaw velocity amplification. The vehicle is driven with

Objective driving dynamics performance measures for BRWC	
CV	**Description**
$\Delta\dot{\psi}_{1s}$	Yaw velocity change at t=1s

Table 2.5: Characteristic values for BRWC

certain different constant velocities at the constant lateral acceleration $a_y = 4m/s^2$. For example, the vehicle drives with a defined constant velocity, v_1. The amplitude of steering is then adjusted, such that the vehicle reaches the lateral acceleration of $a_y = 4m/s^2$. Then, the yaw velocity amplification to the steering angle amplification is recorded. This procedure is then done also for other defined constant velocities, $v_2, ..., v_n$. Then, a course is interpolated among all these recoded amplifications and results in a diagram like figure 2.12 (b).

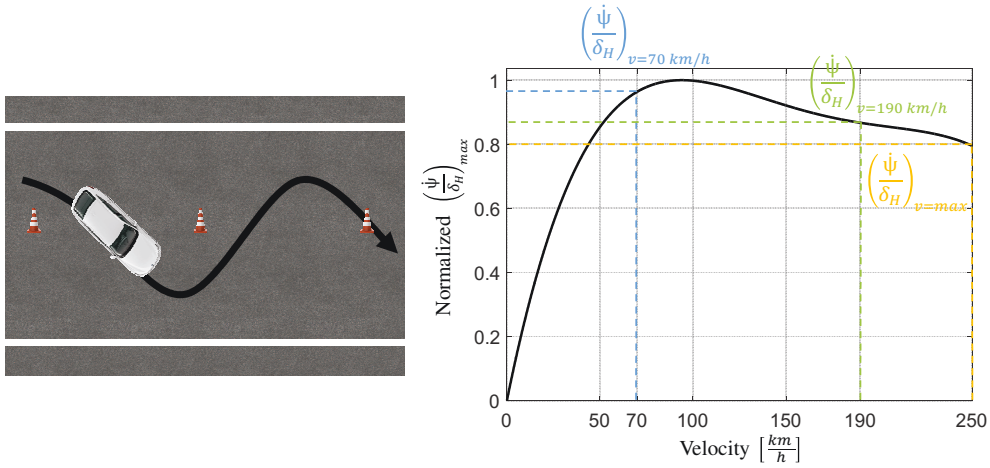

Figure 2.12: WEAVE Maneuver and its associated objective targets

According to this maneuver, various driving dynamics performance measures are assessed, which are listed in table 2.6.

CSST - Continuous Sine Steering

The maneuver CSST is applied for the evaluation of the vehicle transient response. The frequency response of the vehicle is analyzed with concerning the steering stimulation. The vehicle is driven with a sinus shaped steering input

Objective driving dynamics performance measures for SWD	
CV	**Description**
$(\dot{\psi}/\delta_f)_{stat,70}$	Stationary yaw velocity amplification for $v = 70km/h$
$(\dot{\psi}/\delta_f)_{stat,190}$	Stationary yaw velocity amplification for $v = 190km/h$
$(\dot{\psi}/\delta_f)_{stat,max}$	Maximal stationary yaw velocity amplification

Table 2.6: Characteristic values for WEAVE

with rising frequency from $0.5Hz$ until $2Hz$ and a constant amplitude, figure 2.13.

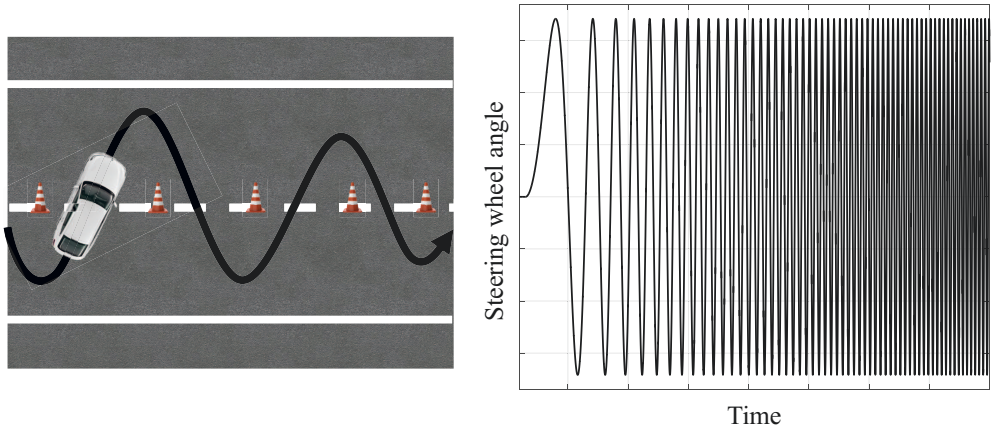

Figure 2.13: Continuous Sine Steering Maneuver

The amplitude is determined based on a pre-maneuver of RAMP steer, such that the vehicle reaches the lateral acceleration of $a_y = 4m/s^2$ during this maneuver. Moreover, the velocity is kept constant at 100 km/h. Different driving dynamics performance measures are evaluated based on this maneuver. For instance, the equivalent time delay $T_{eq,\dot{\psi}/\delta_H}$, computed as follows, represents the agility of a vehicle. The smaller its values, the more agile the vehicle is.

$$T_{eq,\dot{\psi}/\delta_H} = \frac{1}{2 \cdot \pi \cdot \text{freq}_{\dot{\psi}/\delta_H}(-45°)} \tag{2.50}$$

$\text{freq}_{\dot{\psi}/\delta_H}(-45°)$ stands for the frequency, at which the phase of the transfer function $\frac{\dot{\psi}}{\delta_H}$ reaches $-45°$.

Another example is the yaw velocity resonance gain H/H_0, figure 2.14.

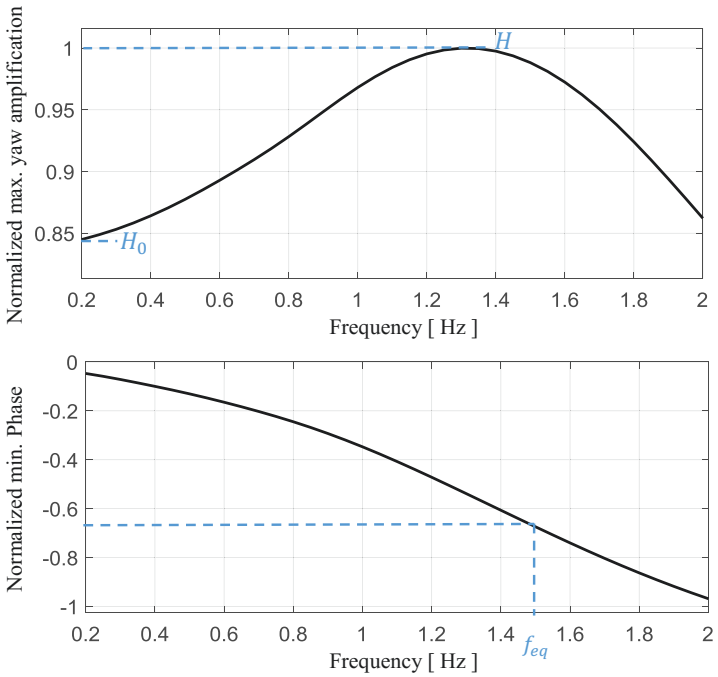

Figure 2.14: The CSST associated objective targets

It denotes the relation between the dynamic yaw amplification at the resonance H and the stationary yaw amplification H_0. The smaller the yaw velocity resonance gain is, the faster the dynamic yaw velocity is damped and the more sporty the vehicle is. All driving dynamics performance measures relevant to this maneuver are listed below:

Objective driving dynamics performance measures for CSST	
CV	**Description**
$T_{eq,\psi/\delta_H}$	Equivalent time delay at phase$(-45°)$
$(H/H_0)_{\dot{\psi}/\delta_H}$	Yaw velocity resonance gain
$T_{a_y/\dot{\psi}}$	Time difference from lateral acceleration to steering wheel angle at $f = 1Hz$

Table 2.7: Characteristic values for CSST

2.5 Simulation environment, Two-track model

The development and design of the control system and the actuators in this dissertation are carried out in a complete vehicle simulation environment. By using the simulink-based tool "ISAR" (Integrated simulation environment for vehicle dynamics with control systems)[38], the developed control systems and actuator models can be tested and evaluated in a simulation environment close to the real vehicle. This vehicle model is based on a non-linear two-track model implanted at BMW in MATLAB. By reducing simplifications of the STM model, i. e. increasing the degree of freedom, the model accuracy is increased. In contrast to the single-track model, the axles of the vehicle are taken into account, which results in the name of the two-track model. In addition, the center of gravity is assumed above the road surface. Effects such as changes in wheel loads, rolling, and pitching can be observed. This is particularly important when considering lateral dynamics, as the wheel load oscillation, due to the center of gravity height, has a significant influence on the driving behavior. The schematic of a two-track model is depicted in figure 2.16. This simulation tool also contains a driver, a traffic, a road model and enables the integration of any arbitrary control system, i.e. logic, actuator and sensor model. It is composed of non-linear characteristics obtained from a multi-body simulation in ADAMS and is able to simulate the vehicle dynamics at an adequate level. The magic formula is implemented in this model for the calculation of the tire dynamics [54]. Accordingly, the lateral forces acting on tyres can be calculated by the following linear equation

$$F_y = c_\alpha \cdot \alpha \tag{2.51}$$

Where α is the tyre slip angle, obtained from equations 2.20 and 2.21 and c_α is the cornering stiffness. However, the above-mentioned linear equation holds until a certain slip angle, as we can see from figure 2.15.

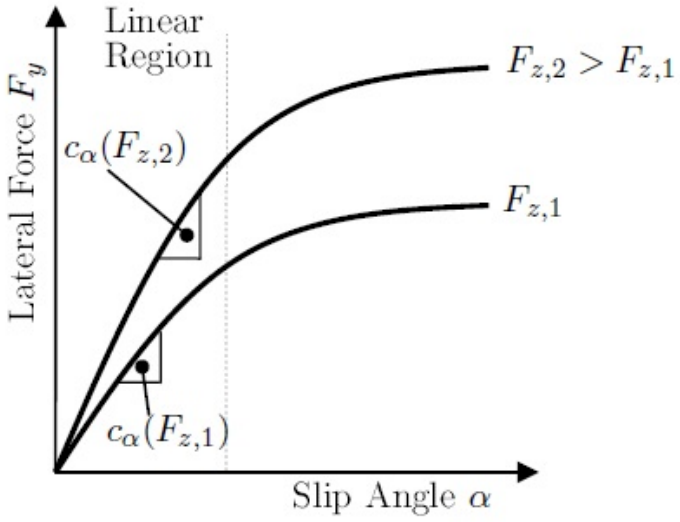

Figure 2.15: Tyre lateral forces and slip angles [66]

Moreover, the load (the force in direction of the z-axis) acting on a tyre can change the behavior of the tyre. In this manner, increasing the tyre load leads to the increase of the cornering stiffness. This fact is very important, because the lateral and longitudinal weight transfer is constantly happening during the ride due to the lateral and longitudinal accelerations.

All in all, it is also possible to evaluate the vehicle in the non-linear range.

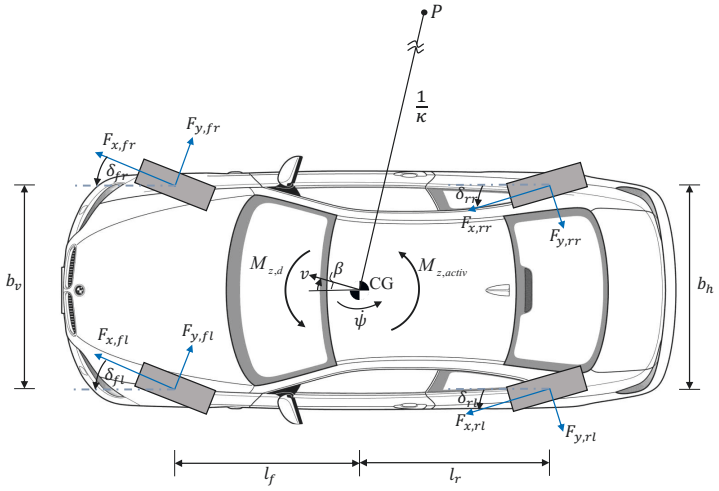

Figure 2.16: Schematic of the vehicle two-track model

Summary

In this chapter, the prerequisite knowledge about the lateral vehicle dynamics has been addressed. We have explained the single-track model with its two-degrees-of-freedom. It is a linearized model of the two-track model, which is the basis for the development of the lateral vehicle dynamics control system introduced in the next chapter. Moreover, the functionality of the active rear steering system (ARS) and one-sided brake intervention has been presented. The ARS enables the vehicle to move agile and stabilize it regarding velocity. However, the one-sided brake intervention proposed in this chapter may make the vehicle become more agile. The conversion factors have been proposed, which transform the yaw moment to the rear steering angle and the brake force. Finally, we have introduced the open-loop maneuvers with their objective driving dynamics performance measures. They are necessary for developing the chassis components by simulations and achieving desirable static and dynamic steering performances in terms of ride and safety. For the stationary cornering, we have introduced the QSSC, BRWC and WEAVE maneuvers. For the dynamic steering, the SWD and CSST maneuvers have been proposed and explained.

3 Lateral vehicle dynamics control systems

The lateral vehicle dynamics control system consists of different functions and is a centralized control system whose output is realized by different actuators assembled in a vehicle. Examples of such actuators are front and rear steering system, brake system and electronic differential lock. The structure of the proposed control system is demonstrated in figure 3.1 with the following units: feedforward control, disturbance feedforward control, driving situation identifier (DSI), feedback controller and priorization, summation and allocation unit. All these functions are concerned to change the yaw velocity regarding the desired vehicle dynamics response. In the following section, we describe how and for which aim each unit works.

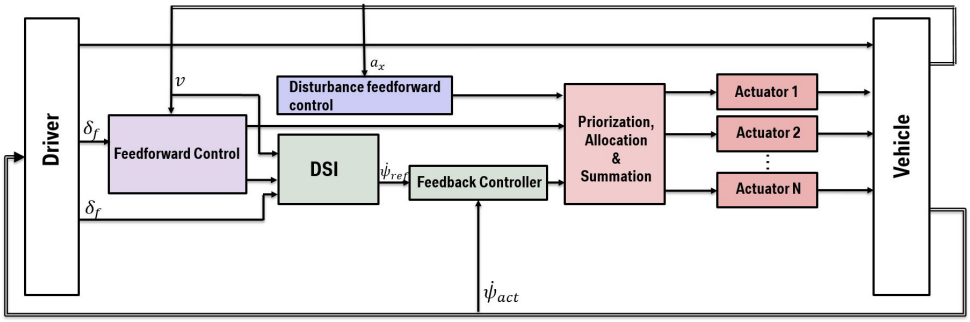

Figure 3.1: Structure of the proposed control system

3.1 Static feedforward control

As a static feedforward control is just a factor, it can be adjusted for each actuator specifically and separately with respect to the desired aim which has to be achieved by the performance of each actuator. The static feedforward control influences mainly the static driving performance measures during steady state cornering and is normally calculated from the front steering wheel angle δ_f, the input of a driver, and the vehicle v. As actuators concerned in this work

are the brake system and the rear steering system, we focus on the structure of the static feedforward control for these actuators.

Static feedforward control for active rear steering

As mentioned before, the rear steering system can enhance the stability as well as the agility of a vehicle. Several approaches have been examined based on different purposes in the last few years for adjusting a factor as static feedforward control associated with the rear steering system [51, 73, 21, 48, 16]. We use the idea in [73] and present a new characteristic curve in figure 3.2 with the following equation:

$$\delta_{r,stat} = f(v, \delta_f)\delta_{r,stat} = i_{ARS}(v) \cdot \delta_f \tag{3.1}$$

where i_{ARS} is a ratio dependent on the velocity of a vehicle.

As we can see from figure 3.2, the value of i_{ARS} is negative under the velocity v_{trans} which means, that the rear steering system turns rear wheels in opposite direction of front wheels, resulting in an increase in the yaw moment and consequently the yaw velocity. Accordingly, the vehicle becomes more agile while cornering and capable in terms of turning. The value of i_{ARS} can also be positive, if the velocity of a vehicle is more than v_{trans}.

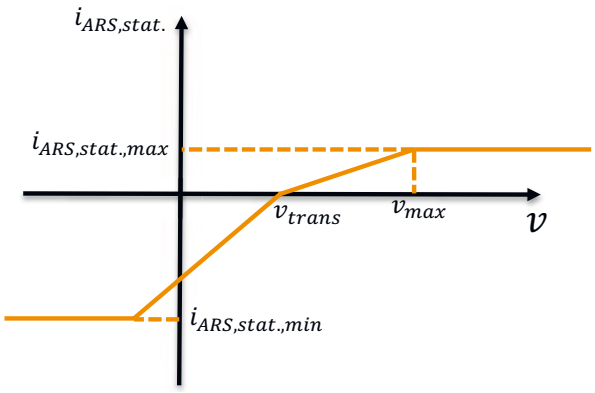

Figure 3.2: Characteristic curve of ARS static feedforward control

In this case, rear wheels are turned in the same direction of front wheels and this leads the vehicle to become more stable during cornering. This fact is depicted in figure 3.3, where it can be interpreted that the yaw velocity amplification (YVA) becomes more than the YVA of a vehicle without a lateral vehicle dynamics control (uncontrolled vehicle) for the velocity less than v_{trans},

i.e. the controlled vehicle is more agile. A reverse effect occurs by all velocities more than v_{trans}, when the controlled vehicle is more stable. This explanation can be illustrated in more details by considering equation 2.9. If the inputs to the vehicle are δ_f and δ_r, then equation 2.9 will be converted to the following form:

$$\begin{bmatrix} \dot{\beta} \\ \ddot{\psi} \end{bmatrix} = \underbrace{\begin{bmatrix} -\frac{c_r+c_f}{mv} & -1+\frac{c_r l_r - c_f l_f}{mv^2} \\ \frac{c_r l_r - c_f l_f}{J_z} & -\frac{c_r l_r^2 + c_f l_f^2}{J_z v} \end{bmatrix}}_{\mathbf{A}} \begin{bmatrix} \beta \\ \dot{\psi} \end{bmatrix} + \underbrace{\begin{bmatrix} \frac{c_f}{mv} & \frac{c_r}{mv} \\ \frac{c_f l_f}{J_z} & -\frac{c_r l_r}{J_z} \end{bmatrix}}_{\mathbf{B}} \begin{bmatrix} \delta_f \\ \delta_r \end{bmatrix} \tag{3.2}$$

Accordingly, the transfer function represented in equation 2.36 will be converted into:

$$\mathbf{G}(s) = (\mathbf{I}s - \mathbf{A})^{-1}\,\mathbf{B} \tag{3.3}$$

$$\begin{bmatrix} \beta \\ \dot{\psi} \end{bmatrix} = \begin{bmatrix} G_{\beta/\delta_f}(s) & G_{\beta/\delta_r}(s) \\ G_{\dot{\psi}/\delta_f}(s) & G_{\dot{\psi}/\delta_r}(s) \end{bmatrix} \begin{bmatrix} \delta_f \\ \delta_r \end{bmatrix} \tag{3.4}$$

Thus,

$$\dot{\psi}(s) = G_{\dot{\psi}/\delta_f}(s)\delta_f(s) + G_{\dot{\psi}/\delta_r}(s)\delta_r(s) \tag{3.5}$$

Where,

$$\begin{aligned} G_{\dot{\psi}/\delta_f}(s) &= \frac{b_{21}s + (a_{21}b_{11} - a_{11}b_{21})}{s^2 - (a_{11}+a_{22}) + (a_{11}a_{22} - a_{12}a_{21})} \\ G_{\dot{\psi}/\delta_r}(s) &= \frac{b_{22}s + (a_{21}b_{12} - a_{11}b_{22})}{s^2 - (a_{11}+a_{22}) + (a_{11}a_{22} - a_{12}a_{21})} \end{aligned} \tag{3.6}$$

with the following parameters:

$$\begin{aligned} a_{11} &= -\frac{c_r + c_f}{mv} & a_{12} &= -1 + \frac{c_r l_r - c_f l_f}{mv^2} \\ a_{21} &= \frac{c_r l_r - c_f l_f}{J_z} & a_{22} &= -\frac{c_r l_r^2 + c_f l_f^2}{J_z v} \\ b_{11} &= \frac{c_f}{mv} & b_{12} &= \frac{c_r l}{mv} \\ b_{21} &= \frac{c_f l_f}{J_z} & b_{22} &= -\frac{c_r l_r}{J_z} \end{aligned} \tag{3.7}$$

In the stationary cornering, $s = 0$, equation 3.5 is as follows:

$$\dot{\psi}_{stat} = (a_{21}b_{11} - a_{11}b_{21})\delta_{f,stat} + (a_{21}b_{12} - a_{11}b_{22})\delta_{r,stat} \tag{3.8}$$

By inserting equation 3.1 into equation 3.8:

$$\dot{\psi}_{stat} = (a_{21}b_{11} - a_{11}b_{21})\delta_{f,stat} + (a_{21}b_{12} - a_{11}b_{22})i_{ARS}(v)\delta_{f,stat} \tag{3.9}$$

Therefore,

$$\left(\frac{\dot{\psi}}{\delta_f}\right)_{stat} = (a_{21}b_{11} - a_{11}b_{21}) + (a_{21}b_{12} - a_{11}b_{22})i_{ARS}(v) \tag{3.10}$$

By inserting the parameters shown in equation 3.7 into the above-mentioned equation:

$$\left(\frac{\dot{\psi}}{\delta_f}\right)_{stat} = \frac{v}{l + \frac{m}{l}\left(\frac{l_r}{c_f} - \frac{l_f}{c_r}\right)v^2} - \frac{v}{l + \frac{m}{l}\left(\frac{l_r}{c_f} - \frac{l_f}{c_r}\right)v^2} \cdot i_{ARS}(v) \tag{3.11}$$

So,

$$\left(\frac{\dot{\psi}}{\delta_f}\right)_{stat} = \underbrace{\underbrace{\frac{v}{l + \frac{m}{l}\left(\frac{l_r}{c_f} - \frac{l_f}{c_r}\right)v^2}}_{YVA_{uncontr}}(1 - i_{ARS}(v))}_{YVA_{contr}} \tag{3.12}$$

From equation 3.12, it can be concluded, that the stationary yaw velocity amplification of a vehicle controlled only by the static feedforward control of the active rear steering system is the multiplication of the stationary YVA of the uncontrolled vehicle with the term $(1 - i_{ARS}(v))$.

By looking again at figure 3.3, we can see, that at $v = 0$ the stationary YVA of the unctrolled vehicle is equal zero, i.e. $YVA_{uncontr} = 0$. Therefore, $YVA_{contr} = 0$. The difference of YVA_{contr} at the velocities below v_{trans} is not significant, because either $YVA_{uncontr}$ or the term $(1 - i_{ARS}(v))$ is small. However, at the high velocities, the drop of YVA_{contr} compared to $YVA_{uncontr}$ is significant, because $YVA_{uncontr}$ is large and the term $(1 - i_{ARS}(v))$ becomes small.

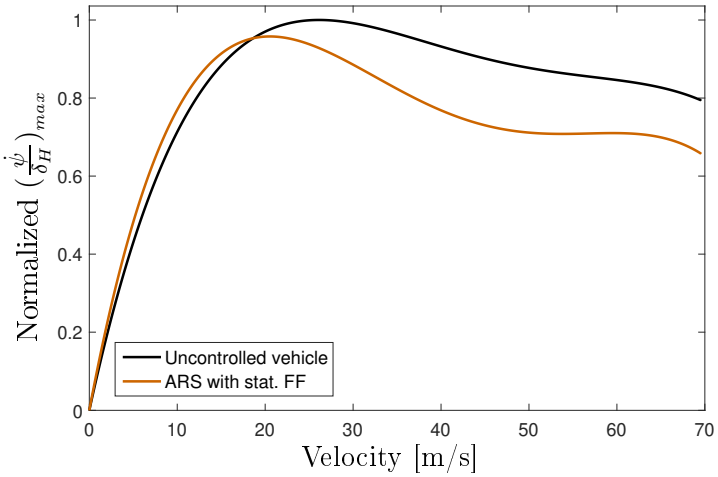

Figure 3.3: Stationary yaw velocity amplification of the uncontrolled and controlled vehicle with only ARS static feedforward control

Furthermore, figure 3.5 indicates that for reaching a certain lateral acceleration under the above-mentioned transient velocity, less self-steering is demanded and vice versa.

Static feedforward control for brake system

Although many researches have been done in the last few decades for designing single-sided braking by the brake system to stabilize the vehicle in critical situations, we use the brake system in this dissertation through single-sided braking just to make the vehicle agile. Because we assume, that vehicles are equipped with DSC, which stabilizes them in critical situations. Therefore, the goal is to reduce the self-steering demand at large lateral acceleration and increase the maximum lateral acceleration in steady state cornering. Thus, we would like to design a characteristic curve which generates brake moment based on the consideration of the lateral acceleration. The real lateral acceleration can be measured directly in a vehicle, after the driver has taken an action and has entered the wheel steering angle. In other words, the measured lateral acceleration is the output of our system. But as we know, the task of a feedforward control is to regulate the vehicle, before the driver input gets into the vehicle. Therefore, we must not use the actual real lateral acceleration as the input of the static feedforward control. Instead, it is beneficial to determine an imaginary lateral acceleration, computed by the drivers's commando, δ_f, v_x. This imaginary lateral acceleration is called Ackermann acceleration and an approximation of the

real static lateral acceleration during cornering.

The Ackermann acceleration is given in the following equation:

$$a_{y,ack} = \frac{v_x^2 \cdot \delta_{eff}}{l(1 + (\frac{v_x}{v_{ch}})^2)} \tag{3.13}$$

where δ_{eff} stands for the effective steering wheel angle computed by the following equation:

$$\delta_{eff} = \frac{\delta_{fl} + \delta_{fr}}{2} - \delta_{r,stat} \tag{3.14}$$

where δ_{fl} and δ_{fr} represent the front steering wheel angle on the left and right side. $\delta_{r,stat}$ stands for the stationary feedforward controlled input of the rear steering system.

Figure 3.4 is the proposed characteristic curve of the brake system static feedforward control for the computation of the brake moment. A brake moment is extracted in real-time from this characteristic curve based on the computed Ackermann acceleration. On the characteristic curve, it is to be recognized that no brake moment is defined below a certain Ackermann acceleration, for instance $a_{y,ack} = 5m/s^2$. In addition, a weighting factor will be defined with respect to the velocity, which will be multiplied with the extracted brake moment. This weighting factor, shown in figure 3.4, prevents the brake system from intervening at low and high velocities. Otherwise, there is high wastage in the brake system.

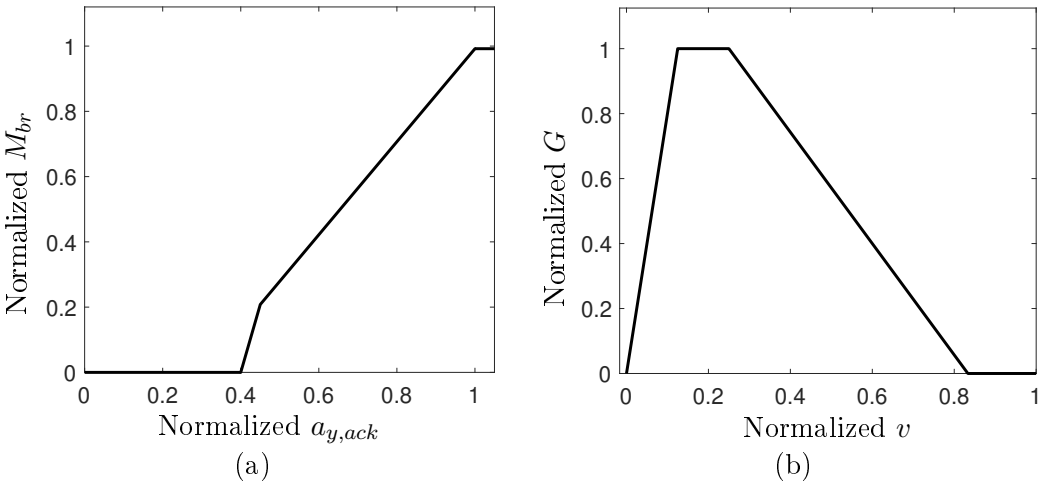

Figure 3.4: Characteristic curves of the brake system static feedforward control: (a): the characteristic curve for the extraction of brake moment regarding Ackermann acceleration, (b): The characteristic curve for the extraction of the weighting factor regarding the velocity

Another important point is the sign of the computed braking moment, which is an index, on which wheel the braking moment should be implemented. Since the brake system is used here to make the vehicle agile, the sign of the brake moment is computed from the sign of the ackermann acceleration and will be multiplied with the calculated brake moment; hence, the generated static brake moment, sent to the brake system, is calculated as following:

$$M_{br,stat} = Sgn(a_{y,ack}) \cdot M_{br}(a_{y,ack}) \cdot G(v) \tag{3.15}$$

Figure 3.5 shows an example of how the static feedforward control of the one sided-brake system changes the self-steering of a vehicle. The controlled vehicle with ARS and BS static feedforward control can tolerate more lateral acceleration in comparison with the uncontrolled vehicle or controlled one by just rear static feedforward control. In addition, for a determined acceleration, the steering demand of a controlled vehicle with BS and ARS is less than the controlled one by just ARS, which also indicates more agility while cornering.

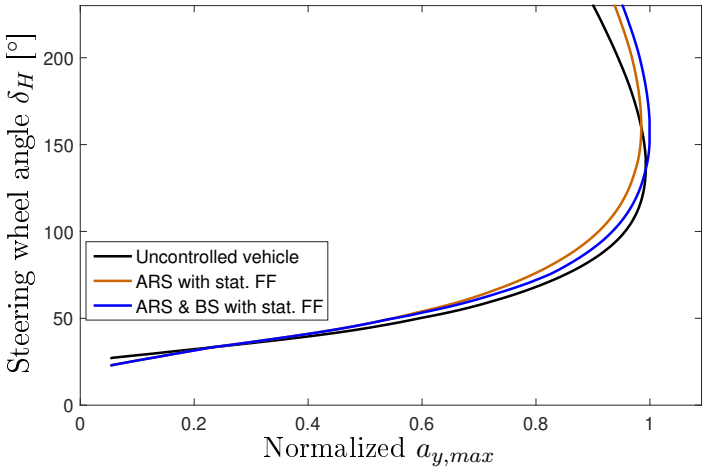

Figure 3.5: The comparison between the self-steering demand of the uncontrolled vehicle (black line), the controlled vehicle with only ARS static feedforward control (orange line) and the controlled vehicle with ARS and BS static feedforward control (blue line)

3.2 Centralized dynamic feedforward control

While the static feedforward control is designed for each actuator specifically, the dynamic feedforward control is a global model-based function and independent from available actuators. In other words, the output of the dynamic feedforward control is a yaw moment which can be implemented by any actuator assembled in a vehicle. In this case, the generated yaw moment must be converted to the relevant signal for each actuator. This topic will be explained in the section of "Prioritization and summation".

By the use of such a dynamic feedforward control, the dynamic response of a vehicle with respect to the driver inputs can be influenced. The effects of a dynamic feedforward control are dependent on how this feedforward control is designed and tuned. In this section, we introduce a new approach for developing a centralised dynamic feedforward control to influence the lateral dynamics of a vehicle. As our target is to manipulate the lateral vehicle dynamics by this feedforward control, the longitudinal dynamics will not be considered. It means, we use equation 2.9. The yaw moment generated by the feedforward control is concerned as $M_{z,ff}$. It should be noticed, that in this case, the inputs into the vehicle, i.e. system, are the wheel steering angle δ_f caused by the act of a driver and the yaw moment, generated by the dynamic feedforward control.

Accordingly, the state space model is:

$$\begin{bmatrix}\dot{\beta}\\ \ddot{\psi}\end{bmatrix} = \underbrace{\begin{bmatrix}a_{11} & a_{12}\\ a_{21} & a_{22}\end{bmatrix}}_{\mathbf{A}} \begin{bmatrix}\beta\\ \dot{\psi}\end{bmatrix} + \underbrace{\begin{bmatrix}b_{11} & b_{22}\\ b_{21} & b_{22}\end{bmatrix}}_{\mathbf{B}} \begin{bmatrix}\delta_f\\ M_{z,ff}\end{bmatrix} \tag{3.16}$$

where

$$\begin{aligned} a_{11} &= -\frac{c_r + c_f}{mv} & a_{12} &= -1 + \frac{c_r l_r - c_f l_f}{mv^2}\\ a_{21} &= \frac{c_r l_r - c_f l_f}{J_z} & a_{22} &= -\frac{c_r l_r^2 + c_f l_f^2}{J_z v}\\ b_{11} &= \frac{c_f}{mv} & b_{12} &= 0\\ b_{21} &= \frac{c_f l_f}{J_z} & b_{22} &= -\frac{1}{J_z} \end{aligned} \tag{3.17}$$

This state space model can be reformulated based on equation 3.18, where $\mathbf{C}$ is a unit matrix. Accordingly, the transfer function of the above-mentioned state space model in the Laplace domain is as follow:

$$\mathbf{G(s)} = \mathbf{C}(s\mathbf{I} - \mathbf{A})^{-1}\mathbf{B} + \mathbf{D} \tag{3.18}$$

$$\begin{bmatrix}\beta(s)\\ \dot{\psi}(s)\end{bmatrix} = \begin{bmatrix}G_{11}(s) & G_{12}(s)\\ G_{21}(s) & G_{22}(s)\end{bmatrix} \begin{bmatrix}\delta_f(s)\\ M_{z,ff}(s)\end{bmatrix} \tag{3.19}$$

The objective is here to change the transient behavior of the vehicle yaw velocity. The dynamic feedforward control is then designed for the following transfer function:

$$\dot{\psi}(s) = G_{21}(s)\delta_f(s) + G_{22}(s)M_{z,ff}(s) \tag{3.20}$$

As already represented in figure 2.4, the damping ratio and the eigenfrequency of a vehicle decreases very fast by increasing the vehicle velocity, while the time constant increases. The dynamic feedforward control should be tuned so that this fact will be compensated.

As explained earlier, the feedforward control is composed of the static feedforward control of the rear steering system ($\delta_{r,stat}$), the static feedforward forward control of the brake system ($M_{br,stat}$), and the dynamic feedforward control. Consequently,

$$M_{z,ff} = M_{z,stat} + M_{z,dyn} \tag{3.21}$$

where, $M_{z,stat}$ is the summation of the static yaw moments generated by the act of the ARS and BS static feedforward control.

$$M_{z,stat} = M_{b,stat} \cdot \Delta M_{br \rightarrow M_z} + \delta_{r,stat} \cdot \delta_{r \rightarrow M_z} \tag{3.22}$$

As we know, each static feedforward control is a function of the front wheel steering angle (δ_f). Therefore, we define a static factor here, which relates the static yaw moment ($M_{z,stat}$) to the front wheel steering angle (δ_f):

$$i_{Mz,ff} = \frac{M_{z,stat}}{\delta_f} \tag{3.23}$$

$M_{z,dyn}$ is defined as follows:

$$M_{z,dyn}(s) = G_{dyn}(s) \cdot \delta_f(s) \tag{3.24}$$

Inserting Equations 3.23 and 3.24 in Equation 3.21, we obtain:

$$M_{z,ff}(s) = i_{Mz,ff} \cdot \delta_f(s) + G_{dyn}(s) \cdot \delta_f(s) \tag{3.25}$$

Placing Equation 3.25 into Equation 3.20 results in:

$$\frac{\dot{\psi}}{\delta_f}(s) = G_{21}(s) + G_{22}(s) i_{Mz,ff} + G_{22}(s) G_{dyn}(s) \tag{3.26}$$

The above-mentioned equation represents how the yaw velocity responds to the front wheel steering angle and the feedforward control. Now, we would like to design G_{dyn} in equation 3.26, such that the yaw velocity achieves a desired response to the act of driver, δ_f. Therefore, we first formulate a desired transfer function from the front wheel steering angle to the yaw velocity as follows:

$$G_{des}(s) = \left(\frac{\dot{\psi}}{\delta_f}(s) \right)_{desired} = ST \cdot \frac{1 + T_{z,des} s}{1 + \frac{2D_{des}}{\omega_{des}} s + \frac{1}{\omega_{des}^2} s^2} \tag{3.27}$$

Where, ST is the static term, $T_{z,des}$ is the desired time constant, D_{des} is the desired damping ration, and ω_{des} is the desired eigenfrequency of the desired transfer function G_{des}. Setting equation 3.26 equal to equation 3.27 results in:

$$G_{dyn} = \frac{G_{des} - G_{21}}{G_{22}} - i_{M_{z,ff}} \tag{3.28}$$

As we see from the above-mentioned equation, G_{dyn} is developed by designing G_{des}, i.e. ST, $T_{z,des}$, D_{des}, and ω_{des}.

As we explained earlier, our goal by developing G_{dyn} is only to change the transient behavior of the vehicle yaw velocity, i.e. $G_{dyn}(s=0)=0$. Thus,

$$G_{dyn}(s=0)=\frac{G_{des}(s=0)-G_{21}(s=0)}{G_{22}(s=0)}-i_{M_{z,ff}}=0 \tag{3.29}$$

$$G_{des}(s=0)=G_{21}(s=0)+G_{22}(s=0)i_{Mz,ff} \tag{3.30}$$

From equation 3.27, $G_{des}(s=0)=ST$. So,

$$ST=G_{21}(s=0)+G_{22}(s=0)i_{Mz,ff} \tag{3.31}$$

Considering equations 3.16, 3.17, and 3.19,

$$ST=\frac{a_{21}b_{11}-a_{11}b_{21}}{-a_{12}a_{21}+a_{11}a_{22}}+\frac{a_{22}b_{12}-a_{11}b_{22}}{-a_{12}a_{21}+a_{11}a_{22}}\cdot i_{M_{z,ff}} \tag{3.32}$$

Another goal to be achieved by designing G_{dyn} is to compensate the decrease of the damping ratio and the eigenfrequency of a vehicle by increasing the vehicle velocity and to manipulate the time constant of the vehicle. Accordingly, we define $T_{z,des}$, D_{des}, and ω_{des} as follows:

$$\begin{aligned} T_{z,des}&=T_z\cdot T_f s\\ D_{des}&=D\cdot D_f\\ \omega_{des}&=\omega_0\cdot\omega_f \end{aligned} \tag{3.33}$$

Where, T_z, D and ω_0 are the time constant, the damping ratio, and the natural frequency of a vehicle, computed by equation 2.38. T_f, D_f and ω_f are tuning parameters. With tuning these parameters, we change the response of the vehicle to the wheel steering angle and can determine the desired transfer function.

For example, figure 3.6 shows how the dynamic feedforward control with the tuning parameters $w_f=1$, $T_f=1$ and $D_f=1.1$ affects the driving performance of the vehicle by executing the CSST maneuver. The maximum of yaw velocity resonance gain $\left(RES_{\frac{\dot{\psi}}{\delta_H}}\right)$ becomes less, which means that the vehicle response to such a dynamic input will be damped. In addition, the equivalent time delay $\left(T_{eq,\frac{\dot{\psi}}{\delta_H}}\right)$ also becomes less. It means, the vehicle responds to the input of a driver faster and with less delay.

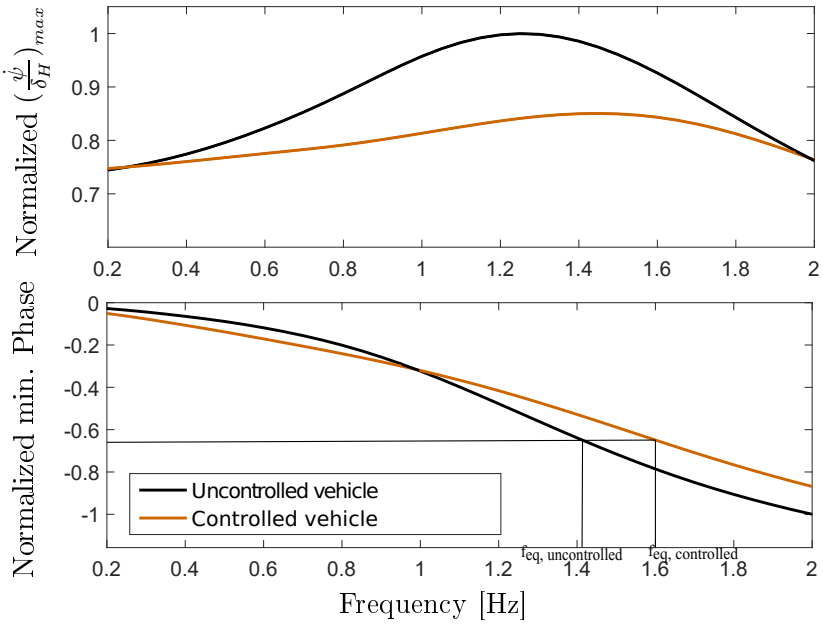

Figure 3.6: The bode diagram of the vehicle dynamics with respect to the CSST maneuver

In addition, the dynamic feedforward control enhances the stability of the vehicle by dynamic maneuvers such as SWD. Figure 3.7 shows how the dynamic feedforward control damps the side slip angle of the vehicle, indicating the stability improvement of the vehicle.

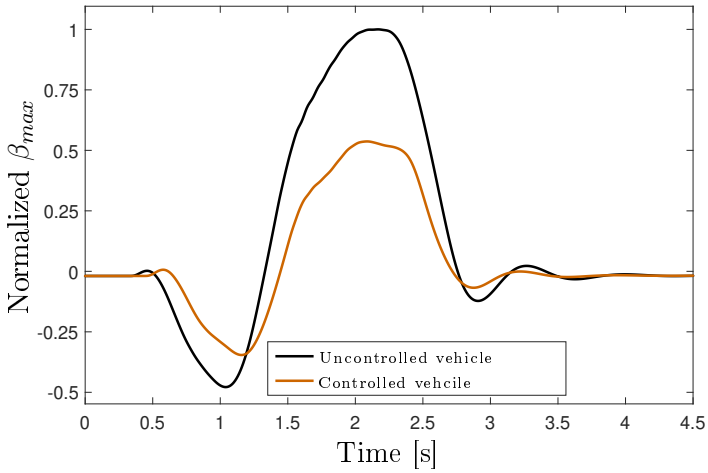

Figure 3.7: The side slip angle response of the vehicle to the SWD maneuver

3.3 Centralized disturbance feedforward control

Different kinds of disturbances affect the vehicle dynamics. Only very few ones can be compensated. For the vehicle lateral dynamics, the effect of the longitudinal dynamics is concerned as disturbance. Due to braking or acceleration during cornering, wheel load changes between front and rear axle. Consequently, the self-steering behavior changes. This change has to be compensated by a driver in the linear domain of the vehicle. For example, during accelerated cornering, more vehicle weight is braced on the rear axle, while the vehicle weight on the front axle decreases. As a result, the vehicle becomes more understeering. The driver must steer the steering wheel more in order to stay on the curve with the same radius. Such an effect should be reduced by means of decoupling the longitudinal dynamics from the lateral dynamics. The design of a proper function for compensating such an effect is unfolded in [52] explicitly. As a consequence, we do not explain the design of this function again. Rather, we describe its functionality.

In order to determine the required yaw moment which compensates this effect, the simple single-track model, i.e. equation 2.9 is compared with the single-track model in equation 2.6 with consideration of the available longitudinal acceleration a_x, shown in figure 3.8. Accordingly, if the sign of the calculated yaw moment ($M_{z,dff}$) is positive, the vehicle drives under drive. In the other way around, the vehicle drives under train, when the sign of $M_{z,dff}$ is negative. This yaw moment will be added to the feedforward control total term before

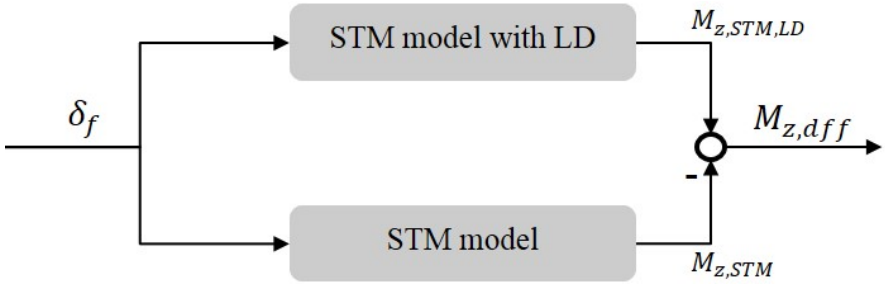

Figure 3.8: The schematic of the generated yaw moment by the disturbance feedforward control

getting in an associated actuator.

The influence of the disturbance feedforward control can be seen in figure 3.9. The plot shows the yaw velocity response of the vehicle with and without disturbance feedforward control, during brake while cornering (BRWC) maneuver. The difference yaw velocity at t=1s is less for the controlled vehicle. In other words, the controlled vehicle stays better on its trajectory while BRWC.

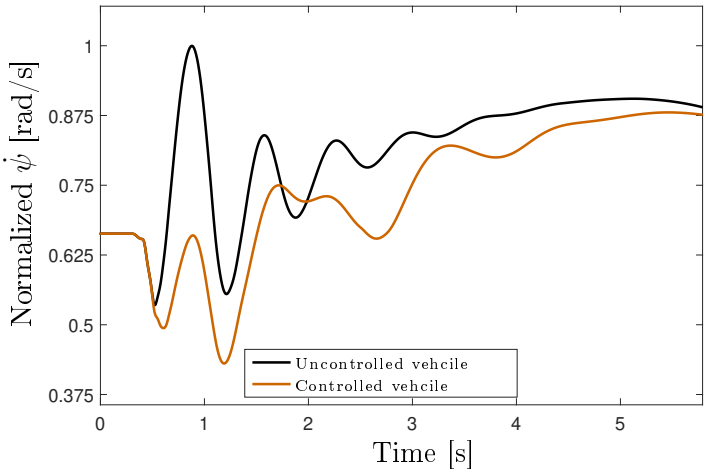

Figure 3.9: The yaw velocity response during the BRWC maneuver: black line stands for the uncontrolled vehicle and the orange one stands for the controlled vehicle by the disturbance feedforward control

3.4 Reference input generator and driving situation identifier

The reference input generator produces a reference yaw velocity for the feedback controller. It obtains an input from the driving observer, which estimates the driving situation. Based on the estimated driving situation, a reference yaw velocity will be calculated.

In this section, we clarify how this reference yaw velocity will be generated and the driving situation will be estimated. For this purpose, the single-track model defined in equation 3.16 with the variables in equation 3.17 is applied. It has to be noticed, that the inputs of this model are the wheel steering angle entered by a driver, the vehicle velocity, and the feedforward control terms in form of a yaw moment, generated by the static and dynamic feedforward controls.

As we know, the behavior of a single-track model is similar to the behavior of a real vehicle during cornering until the lateral acceleration of 4 m/s^2. After this lateral acceleration, there is a deviation between these two behaviors which is due to the non-linear behavior of tires [32].

From the vehicle kinematics, a relationship between the lateral acceleration, the yaw velocity and the side slip angle velocity is defined as follows:

$$\begin{aligned} a_y &= v(\dot{\beta} + \dot{\psi}) \\ \dot{\psi} &= \frac{a_y}{v} - \dot{\beta} \end{aligned} \tag{3.34}$$

This relationship holds also in the non-linear area of tires.

In order to estimate the driving situation, a new variable is defined, namely lateral acceleration yaw velocity ($\dot{\psi}_{a_y}$). This acceleration is calculated from the actual lateral acceleration of the vehicle ($a_{y,act}$) and the side slip angle velocity computed from the single-track model, i.e. $\dot{\beta}_{STM}$.

$$\dot{\psi}_{a_y} := \frac{a_{y,act}}{v} - \dot{\beta}_{STM} \tag{3.35}$$

The actual lateral acceleration refers to the vehicle center of gravity. As a consequence, the effect of rolling during cornering should be considered for computing the actual lateral acceleration. Accordingly,

$$a_{y,act} = a_{y,act,measured} - \phi \cdot g \tag{3.36}$$

where, $a_{y,act,measured}$ is the measured actual lateral acceleration of a vehicle, ϕ represents the roll angle during cornering and g expresses the gravitational

constant.

Accordingly, we are dealing with three different yaw velocities, such as the single-track model yaw velocity $\dot{\psi}_{STM}$ computed from equation 2.9, lateral acceleration yaw velocity $\dot{\psi}_{a_y}$ obtained from Equation 3.35, and the actual yaw velocity $\dot{\psi}_{act}$ measured from the vehicle. $\dot{\psi}_{act}$ can also be rewritten as follows:

$$\dot{\psi}_{act} = \frac{a_{y,act}}{v} - \dot{\beta}_{act} \tag{3.37}$$

The single-track model yaw velocity $\dot{\psi}_{STM}$ has to be bounded by the maximal tolerable of the lateral acceleration of a vehicle which is limited by the roadway friction coefficient [11]. It means, the front wheel steering angle will be bounded as follows and will be inserted in Equation 3.16.

$$|\delta_f| \leq |\delta_{f,max}| \tag{3.38}$$

where,

$$|\delta_{f,max}| = \frac{l \cdot |a_{y,max}|}{v^2} \left(1 + \left(\frac{v}{v_{ch}}\right)^2\right) \tag{3.39}$$

Driving Situations

The idea how to recognize the driving situations is obtained from [74]. Three common driving situations which occur during the explained maneuvers in the section 4.3 can be then classified as follows:

- **Linear:** $\dot{\psi}_{a_y}$, $\dot{\psi}_{STM}$ and $\dot{\psi}_{act}$ have the same sign, and the absolute value of $\dot{\psi}_{act}$ is almost equal to the value of $\dot{\psi}_{a_y}$.

  $$sgn(\dot{\psi}_{a_y}) = sgn(\dot{\psi}_{STM}) = sgn(\dot{\psi}_{act}) \quad and \quad \left|\dot{\psi}_{act}\right| \approx \left|\dot{\psi}_{a_y}\right|$$

  In this situation, the real vehicle behaves like the single-track model. This state holds until the lateral acceleration of $4\frac{\mathrm{m}}{\mathrm{s}^2}$.

- **Oversteer:** $\dot{\psi}_{a_y}$, $\dot{\psi}_{STM}$ and $\dot{\psi}_{act}$ have the same sign, and the absolute value of $\dot{\psi}_{act}$ differs from the absolute value of $\dot{\psi}_{a_y}$ significantly.

  $$sgn(\dot{\psi}_{a_y}) = sgn(\dot{\psi}_{STM}) = sgn(\dot{\psi}_{act}) \quad and \quad \left|\dot{\psi}_{act}\right| \gg \left|\dot{\psi}_{a_y}\right|$$

  In this situation, the side slip angle of the vehicle is increasing and the vehicle is about to become instable due to the fact that the rear tires are about to reach the marginal condition.

- **Counter-steer:** $\dot{\psi}_{a_y}$ and $\dot{\psi}_{act.}$ have the same sign differing from the sign of $\dot{\psi}_{STM}$.

$$sgn(\dot{\psi}_{a_y}) = sgn(\dot{\psi}_{act.}) \neq sgn(\dot{\psi}_{STM})$$

  In this situation, the vehicle does not track the driver's command. Such a situation happens due to an abrupt change of the direction while cornering or rash steering while the vehicle is swinging off.

Based on the above-mentioned situations, we define different reference yaw velocities whose deviation from the vehicle actual yaw velocity has to be regulated by the feedback controller.

In the **linear** domain, the vehicle drives stable. The improvement of the vehicle agility is desirable. As a consequence, the reference yaw velocity is defined as the single-track model yaw velocity ($\dot{\psi}_{STM}$). But, it should be mentioned that this improvement of agility is very small, because in the linear domain, the actual vehicle yaw velocity is almost equal to the single-track model yaw velocity.

$$\dot{\psi}_{ref} = \dot{\psi}_{STM}$$

$$e_{\dot{\psi}} = \dot{\psi}_{STM} - \dot{\psi}_{act}$$

In the **oversteer** domain, the vehicle is about to become unstable and the tires are about to reach the non-linear marginal condition. The vehicle is building up a large side slip angle β. Consequently, β has to be controlled by the feedback controller. As the side slip angle is a state variable but not measurable in a vehicle, we control its velocity $\dot{\beta}$. In this case:

$$\dot{\psi}_{ref} = \dot{\psi}_{a_y}$$

Accordingly,

$$e_{\dot{\psi}} = \dot{\psi}_{a_y} - \dot{\psi}_{act} = \dot{\beta}_{act} - \dot{\beta}_{STM}$$

It means, the controlled variable is the side slip angle velocity of the vehicle, when the reference yaw velocity is the lateral acceleration yaw velocity ($\dot{\psi}_{a_y}$). As long as the error between these two side slip angle velocities is less than a defined upper bound, the vehicle is stil in linear domain. This upper bound is a tuning parameter:

$$\left|\dot{\beta}_{act} - \dot{\beta}_{STM}\right| < \Delta\dot{\beta}_{max}$$

In this dissertation, we empirically set $\Delta\dot{\beta}_{max} = 0.06$.

In the **Counter-steer** domain, the vehicle must be stabilized as fast as possible. In other words, it is desirable to bring the vehicle into a straight ahead line again. Therefore:

$$\dot{\psi}_{ref} = 0 \tag{3.40}$$

To sum up,

$$\dot{\psi}_{ref} = \begin{cases} \dot{\psi}_{STM} & For\ \ linear\ \ domain \\ \dot{\psi}_{a_y} & For\ \ oversteer\ \ domain \\ 0 & For\ \ Counter-steer \end{cases}$$

The point to be considered is that the vehicle yaw velocity responds very fast to a steering wheel stimulation. As a result, the reference yaw velocity can change abruptly regarding driving situations. In order to avoid a rapid change between the reference yaw velocities, we introduce the following equation for the calculation of $\dot{\psi}_{ref}$:

$$\dot{\psi}_{ref} = \dot{\psi}_{STM}(1 - K_{os})(1 - K_{cs}) + K_{os}(1 - K_{cs})\dot{\psi}_{min} \tag{3.41}$$

where,

$$\dot{\psi}_{min} = min(|\dot{\psi}_{STM}|, |\dot{\psi}_{a_y}|) \cdot (sgn(\dot{\psi}_{STM}) + sgn(\dot{\psi}_{a_y}))/2 \tag{3.42}$$

K_{os} and K_{cs} are indicators of the oversteer and counter-steer driving situations, respectively. As soon as the counter-steer situation is detected ($sgn(\dot{\psi}_{a_y}) = sgn(\dot{\psi}_{act}) \neq sgn(\dot{\psi}_{STM})$), K_{cs} is raised to 1. However, recognizing the oversteer situation is slightly more complex than the counter-steer one. As long as $sgn(\dot{\psi}_{a_y}) = sgn(\dot{\psi}_{STM}) = sgn(\dot{\psi}_{act})$ remains the same, we have to look at the deviation value between the side slip angle velocities of the single-track model and the real vehicle, shown in equation 3.43, and the sign of the lateral acceleration ($a_{y,act}$).

$$\Delta\dot{\beta} = \dot{\beta}_{act} - \dot{\beta}_{STM} \tag{3.43}$$

Accordingly,

$$K_{os} = \begin{cases} 1 & \Delta\dot{\beta} \cdot sgn(a_{y,act}) \geq \Delta\dot{\beta}_{max} \\ 0 & \Delta\dot{\beta} \cdot sgn(a_{y,act}) < 0 \end{cases}$$

Once $\Delta\dot{\beta} \cdot sgn(a_{y,act}) \geq \dot{\beta}_{max}$, the indicator K_{os} is set to 1. Once the vehicle

gets to this situation, K_{os} is not set to 0, until the $\Delta\dot{\beta}$ becomes less than 0.

A typical course of $\Delta\dot{\beta}$ and calculation of K_{os} is shown in figure 3.10.

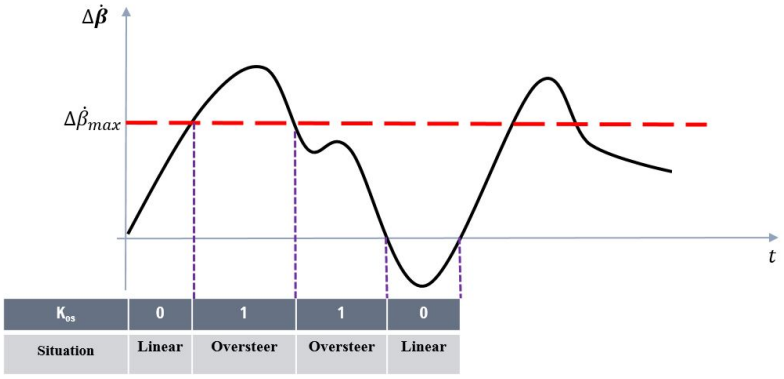

Figure 3.10: An example of the calculation of the oversteer indicator K_{os}

All these procedures will be carried out in a so-called Driving Situation Identifier (DSI) unit. In this unit, the reference yaw velocity is also computed. Figure 3.11 represents which inputs and outputs get inside and outside of the DSI.

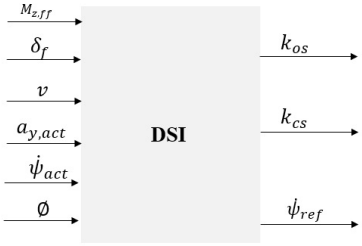

Figure 3.11: Driving Situations Identifier (DSI) unit

3.5 Centralized feedback controller

In addition to the static and dynamic feedfoward control and the disturbance feedfoward control, we develop a centralized feedback controller in this section. The feedback controller has the following tasks [74]:

- Damping the yaw velocity dynamics.

- Optimization of the vehicle handling properties.
- reduction of the vehicle side slip angle velocity build-up.

Damping the yaw velocity dynamics means that if the yaw velocity is excited to oscillate, the feedback controller has to attenuate the oscillation. Moreover, the controller should assist the driver to have a better handling in the linear domain of the vehicle dynamics. If a vehicle is about to build up a large side slip angle which makes the vehicle over-steer and uncontrollable for a normal driver, the controller has to control the side slip angle and reduce it before the vehicle swings off. With respect to all these requirements, it does not make sense to just control the yaw angle velocity dynamics. Because, such a controller can destabilize a vehicle, since it does not then consider the side slip angle of the vehicle. This in turn causes a vehicle to spin in critical situations. However, the side slip angle is not measurable in a vehicle during the ride. Rather, the side slip angle velocity can be measured based on the kinematics of the vehicle. As a consequence, we consider this fact and try to design a controller to control both the yaw angle velocity and the side slip angle velocity.

Accordingly, a reference yaw velocity will be defined whose deviation from the actual yaw velocity in the vehicle will be controlled as follows:

$$e_{\psi} = \dot{\psi}_{ref} - \dot{\psi}_{act} \tag{3.44}$$

Where ψ_{ref} and ψ_{act} stand for the reference yaw velocity and the actual yaw velocity, respectively.

A candidate feedback controller can be a trivial PID-controller. However, the integral term (I-term) is not necessary to be applied. Because, the I-term is responsible for regulating the stationary accuracy of the closed-loop system. But, the main vehicle states, such as oversteer and counter-steer, controlled by this feedback controller are non-stationary. Moreover, the I-term brings a phase shift of $-\pi/2$ into the closed-loop. But in such vehicle states, such a phase shift in the controlled input makes the driver confused. The driver is also a controller of the vehicle. In such non-stationary states, he also tries to regulate the vehicle. A phase shift in the controlled input brings a phase shifted intervention and makes the driver nervous and confused by controlling the vehicle. The D-term can be neglected, as the designed dynamic feedforward control takes over the task of improving the dynamic response of the vehicle yaw angle velocity; hence, the proposed feedback controller in this dissertation has only the proportional term. (K_p) should be large enough in order to make the feedback controller react quickly to the error. The output of the controller is a yaw moment, shown in figure 3.12, which will be then added to the feedforward

control terms and sent to the actuators.

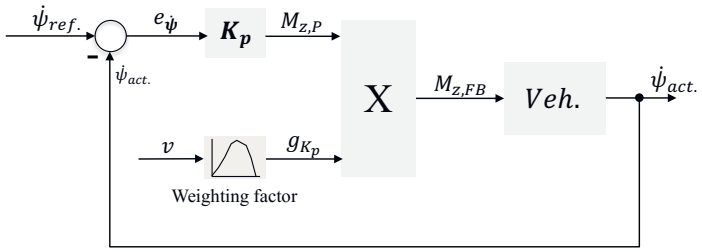

Figure 3.12: Feedback controller

The reference yaw velocity changes during a ride based on the identified situations of the vehicle by the DSI. This fact makes the closed-loop system non-linear. Therefore, the whole transfer function of the closed-loop system, vehicle, and controller including actuators, cannot be defined straightforward. Additionally, the controller proportional term cannot stay constant while the velocity changes, because the agility and specifically stability of a vehicle depends on the vehicle velocity. Subsequently, the controller proportional term must be weighted by the change of the velocity, illustrated in figure 3.12. As a consequence,

$$M_{z,FB} = f(v, e_{\dot{\psi}}) = K_p \cdot e_{\dot{\psi}} \cdot g_{K_p}(v) \tag{3.45}$$

wheres g_{K_p} is a weighting factor, depending on the velocity. Since too large K_p makes a vehicle unstable at high and low velocities, the weighting factor should reduce the proportional gain significantly at these velocities. Figure 3.13 is, hence, used as characteristic curve for this weighting factor in this dissertation.

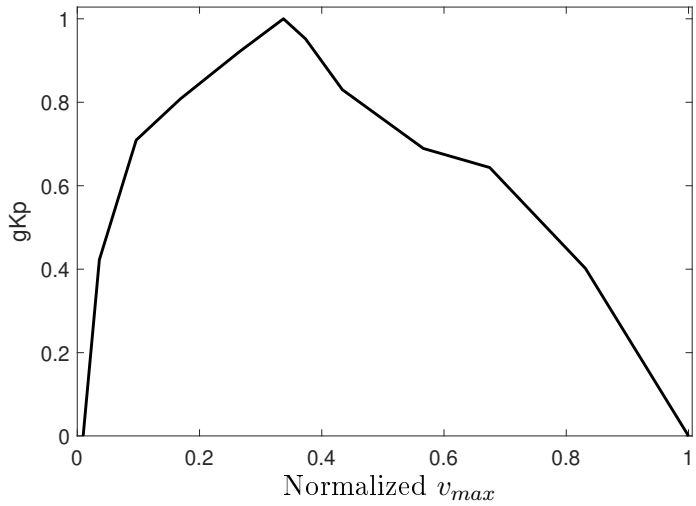

Figure 3.13: The proposed characteristic curve as the weighting factor of the controller propotional term

We reveal the impact of the feedback controller by means of an example. Figure 3.14 depicts the simulation results of the SWD maneuver. The simulation is executed one time for $SAF = 4.5$ and one time for $SAF = 5$. By the simulation with $SAF = 4.5$, it can be seen that the yaw angle velocity and the side slip angle amplitude of the controlled vehicle (blue line) are more damped and less than those of the uncontrolled vehicle (black line). By the simulation with $SAF = 5$, the uncontrolled vehicle (orange line) becomes completely unstable. However, the driving situation identifier (DSI) predicts this behavior during the execution of this maneuver, sets the reference yaw velocity to $\dot{\psi}_{a_y}$ and attempts to prevent the vehicle to build-up side slip angle. As a consequence, the controlled vehicle stays stable during this maneuver, which is to be seen in Figure 3.14(b) (purple line).

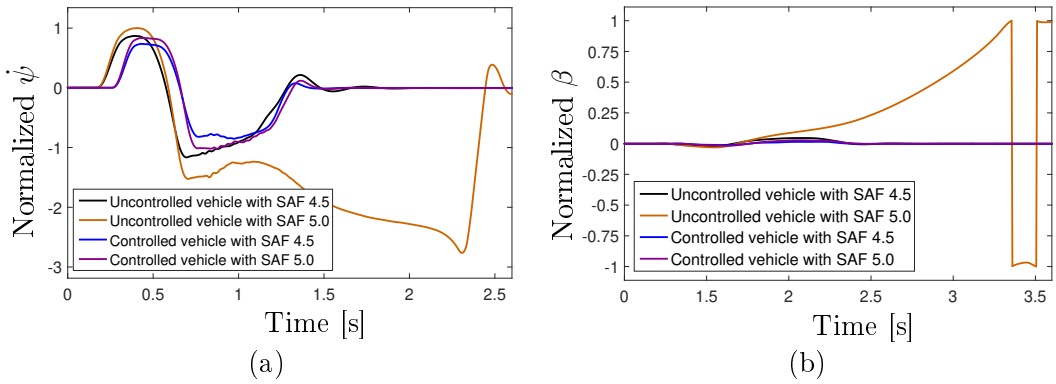

Figure 3.14: (a) vehicle yaw angle velocity and (b) side slip angle during the execution of the SWD maneuver with $SAF = 4.5$ and $SAF = 5$

3.6 Priorization, allocation and summation unit

As we have seen before, all units of the proposed control system, except the static feedforward control, are centralized and generate a yaw moment. Furthermore, there are different actuators assembled in a vehicle, i.e. rear steering system, electronic power steering system, electronic differential lock, braking system, etc. The generated yaw moment should be first converted into the form of a signal associated with an actuator and then sent to it. If there is only one actuator available in the chassis, then the whole generated yaw moment will be turned into the associated signal. The actuator locates the signal in the vehicle, until it reaches its maximum physical limits. However, there must exist a strategy for the distribution of the yaw moment, if there are more than one actuator configured in the chassis. The distribution can take place in different ways. We consider just two of them for the sake of easiness. Either all the generated yaw moments from various control system units are added together and the whole yaw moment is distributed between all actuators, depicted in Figure 3.15, or each yaw moment generated by each control system unit is first distributed among actuators and the total controlled input for each actuator is then calculated and sent to each actuator, figure 3.16.

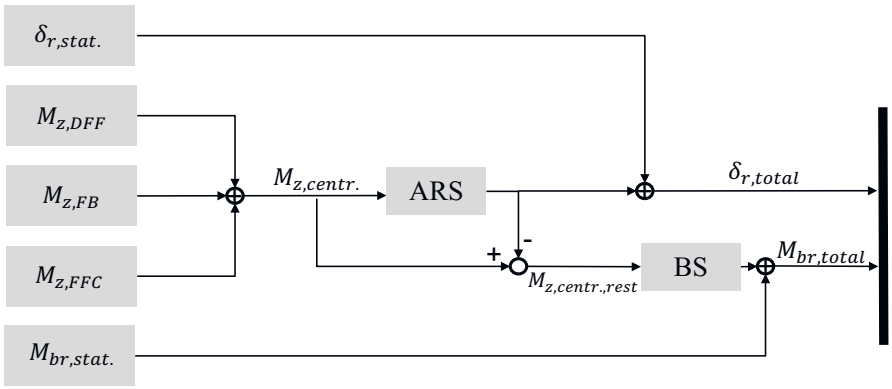

Figure 3.15: All the generated yaw moments from various control system units are added together and the whole yaw moment is distributed among all actuators

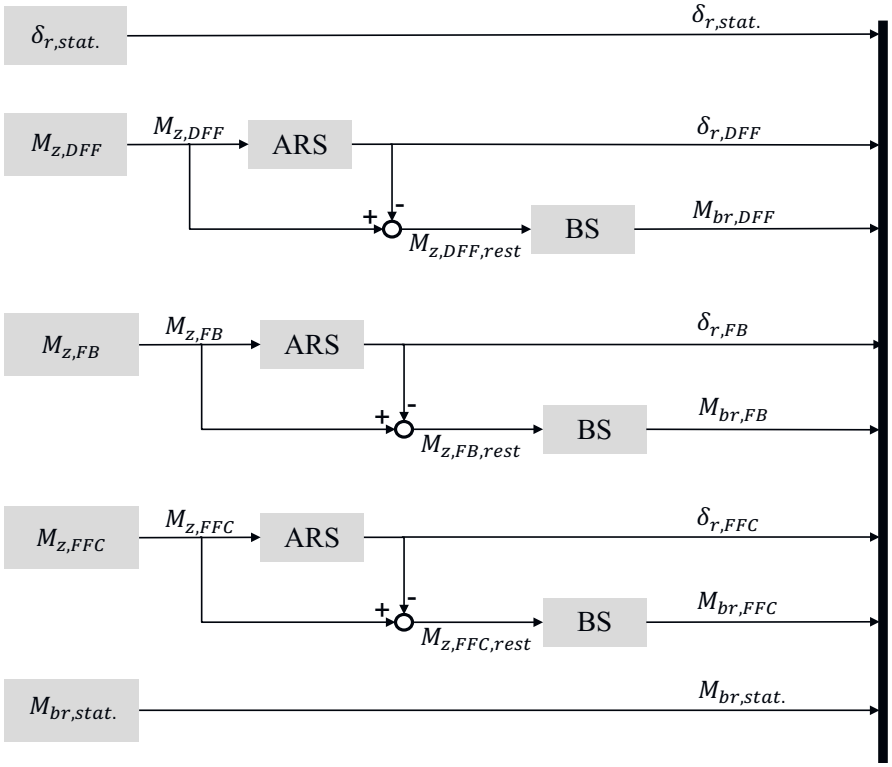

Figure 3.16: Each yaw moment generated by each control system unit is first distributed among actuators and the total controlled input for each actuator is then calculated and sent to each actuator

We apply the second way in this dissertation. One reason is that each control system unit can be tuned in this manner separately and with respect to the development stages of the chassis and the driving dynamics performance measures. Mostly, in the early stage of the chassis development, the so-called integration level 300 (I-300), only static and dynamic feedforward controls are tuned based on the driving dynamics performance measures. Another reason is, the output of each unit can be priorized based on the driving situation. For instance, if the vehicle gets out of control (oversteer), the static feedforward control of the braking system, whose task ist to make the vehicle agile, may not have to send any signal to the braking system anymore. Rather, the braking system should follow the DSC interventions stabilizing the vehicle. Figure 3.17 demonstrates, for example, how the generated yaw moment by the dynamic feedforward control is distributed and priorized.

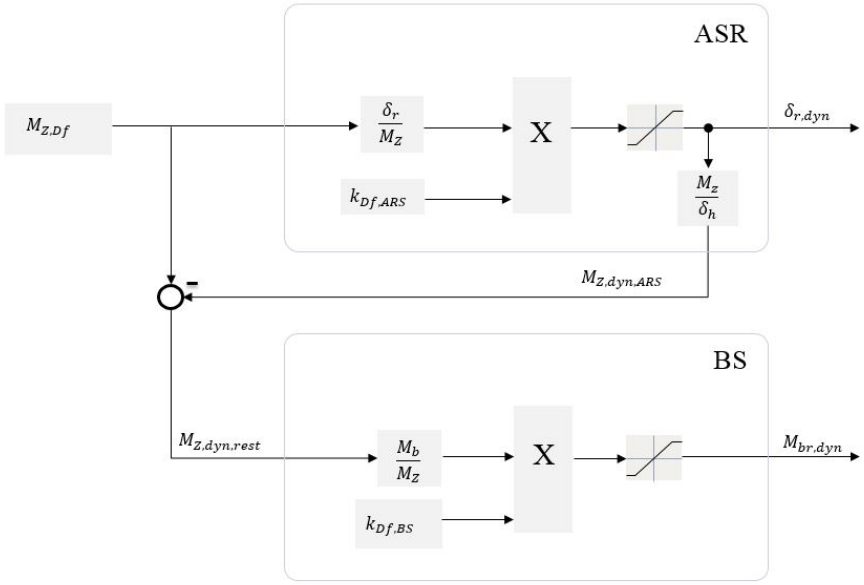

Figure 3.17: The generated yaw moment by the dynamic feedforward control is distributed and priorized among actuators

The generated yaw moment by the dynamic feedforward control is first assigned to the ARS module. There, it will be converted to a rear steering angle through the conversion factor $M_{z\rightarrow\delta_r}$. The calculated rear steering angle will be bounded by the actuator maximal rear steering angle, a specification of an actuator defined by the supplier. The bounded rear steering angle is then sent to the actuator and converted again into a yaw moment through the conversion factor $\delta_{r\rightarrow M_z} = \frac{1}{M_{z\rightarrow\delta_r}}$. This yaw moment is subtracted from the original generated yaw moment by the dynamic feedforward control. The rest is sent into the brake system module. There, it is converted into the brake moment by the conversion factor $M_{z\rightarrow\Delta M_{br}}$. The computed brake moment is also bounded with respect to the maximum brake moment, permitted to be implemented on the rear axle. The maximum brake moment on the rear axle is defined by the functional safety department. The computed brake moment should also be priorized with respect to driving situations. As mentioned above, if the vehicle is in the oversteer or counter-steer situation, it needs a stabilization yaw moment. Therefore, the computed and bounded brake moment may not be implemented in these situations, if the vehicle is getting agile by this moment. As shown earlier, the order of assigning the yaw moment to the actuators is first ARS and then BS. Because, the ARS can stabilize and make the vehicle agile and

the BS may just make the vehicle agile. Generally, the braking system should be the last actuator in this daisy chain which implements the yaw moment, otherwise, high braking wastage arises.

The distribution is carried out anyway by a daisy chain concept. Based on the daisy chain distribution, all actuators are not involved at the same time, which reduces the attrition of an actuator. In addition, each actuator is priorized based on its efficiency. In our case, the active rear steering system tries first to implement all requirements of each control unit. If it is not able to realize all requirements in form of a rear wheel steering angle, the rest of requirements will be sent to the brake system attempting to implement them in form of a brake moment.

Summary

In this chapter, we have demonstrated the structure of the lateral vehicle dynamics control system. The simulation model is then developed which consists of different units such as the static and the dynamic feedforward control, the disturbance feedforward control, the driving situation identifier, the feedback controller, and the priorization and allocation unit. The static feedforward control has been designed for ARS and one-sided brake intervention separately. The output of the characteristic curve of the ARS static feedforward control is a rear steering angle. The characteristic curve of the one-sided brake intervention calculates a brake moment with respect to the Ackermann lateral acceleration, which can also be weighted by the weighting factor, a function of the velocity. The dynamic feedforward control was centralized and produced a yaw moment based on the desired transfer function. It has enhanced the performance of the vehicle during the dynamic maneuvers. The centralized disturbance feedforward control has improved the behavior of the vehicle by braking or accelerating while cornering, since it rejects the impact of the longitudinal acceleration on the lateral dynamics by generating a yaw moment. The driving situation identifier has been proposed, which observes and compares the actual yaw velocity, the lateral acceleration yaw velocity, and single-track model yaw velocity. Based on this comparison, it could recognize the driving situation, such as oversteering, understeering or counter-steering, and generate a reference input for the feedback controller. The centralized feedback controller then controlled the deviation between this reference input and the actual yaw velocity by producing a yaw moment. All these generated yaw moments from different units had to be allocated to various actuators in the chassis. We have shown how this is done by the daisy chain method and with respect to the

driving situation in the priorization and allocation unit.

4 Functional actuator modeling

In the last few decades, some researches have been done for modeling actuators of the chassis. However, in most control engineering literatures, an actuator is considered as uncertainty in the model of a plant. In the vehicle industry, it is very important to specify an actuator, as it should most probably be able to deal with not only one vehicle, rather different vehicle variants. Otherwise it would be highly expensive to construct a specific actuator for each vehicle. For example, a common rear steering system is implemented in BMW 5, 6, 7, x3 and x5 series [68].

Designing and specifying actuators' properties for new vehicle generations can be done by assuming a similar system behavior to predecessors. In this way, it is important, in the first place, to have an appropriate model from the predecessors. The question arising here is which kind of model is required for this purpose. [19] attempts to answer this question regarding the development phases discussed in the introduction. The focus of this chapter lies on finding a proper method for modeling actuators in the early phase of vehicle dynamics development.

4.1 Modeling methodology

In the early stage of vehicle dynamics development, it is desirable to have a model which is as simple as possible and as complex as necessary. It means, we are interested to find a model of an actuator which describes its dynamics and physical limitation by a small number of parameters. This model simplicity helps us later define the specifications of new actuators more easily. In the system identification, we can divide the modeling methodology into three categories: empirical, physical and semi-physical modeling approach.

4.1.1 Empirical modeling procedure

The empirical modeling approach describes a system through mathematical models determined by observing the relationship between inputs and outputs of the system. An example of such models is a first- or second-order transfer function with parameters like static gain, time constant, natural frequency,

and damping ratio. In the system identification, it is necessary to formulate a procedure for finding such models. Based on [42], the method of empirical modeling can be laid out as follows.

1. **Experimental design:** A test rig has to be built up. In this step, different kinds of tests under specific conditions have to be determined, which result in maximum informative Input-Output data.

2. **Experiments:** The defined tests must be carried out. Here, it is important to reduce or preferably avoid any noises in order to have better data for interpreting the system behavior.

3. **Model structure:** This is the most important step of the system identification. A candidate model structure must be denoted based on the engineering intuition as well as properties of the gathered input-output data. In this section, having an insight into the physical components of an actuator is very helpful.

4. **Formulation of requirements:** Often, the outputs of the system model deviate from the outputs of the real system, i.e. an actuator [36]. As a result, the formulation of requirements on the permissible deviation becomes important.

5. **Parameter estimation:** Here the parameters of the candidate model selected in the section of model structure should be identified based on the recorded input-output data. This is done by identification and optimization methods.

6. **Model validation:** In this part, the outputs of the model are compared with the outputs of the real system. The procedure finishes if the deviation between these two outputs corresponds with the formulated requirement. Otherwise, the above-mentioned procedure or the adjustment of the system model parameters must be carried out again.

The empirical modeling procedure is summarized in figure 4.1.

There are different reasons to obtain insufficient models based on the explained procedure. In order to avoid such failures we have to:

- find a proper numerical procedure for the parameter estimation.
- choose appropriate requirements.
- figure out which kinds of data sets are informative enough.

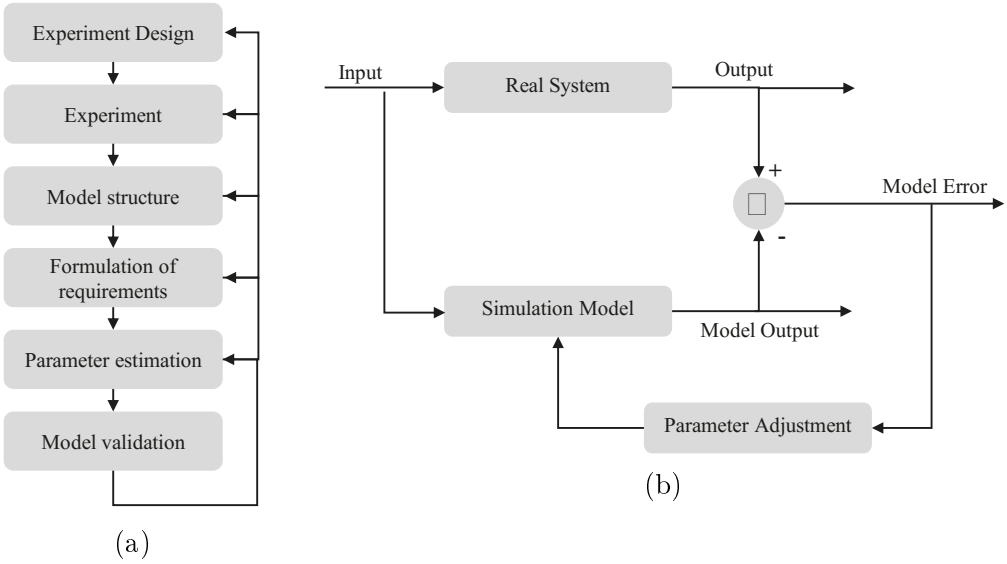

Figure 4.1: Empirical modeling: (a) Procedure of empirical modeling, (b) Deviation of the real system from the simulation model

In the end, it should be mentioned, that it is not desirable to find the most proper model for all purposes, rather a single model which deals with the defined requirements well.

4.1.2 Physical and semi-physical modeling procedure

Based on the physical modeling, a system will be modeled regarding its detailed components. Each mechanical, electrical or thermal parameter will be modeled. Examples of such parameters are mass, friction coefficient, inductance, capacitance or thermal resistance. In this way, each kind of non-linearity in the system has also to be modeled. Non-linearities can arise due to frictions or compliance of mechanical components or a power limitation of electrical ones. The advantage of this kind of modeling is, it gives a detailed view of the system under investigation. Moreover, it is expected that the model output rarely deviates from the real system output. However, such a modeling procedure takes much time due to its complexity and is highly dependent on the system under investigation as each system consists of different kinds of mechanical and electrical components. The system model also needs high computing capacities for the simulation and design procedure. But, in most cases, it is almost impossible to figure out all the subcomponents of an actuator, since they are properties made

by suppliers. In addition, such models are highly time-consuming and need high computing capacities for the simulation and design procedures. Therefore, such physical models are not appropriate in the early stage of product development, since in this stage, the goal is to have a simple model with reasonable accuracy and quick simulation time.

Consequently, we introduce a new kind of modeling which combines the idea of empirical and physical modeling. This way, we obtain a model with a good accuracy and less time consumption for the designing procedure [6]. Semi-physical modeling can then be the serial arrangement of two sub-models, figure 4.2. The sequence of the serial model structure does not matter.

Based on semi-physical modeling, a system is modeled empirically but with the consideration of physical limitations: for example non-linearities, observed from recorded input-output data. Such models should cover the behavior of a system in the frequency as well as time domains. In these both domains, the deviation of the model output from the system output still has to follow the requirements introduced in the section of empirical modeling.

Figure 4.2: Structure of semi-physical modeling

4.2 Application to rear steering system

The methodology of semi-physical modeling will be applied in this section to model an active rear steering system (ARS). It means, we model the ARS actuator first of all by application of empirical modeling methodology. Afterwards, we apply the methodology of physical modeling to model the physical limitations of ARS relevant to the lateral vehicle dynamics. Based on experimental design, the first step in empirical modeling is to build up a test rig with specific situations. As seen in figure 4.3, the ARS actuator is connected to the wheels through the tie rod and the mechanical lever arm.

The movement of the tie rod is calculated by the transmission ratio which is defined by the supplier. Additionally, the maximum rear wheel steering angle is defined by the supplier and equal to 3 degrees. These properties can be briefly seen in table 4.1.

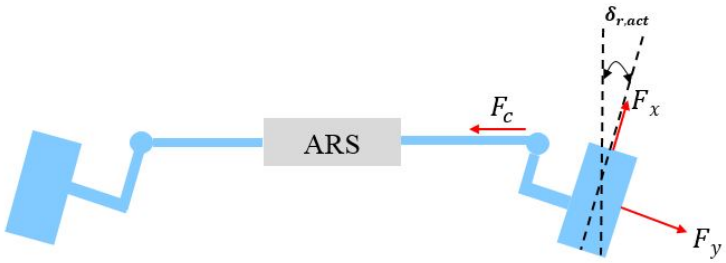

Figure 4.3: schematic interface of the active rear steering actuator and the rear axle

ARS actuator kinematics properties	Value
Maximum rear wheel steering angle	$\pm$ 3°
Transmission ratio (mean value)	$\pm$ 2.679 $\frac{mm}{°}$

Table 4.1: The kinematics properties of the active rear steering system

Experimental design

The set-up of the test rig is shown in figure 4.4. The tie rod is attached from the left side to a sensor which measures the movement and from the right side to a hydraulic cylinder which produces a constant counter force (F_c). The following conditions are met for the test-rig:

- The measurements are executed by the temperature 20° Celsius. The alteration of the temperature is not taken into account, as it is no point of interest in the early stage of vehicle dynamics development.
- The hydraulic cylinder produces only static forces.

In this step, it is also important to define different tests which can identify the behavior of the actuator in the steady and transient states. As a consequence, we use:

- step inputs for investigating the steady state and time transient profile of the actuator.
- sinusoidal inputs with an increasing frequency for investigating transient behavior of the actuator in the frequency domain.

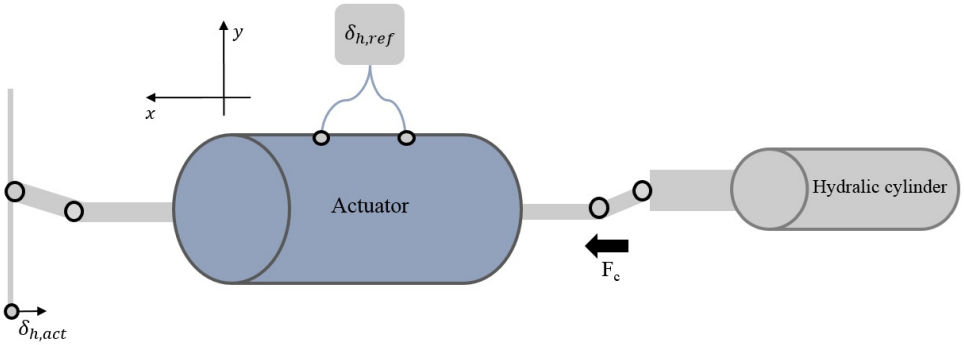

Figure 4.4: Schematic of the test rig setup of ARS

Moreover, these tests should not be executed with respect to only one counter force rather diverse counter force values. In this manner, we can find out how the response of the actuator varies regarding the amplitude and the direction of counter forces. This happens on the tie rod during the ride because of the longitudinal and lateral acting on the tires.

The step test is utilized for exploring the performance of the actuator in time domain. Moreover, it contributes to figure out whether the actuator includes physical limitations caused by friction, inertias, transport delays, etc. The chosen properties for the step test are illustrated in table 4.2.

Step test properties	**Value**
Counter forces	± 5.5, 0 [kN]
Amplitude	1.87°

Table 4.2: Properties of the step test

The counter force values are considered at no load condition (0 kN) and maximum tolerable counter force (5.5 kN). In this way, we can determine the performance of the actuator at normal and extreme operation points.

In order to catch the response of the actuator in the frequency domain, we outline a sinusoidal test with the information summarized in table 4.3

The test starts with the frequency of 0.1 Hz and is carried out with a duration of 7 periods, in order to stabilize the amplitude and phase shift response at each frequency. In addition, the consideration of a rest time between each frequency is required, in order to bring the system to the steady state and not to influence the next excitation. The schematic of the test input is shown in figure 4.5.

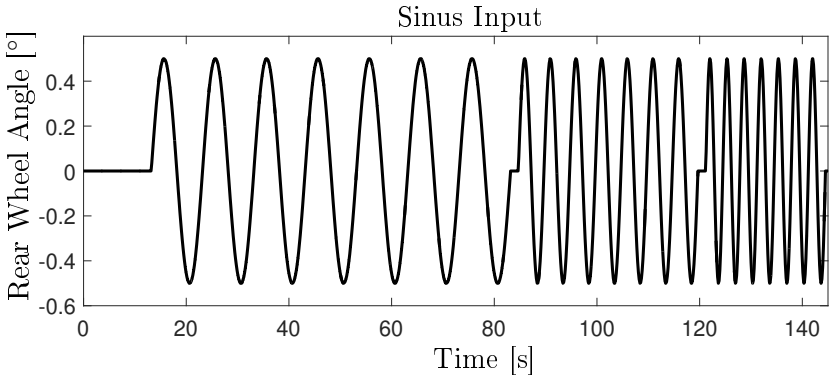

Figure 4.5: Schematic of the sinus input

The maximum counter force is set to ±5 kN, as this was specified by the supplier. Other counter forces are concerned for producing more informative input-output data.

Sinusoidal test properties	**Value**
Counter forces	± 5.5, ± 2.2, 0 [kN]
Amplitude	0.5°
Periods per frequency	7
Starting frequency	0.1 [Hz]
End frequency	5 [Hz]

Table 4.3: Properties of the sinusoidal test

Experiments

In this part, the defined tests are conducted. Figure 4.6 represents how the actuator reacts to the sinus input, where the counter force, for example, is set to +5.5 kN.

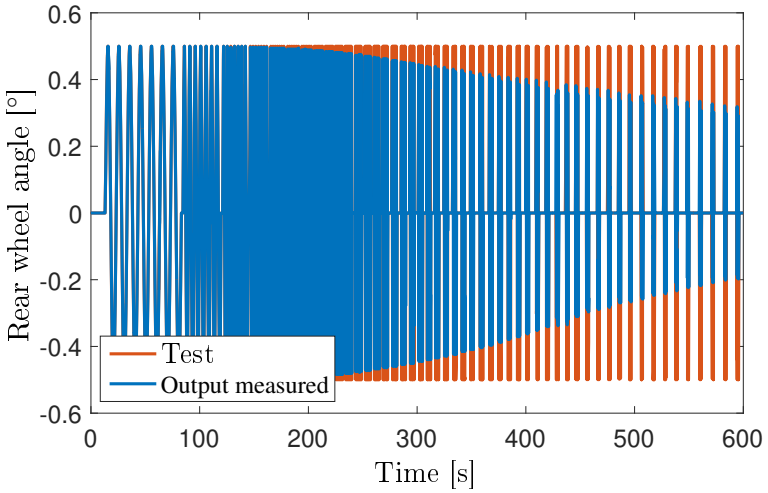

Figure 4.6: Sinus response of the ARS actuator regarding $F_c = 5.5$ kN

Additionally, the step test is executed with respect to the defined counter forces, figure 4.7. The dash lines demonstrate the response of the actuator to each counter force.

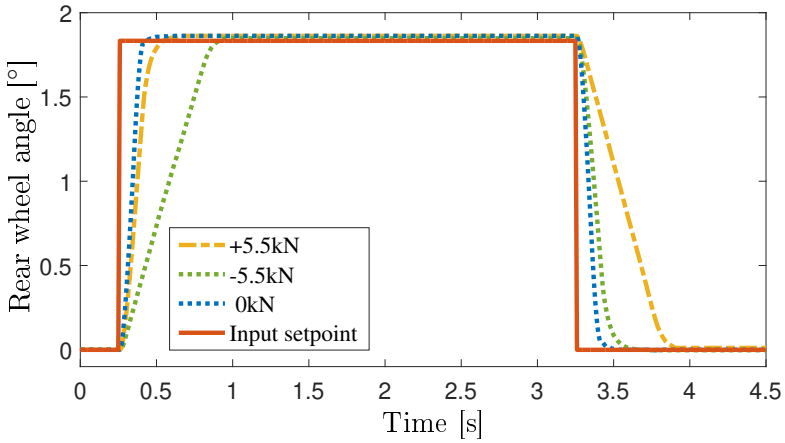

Figure 4.7: Comparison between measured step response regarding the defined F_c

Model structure

Often, the model structure is determined with respect to prior knowledge about physical components of an actuator, engineering intuition, and formal properties of the model needed to be taken into account. As mentioned above, over-parametrization must be avoided and the model should be as simple as possible. By looking at the response of the ARS actuator to the step and sinusoidal input figure 4.7 and figure 4.6, one can assume that a first-order transfer function with a time delay is a good choice for the empirical model structure [7]. However, by considering a second-order transfer function with or without zero we can reach more accuracy for modeling the recorded input-output data. In this case, one can also consider the second-order transfer function with or without zero and with or without time delay [40]. As all mechanical components have a delay at the beginning by implementing the coming signal, we choose a second-order transfer function with a time delay as a candidate for the model structure:

$$G_{ProcessModel}(s) = \frac{K_P}{1 + 2\,D\,T_w\,s + (T_w s)^2}\; e^{-T_d s} \tag{4.1}$$

Where K_P, D, T_w, T_d stand for static gain, damping ratio, time constant, and time delay, respectively.

Formulation of requirements

The formulation of requirements on the error between the model output and the real system output is crucial, since the permissible deviation between them must not violate the ultimate goal. Before giving a deep insight into the requirements, first the term $FitPercent$ will be introduced. It is the normalized root mean square error emerged from model outputs and real system outputs in frequency domain. It means the output of the model and the real system, i.e. ARS actuator, are converted from time domain into frequency domain by means of Fast Fourier Transform (FFT). $FitPercent$ is shown in equation 4.2.

$$FitPercent = 100 \sum_{k=1}^{N} \left(1 - \frac{\|G_0(\omega_k) - G_{\mathbf{q}}(j\omega_k)\|}{\|G_0(\omega_k) - mean(G_0(\omega_k))\|}\right) \tag{4.2}$$

Where G_0 stands for the transfer function calculated from the measured output to the input, G_q represents the transfer functions from the estimated model output to the input and k corresponds to each frequency.

Now, the requirements are defined as follows:

- The $FitPercent$ should not be less than 75%.

- The amplitude deviation must not be more than 10%.
- The time shift must not be more than 15 ms.

Parameter Estimation

There are various approaches for the parameter estimation of a model [25, 57, 39, 71]. In our case, the second-order transfer function with a time delay has been chosen. The applied approach for estimating the introduced model 4.1 is the frequency domain prediction error method (FPEM). The prerequisite knowledge about this method can be found in details in [41]. It attempts to find the best configuration of parameters of the transfer function whose bode-diagram fits well to the realized bode-diagram from the recorded input-output data of the sinusoidal test. FPEM is already implemented in MATLAB [41], in the system identification toolbox. Before using this tool and approach, the input-output data must be converted from time into the frequency domain by the Fast Fourier Transformation (FFT) [5]. Figure 4.8 expresses the amplitude spectrum obtained by the conversion of the input-output data from sinusoidal test with respect to the counter force 0 kN. This procedure will be executed for all counter forces.

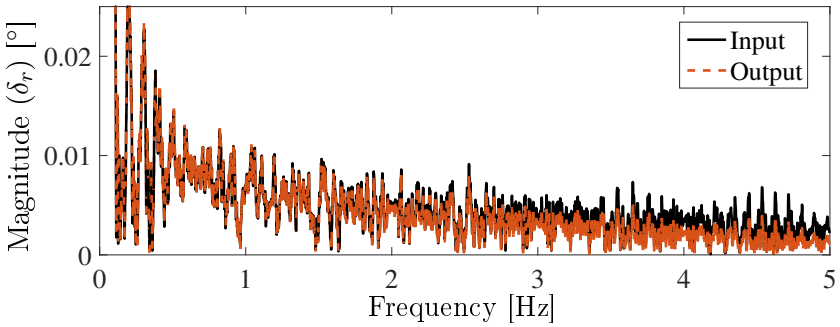

Figure 4.8: Fast Fourier Transform for the sinus response and counter force of +5.5 kN

The converted output of the sinusoidal test is divided by the converted input for each counter force, where the bode-diagram can be represented, figure 4.9. It can be seen, the bode diagram of the response of the ARS actuator to the sinus input for all counter forces has a very similar behavior up to 3 Hz. As mentioned in chapter 3, the lateral vehicle dynamics is defined in the range of 0 until 2 Hz. Consequently, it is sufficient to find one transfer function based on equation 4.1 with a suitable parameter configuration which covers the bode

diagram up to 3 Hz very well and fulfills the above-mentioned requirements. FPEM is then applied and a set of parameters is found, which is represented in table 4.4. The fitting percent of this transfer function is calculated for each counter force based on equation 4.2 and is shown in table 4.5.

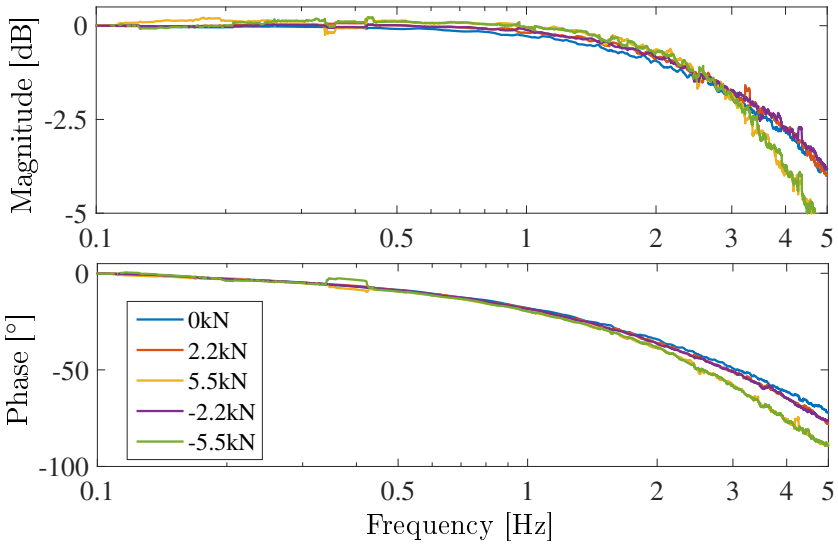

Figure 4.9: Bode diagram of the sinus responses of the ARS regarding all counter forces

Set of parameters			
K_P	D	Tw	T_d
1	3.6	0.0068	0.01122

Table 4.4: Predicted parameters for the candidate transfer function

As a consequence, the predicted empirical model is as follows:

$$G(s) = \frac{1}{1 + 0.01604s + (0.0068s)^2}\, e^{-0.01122s} \tag{4.3}$$

As can be seen from figure 4.10, the course of the model's bode diagram with the predicted parameters fits to all the bode diagrams very well and the FitPercent is still more than 75%, i.e. the first requirement is met. But we have to validate this model now in terms of the amplitude error and the time shift for both sinus and step input.

Fitting Percent					
Counter Force [kN]	−5.5	−2.2	0	+2.2	+5.5
FitPercent [%]	81.9	91.92	93.2	78.92	80.13

Table 4.5: FitPercent of the calculated transfer function for all counter forces

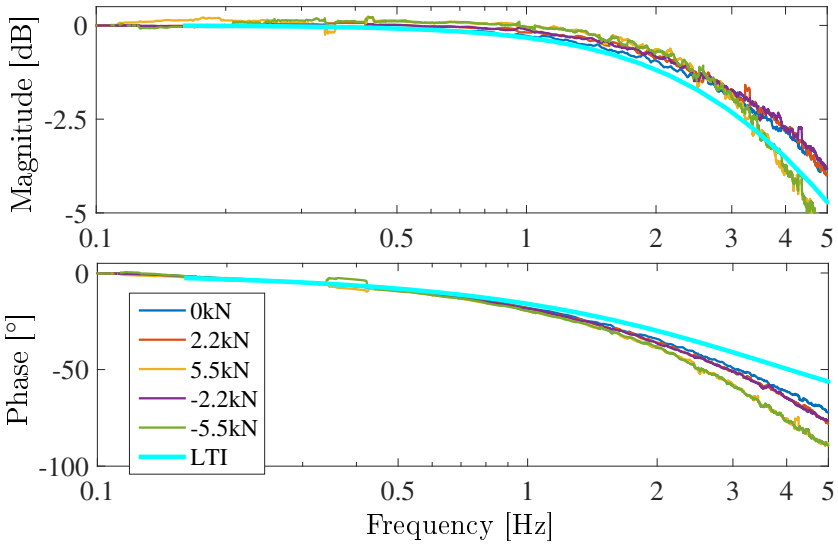

Figure 4.10: Bode Diagram of the sinus response of the ARS actuator and the predicted model with respect to all counter forces

Model Validation

This part has to be carried out based on the defined requirements in the section of formulation of requirements. As already mentioned, the transfer function with the predicted parameters meets the first requirement properly. It is clear from figure 4.11, the amplitude error and the time shift between the system output and the model output regarding the counter force 0 kN at 0.5 Hz, the initial frequency, are almost zero and at 3 Hz, the maximum considered frequency, 3.3 % and 9 ms, respectively.

Figure 4.12 represents the input, the system output, and the model output at 0.5 Hz and 3 Hz for the case, where the counter force +5.5 kN is. The amplitude error and time shift at 0.5 Hz are almost zero and at 3 Hz, 1.48% and 11 ms, respectively.

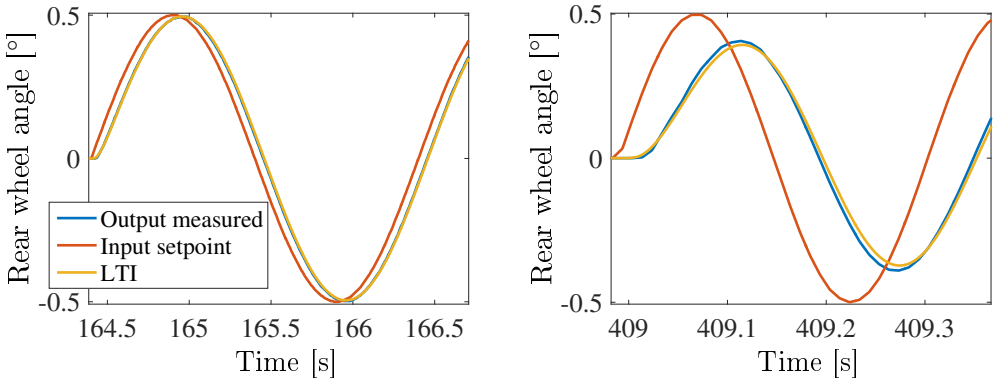

Figure 4.11: The response of the ASR actuator and the model to the sinus input regarding $F_c = 0$ kN: (a) Response at 0.5 Hz, (b) Response at 3 Hz

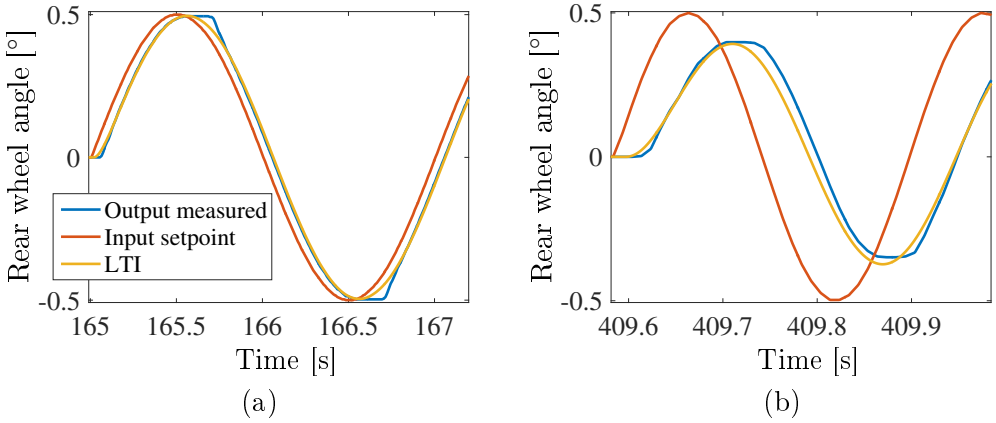

Figure 4.12: The response of the ASR actuator and model to the sinus input regarding $F_c = +5.5$ KN: (a) Response at 0.5 Hz, (b) Response at 3 Hz

Last but not least, it can be figured out from figure 4.13 that the amplitude error and time shift between the system output and the model output in terms of the counter force -5.5 kN are zero at 0.5 Hz and 1.48% and 11 ms at 3 Hz, respectively.

Table 4.6 illustrates the amplitude error and time shift for all counter forces

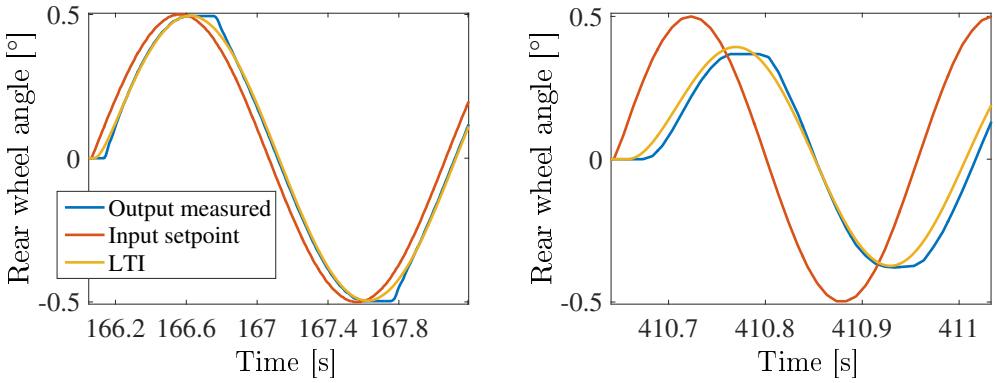

Figure 4.13: The response of the ASR actuator and model to the sinus input regarding $F_c = -5.5$ kN: (a) Response at 0.5 Hz, (b) Response at 3 Hz

at 3 Hz.

Model validation for the sinus response					
Counter Force [kN]	-5.5	-2.2	0	$+2.2$	$+5.5$
Amplitude error [%]	6.74	2.7	3.3	2.1	1.48
Time shift [ms]	11	9	9	8	11

Table 4.6: Comparison of the model output with the system output at the frequency 3 Hz

As a result, it is to be concluded that the model responses at the frequencies $[0.5 - 3]$ Hz for all counter forces meet the requirements.

The model validation has also to be done for the step test. The step input is also given into the transfer function 4.1 with the predicted parameters 4.4. Figure 4.14 demonstrates the response of the system and the model to the step input. The time shift fulfills its requirement. However, the amplitude error fails to meet the formulated requirement, as it can visually be seen that the amplitude error is significantly high. It indicates that the velocity of the system response is much less than the expected velocity, represented by the step response of the predicted model 4.3. This fact results from non-linearities in the ARS actuator, i.e. maximum speed of the actuator's tie rod travel. However, This fact cannot be seen in the sinus responses, as the velocity of the sinus

input is not so high that the actuator runs in the velocity saturation. As a result, the semi-physical modeling is applied to get further improvement in the empirical modeling.

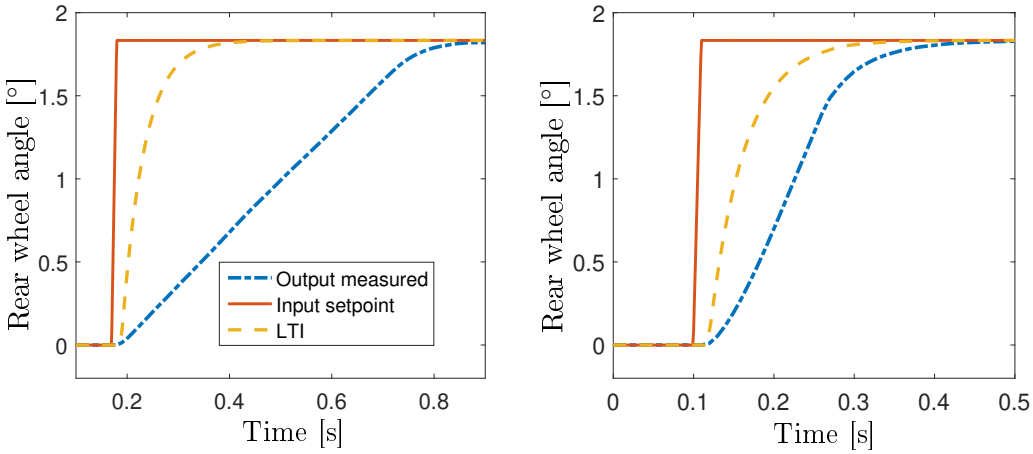

Figure 4.14: Comparison between step input, measured output and predicted output (LTI) for counter force: (a) $F_c = -5.5$ kN, (b) $F_c = +5.5$ kN

Semi-physical modeling

As explained in this chapter, the semi-physical modeling is an extension of the empirical modeling with the consideration of physical limitations. We have concluded from the last section, that the physical limitation in the ARS actuator refers to the maximum speed. This limitation can be incorporated in the empirical model, as shown in figure 4.2, by trying to map the power or torque characteristic curves. The step responses of the actuator regarding the defined counter forces are analyzed. For each step response, the velocity is calculated for each time sample point (interval of 1 second) from the beginning until the steady state of the response. As a consequence, the graphic shown in figure 4.15 is generated.

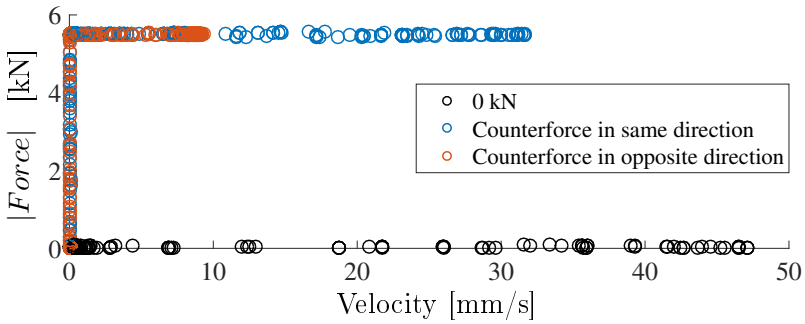

Figure 4.15: Force and velocity measurements for a step input subjected to different counter forces

This gives us the idea how to define the power characteristic curve of the actuator. The characteristic force-velocity limitation is then formulated mathematically as follows:

$$\dot{\delta}_{out} = \begin{cases} \dot{\delta}_{cu} & |F_C| \geq F_{C,c} \;\;\&\;\; F_C \cdot \dot{\delta}_{in} > 0 \\ \dot{\delta}_{TF} & |F_C| < F_{C,c} \\ \dot{\delta}_{cl} & |F_C| \geq F_{C,c} \;\;\&\;\; F_C \cdot \dot{\delta}_{in} < 0 \\ 0 & otherwise \end{cases} \tag{4.4}$$

$$\dot{\delta}_{cu} = \frac{v_{noload} - v_{u,F_{max}}}{F_{max}} \cdot \dot{\delta}_{TF} \pm v_{noload} = (0.0027 \cdot \dot{\delta}_{TF} \pm 47.1)\, \frac{mm}{s} \tag{4.5}$$

$$\dot{\delta}_{cl} = \frac{v_{noload} - v_{l,F_{max}}}{F_{max}} \cdot \dot{\delta}_{TF} \pm v_{noload} = (0.0069 \cdot \dot{\delta}_{TF} \pm 47.1)\, \frac{mm}{s} \tag{4.6}$$

where $\dot{\delta}_{in}$ and $\dot{\delta}_{out}$ stand for the velocity of the input signal and semi-physical model output, respectively. $\dot{\delta}_{TF}$ refers to the velocity of the signal output coming out from the transfer function, F_C expresses the counter force and $F_{C,c} = 5.5$ kN is the maximum critical counter force. $\dot{\delta}_{cu}$ and $\dot{\delta}_{lu}$ are defined as upper and lower bound of the model output velocity when the product of the input velocity with the counter force is positive and negative, respectively.

Figure 4.16 depicts the characteristic curve with the parameters defined in

table 4.7.

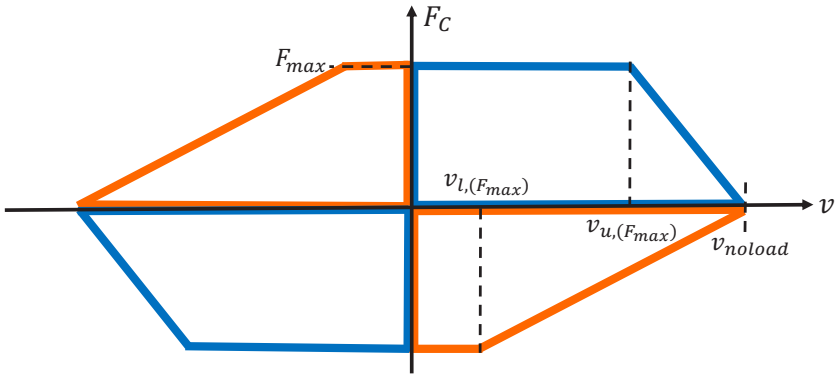

Figure 4.16: Power characteristic curve of the ARS actuator

Table 4.7: Parameters for the actuator force speed characteristic curve

Force speed curve parameters	**Value**
F_{MAX}	$5.5[kN]$
$v_{u,F_{MAX}}$	$32\,[mm/s] = 11.9\,[°/s]$
$v_{l,F_{MAX}}$	$9.3\,[mm/s] = 3.5\,[°/s]$
v_{noload}	$47.1\,[mm/s] = 17.6\,[°/s]$

The characteristic curve 4.16 is implemented as rate limiter (RL) in the semi-physical model of the ARS, which limits the velocity of the output signal obtained from the transfer function 4.3.

Now, we return to the validation part and show that the proposed semi-physical model, shown in figure 4.17, also meets the requirements for the step response.

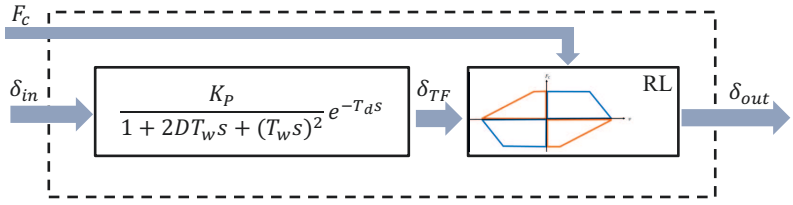

Figure 4.17: Semi-physical model of the ARS actuator

where δ_{in} stands for the δ_r calculated from the lateral vehicle dynamics control system explained in the last chapter and F_c represents the counter force acting on the tie rod and resulted from the longitudinal as well as the lateral forces of the rear wheels.

The results of the step response to the model demonstrated in figure 4.17 are depicted in figure 4.18. As expected, the model approximates the measured output very well and we observe significant improvements. The amplitude deviation between the model output (LTI+RL) and the system output (measured output) is less than 10% and the time shift is approximately zero. This points out, that the semi-physical model meets all the determined requirements.

4.2.1 Summary

In this chapter, the importance of different kinds of modeling approaches has been demonstrated. We have pointed out that the empirical modeling describes a system through mathematical models determined by observing the relationship between inputs and outputs of the system. We have also explained that the physical modeling models a system regarding its detailed components and the semi-physical modeling is compound of the empirical and physical modeling. As illustrated, a semi-physical model of an actuator is sufficient in the early stage of the vehicle dynamics development. Based on the proposed approach, the actuator was modeled first empirically with respect to the specific steps cleared in this chapter. The model had to be verified regarding the verification tests. If the model could not pass all the tests, then it should be adapted. The adaptation was the expansion of modeling to the semi-physical modeling, where the non-linearities in the actuator could also be modeled. We have applied this methodology on the ARS. The ARS semi-physical model has passed all the verification tests in the frequency and time domain. We have also shown that the model is accurate enough for the development of the new generation actuators.

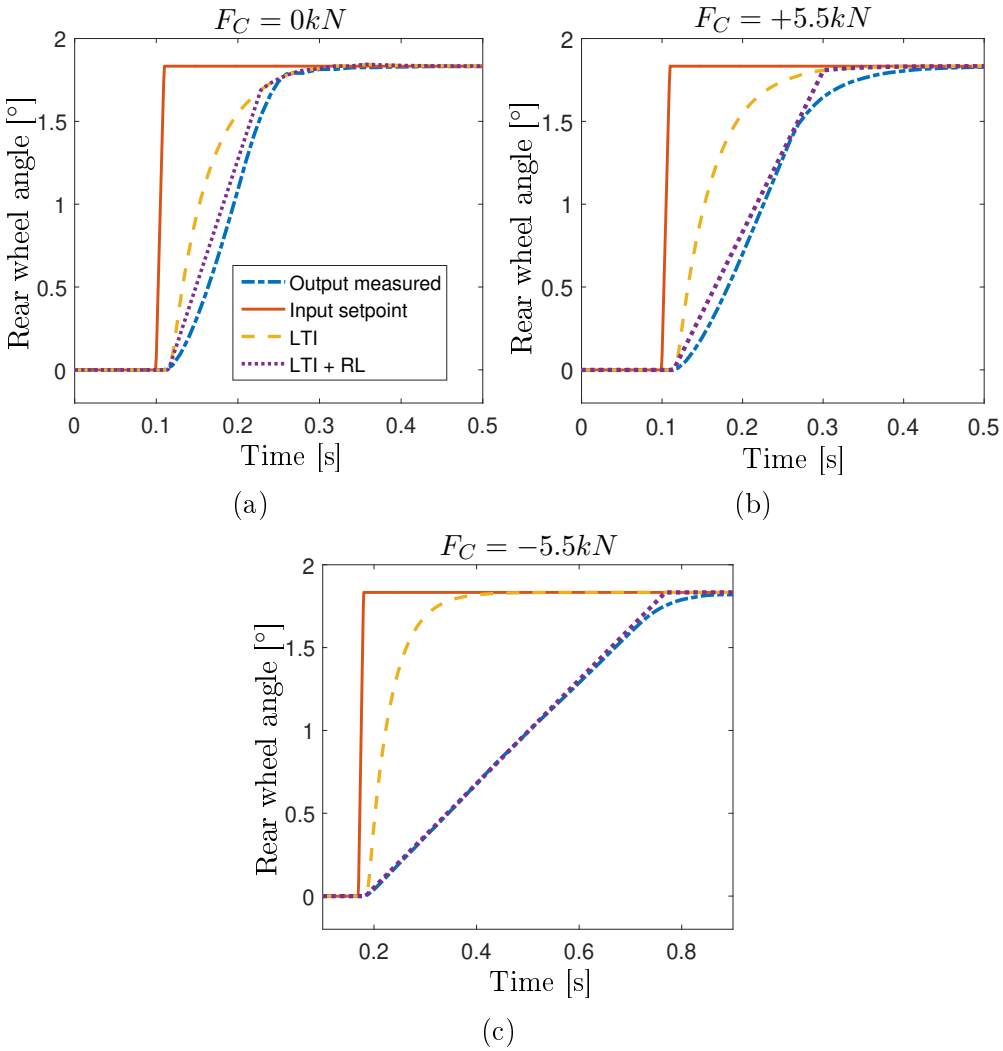

Figure 4.18: The response of the ASR actuator, empirical model (LTI), semi-physical model (LTI+RL) to the step input regarding: (a) 0 kN, (b) +5.5 kN and (c) −5.5 kN

5 Robust design of actuators and control systems

Problem statement

As mentioned in the section of state of the art, there exists research about robust design of actuators and parameterization of control systems. However, almost all of it needs a linear or a linearized system model. In addition, most of the proposed methods find a parameter space for parametrization of only a feedback controller with respect to unstructured uncertainties in the dynamic model of a plant and consider an actuator also as an uncertainty. The most used criterion in such methods is only the stability of the closed-loop system.

We have seen in the last chapters that the vehicle, the control system, and the actuators are together an example of a highly non-linear large-scale system with uncertainties, which makes the design procedure very complex, particularly in the early stages of the vehicle dynamics development. In addition, beside the stability criterion, there are many other requirements on the driving dynamics performances, which also have to be satisfied with a proper design of such a large-scale system. One way to carry out such a design is an iterative design. It means, designing actuators and parameterizing control systems can be accomplished by designing each subsystem of a control system and an actuator separately. In this case, each subsystem must be developed, so that the overall performances of the vehicle will be achieved. However, such an approach may lead to conflicts of goals regarding overall performances, since each subsystem attempts to accomplish the overall performance and does not take into account the contributions of other subsystems. Moreover, this approach cannot cope with complexities during the design procedure. These complexities refer to the fact that actuators and control systems have to be developed for diverse vehicle variants by numerous development departments and based on different driving dynamics performances. As a consequence, there is a necessity for finding a proper method, which confronts the complexity and can find a robust design of actuators and control systems with respect to all driving dynamics performances and uncertainties during the development procedures.

The proposed method in this chapter is based on the general idea of design-

ing large-scale systems with respect to uncertainties, presented in [78]. The basis of this method is the so-called V-model [28]. The V-model is an effective way to decompose qualitative requirements of a large-scale system into subsystem's requirements, figure 5.1. However, it is not straightforward to produce quantitative requirements of the subsystems by this model.

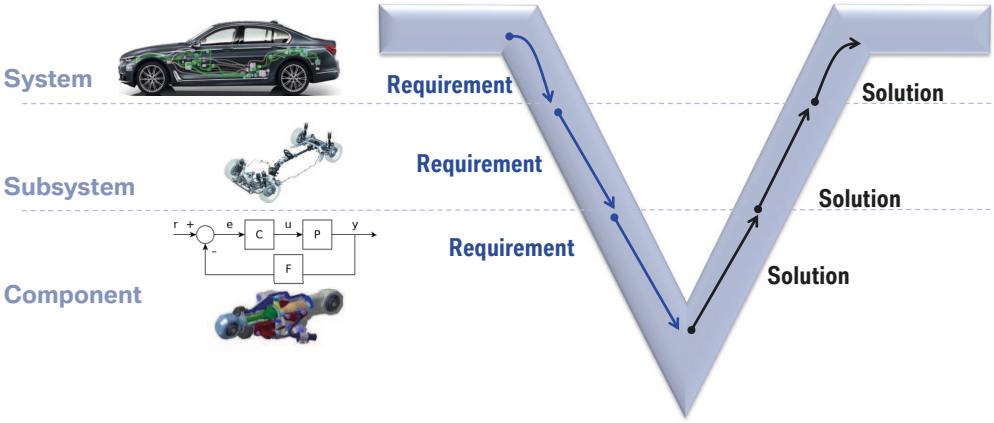

Figure 5.1: Design procedure based on the V-Model

Therefore, additional steps have to be incorporated into this model to make it possible to derive quantitative requirements of subsystems from overall requirements of a large-scale system [78].

In the first step, it should be clarified, which design variables of each subsystem influence which objective quantities, possibly interact with other design variables of other subsystems, and affect the overall performances of a large-scale system. This is done by creating a so-called dependency graph. In the second step, so-called bottom-up mappings, here surrogate models, have to be established, which evaluate the quantitative performances of a large-scale system, depending on the design variables of the subsystems. Surrogate models must be as simple as possible and as complex as necessary. In the third step, the so-called top-down mappings, permissible ranges of design variables are derived from quantitative requirements formulated on the large-scale system. Figure 5.2 shows the overview of all these three steps.

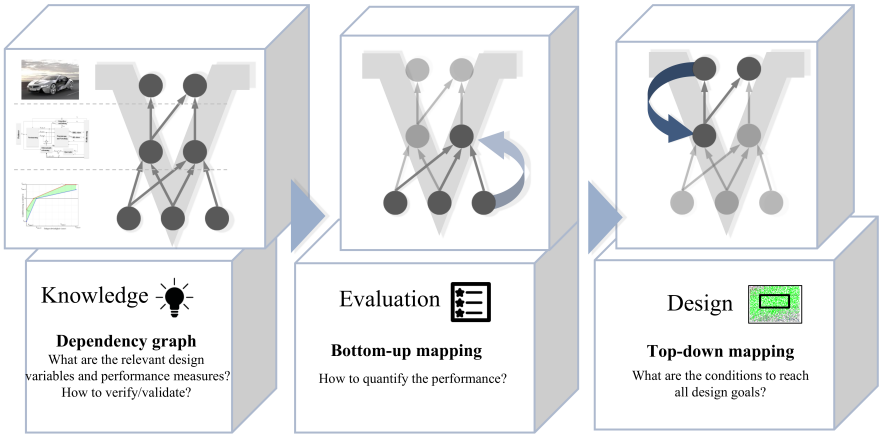

Figure 5.2: Three-enablers for deriving the quantitative requirements of subsystems from the overall requirements of a large-scale system

We first clarify what a dependency graph is and how it is constructed. Second, we explain the buttom-up mapping procedure and necessary mathematical and physical surrogate models for control systems, actuators, and vehicles. Third, we describe the procedure of top-down mapping and give a brief review of the optimization method which delivers permissible ranges of design variables of actuators and control systems with respect to uncertainties and objective driving dynamics performance measures.

5.1 Dependency graph

In the process of designing an actuator and parametrization of a control system, a structured model is required which documents the dependencies among the design variables of the subsystems and the objective driving dynamics performance measures. This model is important, as it can manage know-how in the process of the development. A so-called dependency graph is used for this purpose.

As explained in chapter 2, the vehicle performance is identified in different dynamics domains, namely longitudinal, lateral and vertical domain. Each domain is assessed by different assessment indices (AI). These AIs are targets on the highest level of the V-model, i.e. on the system Level depicted in figure 5.1. Each AI is characterized by different maneuvers and the relevant objective driving dynamics performance measures of these maneuvers. For example, "AI cornering" is one of the assessment indices in the domain of vehicle lateral

dynamics. This AI is evaluated by different maneuvers such as acceleration while cornering (ACWC), brake while cornering (BRWC), quasi steady state cornering (QSSC), Ramp steer, etc. Referencing again to the chapter 2, each of these maneuvers has different objective driving dynamics performance measures which are altered by the chassis' properties, namely subsystem properties in the V-model. These subsystem properties are also affected by the properties of components composing the subsystem. The examples of such components in the chassis are control systems and the actuators.

So, a **dependency graph** is a graph in which the **measurable system** (AIs), objective driving dynamics performance measures and **component** properties (control system parameters and actuators design variables) are displayed as **vertices**. Their dependencies are expressed as an arrow.

5.2 Bottom-up mapping

For bottom-up mapping, quantitative evaluation of outputs as a function of inputs, a model is required which represents the physical relations between inputs and outputs, i.e. design variables of actuators and control systems and objective driving dynamics performance measures. The physical model of the vehicle, functional model of the actuators, and the model of the control system have been pointed out in the previous chapters. Simulation of these models and later optimization of the outputs of the simulation are usually restricted by very large computational time. A single simulation of our complex model takes several hours or even a day. Therefore, the optimization problem, finding permissible ranges of design variables, is very time-consuming, because it usually needs more than thousand simulation iterations. Therefore, substitute models, based on mathematical functions, can be applied in order to approximate and predict the real model behavior with extremely lower calculation time [31], but at a price of yielding a small error on the final result. As mentioned before, a meta-model can also predict the output of the physical model with respect to new sets of design variables without a need for further simulations.

Meta-models used in this work are associated with classification and regression methods of the supervised learning technique of machine learning, which are trained by already known input and output data and are then able to predict the output under new combination of input parameters [62]. The used regression models in this work are artificial neural networks. The support vector machine is then used for the classification. These meta-models need an adequate number of inputs and outputs. As a result, we introduce in the next section the idea of design of experiments (DoEs), responsible for the preparation

of inputs and outputs. Afterwards, we give a brief review of how the artificial neural networks (ANN) and the support vector machine (SVM) work and why we need both of them.

5.2.1 Design of experiments

In order to train ANN and SVM properly, we have to consider two requirements on the design space of all design variables (inputs to ANN and SVM):

- The sample of the design space must be well distributed.
- The design space must be covered as much as possible with minimal number of sample points in order to accelerate the process of the simulation and optimization.

The consequence of the realization of these two requirements is that the metamodel can be well fitted to the real model and later predict the output well for a new combination of input variables.

There are different kinds of sampling methods [69]. Some of them are

- Sobol sequence
- Scramble Sobol sequence
- Full factorial sequence
- Halton sequence
- Scramble Halton sequence

The question arises, which method fulfills the above-mentioned requirements most properly. Therefore, we introduce a term, called discrepancy, which differentiates between sampling methods. Imagining that the number of design variables is P, the design space is labeled as Ω_{ds} with N samples, and z is an arbitrary point from the design space Ω_{ds}, $b[0,z]$ is defined as a box containing all points located in the box from origin to z. $n(b)$ is the number of points in this box and $Vol(b)$ shows the volume of the box. Accordingly, the discrepancy of the point z is computed as follows:

$$Discrepancy(z) = \left| \frac{n(b)}{N} - Vol(b) \right| \tag{5.1}$$

Another term is defined as follows:

$$D_\infty = \max_{z \in \Omega_{ds}} (Discrepancy(z)) \tag{5.2}$$

The smaller D_∞ is , the better the method is in terms of the defined requirements. It means, the method with the smallest D_∞ can sample the P-dimensional design space Ω_{ds} efficiently by covering most of its corners and edges. In this way, the data will be more informative by minimum possible number of samples and accordingly simulations. [72] investigates all possible methods of sampling based on the introduced terms. The result is that Scramble Sobol sequence and Scramble Halton sequence are the best options in terms of D_∞, figure 5.3.

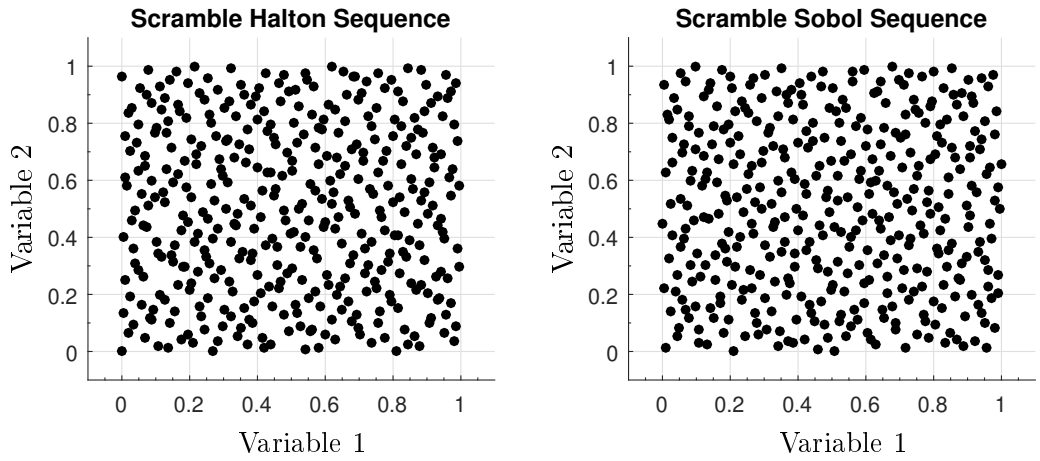

Figure 5.3: The most two efficient sampling methods in terms of discrepancy

As mentioned earlier, input-output data is necessary for training of meta-models. The procedure of generating input-output data is summarized below:

- Identification of design variables of the actuator and the associated control system.
- Choosing a proper method for sampling the design space of the design variables.
- Sampling the design space.
- Choosing desirable driving dynamics maneuver.

- Simulating the whole system model, i.e. vehicle, control system, and actuator model, regarding determined driving dynamics maneuvers and the sampled design space.
- Evaluation of the simulation results for calculating the objective driving dynamic targets of each driving maneuver.

This procedure is depicted in figure 5.4. Consequently, the inputs to a meta-model are sample points of the vehicle-genes, the control system, and the actuator design variables. The outputs are the evaluated objective driving dynamics of each driving maneuver.

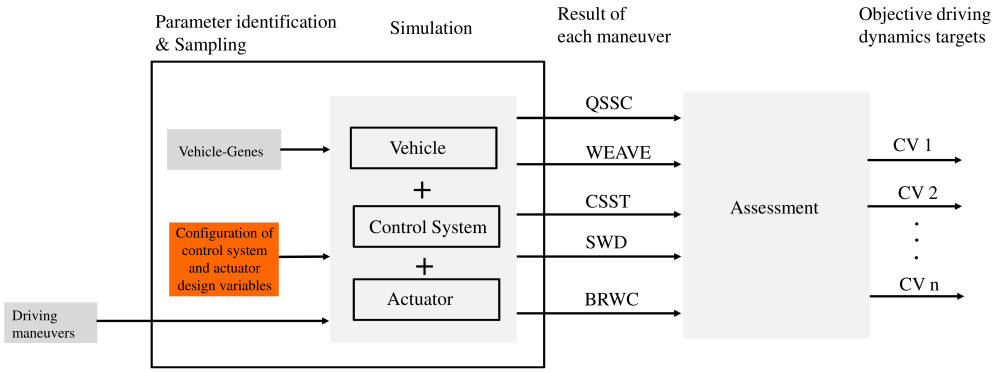

Figure 5.4: The procedure of generating input-output data

5.2.2 Response surface model

After gathering enough input-output data, a meta-model has to be trained. In our case, for each output, we train an individual neural network, multiple input and one output model. It should be noticed, a meta-model approximates a simulation model which is itself an approximation of the real system. As a result, it is desirable that these two approximations have errors as small as possible in order to avoid a big deviation in the final design result [35].

As discussed above, we use the artificial neural networks (ANN) for training the data. ANNs are quasi-mathematical surrogate models, based on the interconnection of numerous biological neurons. One can effectively overcome the non-linear problems with high complexity and many dimensions with ANNs [69].

Currently, there exist different types of neural networks, e.g. Feedforward Neural Network, Convolutional Neural Network, Modular Neural Network, Radial Basis Function Neural Network, Recurrent Neural Network, etc. [33]. In

this dissertation, we use the Feedforward Neural Network with Backpropogation algorithm. Figure 5.5 demonstrates a typical schematic of a simple feedforward neural network. The network is split in three layers: Input layer, hidden layer, and output layer. The input layer gets all samples of the control system and actuator design variables, and vehicle genes.

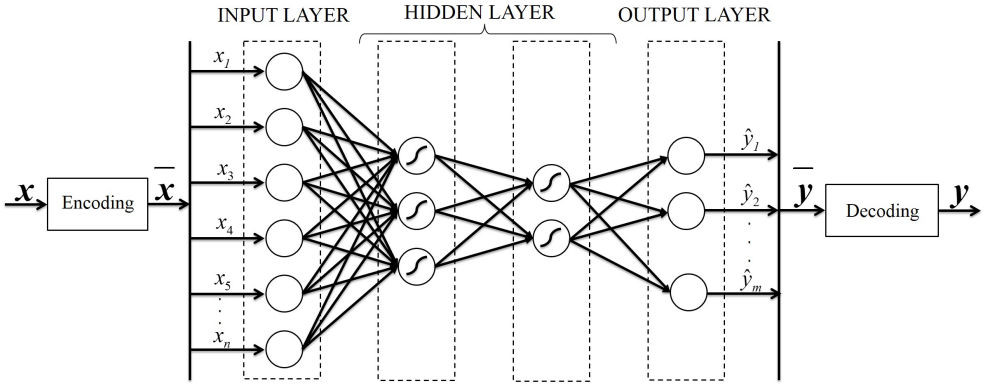

Figure 5.5: A typical schematic of a simple feedforward neural network

All design variables are scaled between 0 and 1 by an encoder before entering the network, since it is easier for the backpropogation algorithm to find the optimal weights more quickly. As a result, decoding of the outputs should be carried out at the end. The output layer includes the evaluated objective driving targets, i.e. CVs, of all maneuvers. Between these two layers, one or more hidden layers are situated. Each hidden layer can have an arbitrary number of neurons, whereby no more than 2 layers are usually needed for most of the problems in this dissertation.

As mentioned before, a separate neural network is defined for each CV (objective driving performance measure), so that the network structure, i.e. number of hidden layers and neurons of each layer, is especially constructed with respect to each output. Each neuron of a hidden layer is connected to all neurons in the previous and the subsequent layer (fully connected neural networks). Figure 5.6 shows, how a neuron in the $j+1$-th layer gets its information by the activation of all neurons of the previous layer. If the j-th layer has k neurons with weighting w_{ji} and the activation function is defined as φ, the activation of a neuron in the next layer proceeds as follows:

$$Net_{j+1} = w_{j0} + \sum_{i=1}^{k} w_{ji} \cdot x_{ji} \tag{5.3}$$

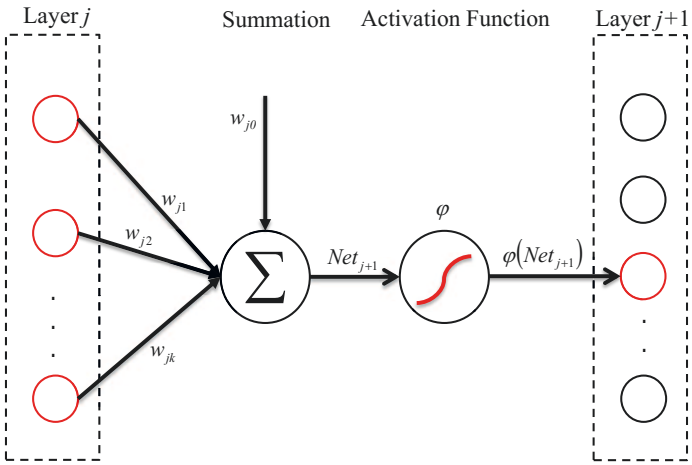

Figure 5.6: Schematic of the activation of a neuron

where, w_{j0} is the so-called bias and a constant value. x_{ij} represents all the neurons in the j-th layer. The activation function φ can be, for instance, sigmoid logistic or sigmoid hyperbolic tangent. In this work, we use sigmoid logistic as activation function:

$$\varphi(Net_{j+1}) = \frac{1}{1 + e^{-Net_{j+1}}} \tag{5.4}$$

Model Quality

Model quality of a computed neural network is very important in terms of the prediction of the real model, since an overfitting of an ANN leads drastically into failed predictions of unseen data. Figure 5.7 [69] represents an overfitting scenario. The network is well trained on the training data and can predict the output of the training data very well. But, as soon as the input data of the trained network is not the training data, it fails to predict the correct output. As a consequence, data is divided in two groups: training data and test data. Usually, the test group is smaller than the training group.

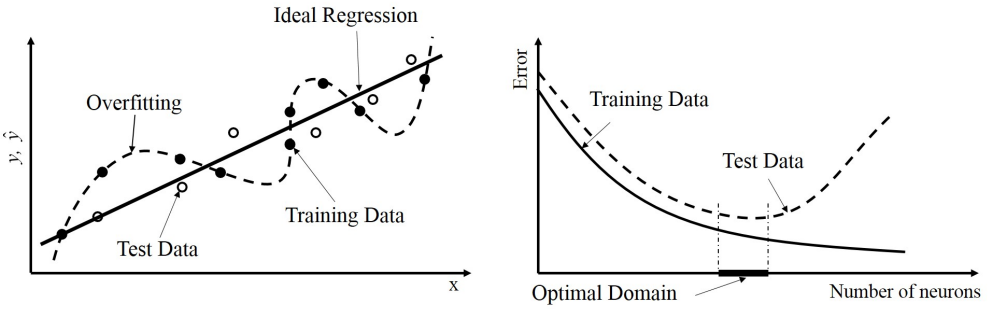

Figure 5.7: Model Quality, the procedure of overfitting

The meta-model, ANN, is trained with the training data. A desired ANN is one, which has the smallest prediction error. The prediction error is measured in different ways. The classic one is the coefficient of determination R^2, computed as follows:

$$R^2 = 1 - \frac{\sum_i^N (y_i - \hat{y}_i)^2}{\sum_i^N (y_i - \bar{y})^2} \tag{5.5}$$

where, y_i, $\hat{y}_i$ and $\bar{y}$ are the real output, the predicted output, and the average of all predicted output, respectively. In order to avoid any overfitting, the quality of the meta-model ANN is compared with the samples from the test data. For this purpose, the cross validation method is applied [69]. In this dissertation, the model quality equal or larger than 0.9 is considered as a good quality.

Proposed Algorithm

As mentioned above, the number of hidden layers as well as neurons can vary with respect to the structure of the feedforward neural network. Increasing the number of neurons and hidden layers can enhance the prediction of more complex relationships between inputs and outputs, which can deliver a very good quality for the training data. However, it may lead into model overfitting. It should also be considered that there is no calculation to determine the best structure of an ANN with the best model quality. Subsequently, we introduce here a pragmatical procedure to find the best structure for our application with the best model quality without meeting any kind of overfitting.

The number of the hidden layers and neurons is varied. For example, the number of hidden layers is set to one at the first attempt and the neurons are varied from 5 to 20. The model quality of each ANN is saved individually.

Here, in order to avoid any overfitting, the quality of the meta-model ANN is compared with the one from the test data. At the second attempt, the number of the hidden layers is increased to 2 and the neurons are varied again from 5 to 20. The model quality of each ANN is saved again individually. This procedure can be done also for more than 2 hidden layers and is repeated for all the outputs. In the end, all the model qualities are compared with each other, and the structure with the highest model quality is picked out.

5.2.3 Classification

In the beginning of this section, we clarified why we need meta-models and which ones we use in this work. After a brief review of the ANN, now the support vector machine (SVM) is introduced as a classification operator. The first question is that why a SVM is required at all?

In the section of *Design of Experiments*, we have declared, that the outputs of the simulation are the results of each driving dynamics maneuver. In order to train ANNs, we need enough data. As a result, the number of simulations to be executed, which is around 4000, depends on the number of design variables. As all simulations are automatically carried out, there are simulations which have been aborted due to unstable configurations of design variables. Therefore, the results of the simulations are either numerical or empty outputs, which stand for the aborted simulations. The numerical outputs should be assessed to compute the objective driving dynamics performance measures of each maneuver, figure 5.4. While automatically assessing, the simulation results, which are not in the predefined range of objective driving dynamics performance measures (CVs), will not be evaluated and will be dropped out of the evaluation procedure and will be represented as an empty evaluation. For example, the CVs associated with the CSST maneuver are defined in the range of [0,2]Hz. If the evaluated CVs are out of this range, they will be dropped out of the assessment procedure.

Accordingly, the outputs obtained from the evaluation procedure can be categorized in three groups:

1. Evaluated CVs (non-empty).
2. Empty CVs due to the fact, that they are out of predefined ranges.
3. Empty CVs due to the fact that simulations have been aborted because of unstable configurations of design variables.

ANNs are trained with all data including all three above-mentioned categories of data. The problem appearing here is that ANN interpolates all empty

outputs. Consequently, the solution space of the design space after setting constraints on the design space is not really reliable. This will be clarified with an example.

Imagining, there are two design variables and all the driving dynamics maneuvers have been simulated for numerous configurations of these two design variables, the outputs applicable for training ANNs are the evaluation of the simulation outputs, CVs. They are either empty or evaluated. Figure 5.8 shows available outputs after the evaluation. The green and black dots represent the evaluated and empty outputs, respectively, for all configurations of the design variable one and two.

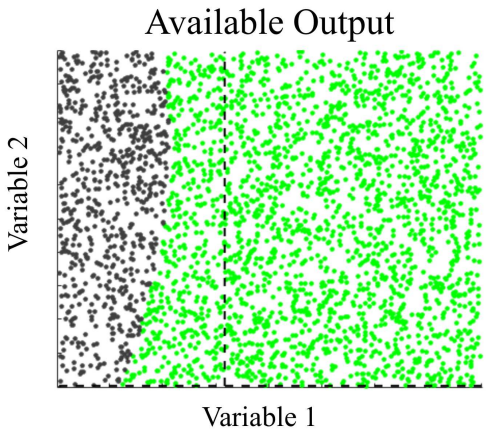

Figure 5.8: Available Outputs

These outputs are trained with an ANN. A constraint is then set on the outputs of the trained network which cuts the design space like in figure 5.9.

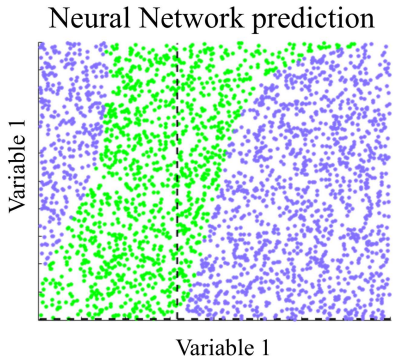

Figure 5.9: ANN Prediction of a constraint on the meta-model output

As can be seen from figure 5.10, the design space, trained by ANN, is wrongly interpolated, since the area of black dots must be considered by the network. As a consequence, there is a need to apply a classification operator, which separates the empty outputs from the evaluated ones.

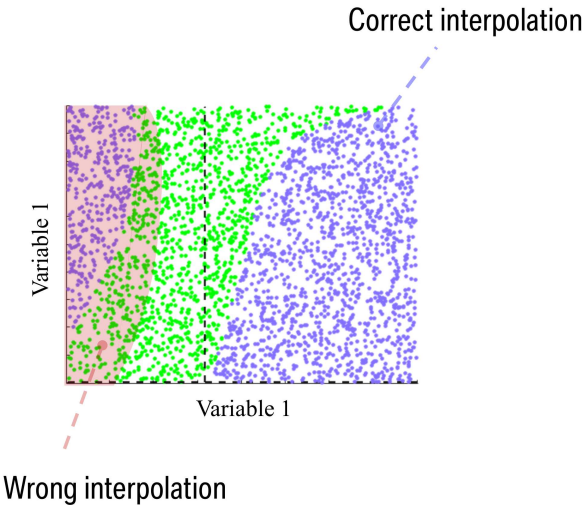

Figure 5.10: Wrong interpolation of ANN

The applied classification in this work is the Support Vector Machine (SVM).

Support Vector Machine - SVM

A support vector machine is a classification operator which classifies data into two classes by finding the hyperplane which maximizes the margin between

them. In our case, it classifies the assessed objective driving dynamics performance measures from simulation results into the evaluated and empty classes, represented by 1 and -1, respectively.

Functonality

Looking at a two-dimensional design space, shown in figure 5.11, the red and green dots represent two different classes. The task of support vector machine is to find the best line in two dimensional design space or a hyperplane in high dimensional design space in order to separate the two classes. The SVM attempts to try the closest two dots from two classes. These two dots are called support vectors. A line is drawn between these two dots and the SVM finds the best line which bisects and is perpendicular to the connecting line.

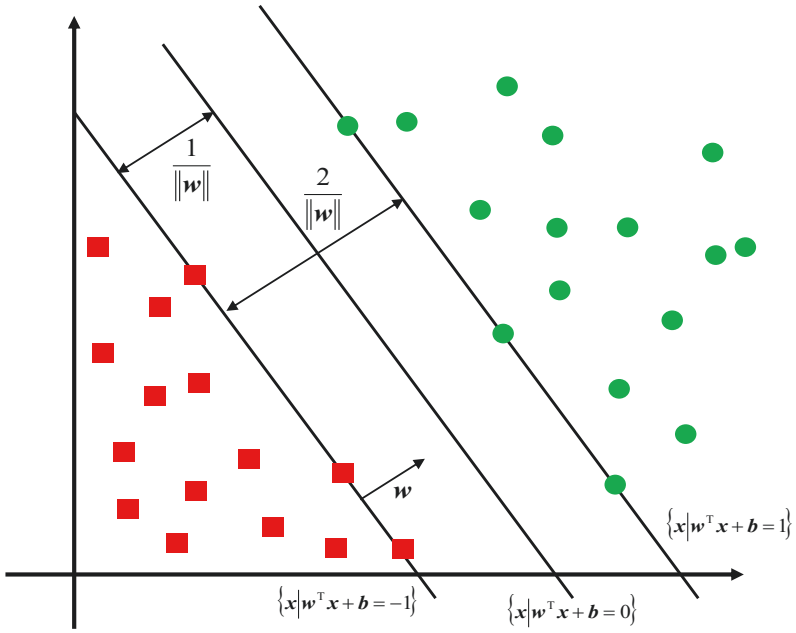

Figure 5.11: The schematic of SVM functionality for two dimensional design space

Mathematical Problem Formulation

A given dataset can be represented as:

$$D = \{(x_1, y_1), (x_2, y_2), \cdots, (x_n, y_n)\} \tag{5.6}$$

where n is the number of training data, y_i is the class associated with the i-th dot x_i and $x_i \in \Omega_{ds}$. y_i is either 1 or -1.

A linear classifier has the following form:

$$f(\mathbf{x}) = \mathbf{w}^T\mathbf{x} + b \tag{5.7}$$

where $\mathbf{w}$ is the normal vector to the hyperplane. Here, support vectors are the dots closest to the hyperplanes. The margin between these two hyperplanes is calculated by $\frac{2}{\|\mathbf{w}\|^2}$. The goal is to find $\mathbf{w}$ and b in Equation 5.7 such that the margin will be maximized. It means,

$$\begin{aligned} &\text{maximize} && \frac{2}{\|\mathbf{w}\|^2} \\ &\text{subject to} && y_i((\mathbf{w^T}\cdot\mathbf{x_i}) + b) \geq 1, \quad i = 1, ..., n \end{aligned} \tag{5.8}$$

This problem refers to an optimization of a quadratic function, subject to linear constraints [44]. In this way, the classification is conservative and the misclassification is therefore as small as possible.

Soft Margin Solution

Sometimes, the above-mentioned optimization problem is not solvable and the data is therefore not separable or the found classification hyperplane delivers a very narrow margin. In this case, some misclassifications can be allowed, through relaxing the inequality in equation 5.8, which leads to a wider classification margin. As a consequence, we introduce two new variables C and ϵ_i, called box constraint and slack variable, receptively, and bring them into equation 5.8:

$$\begin{aligned} &\text{maximize} && \frac{2}{\|\mathbf{w}\|^2} + C\sum_{i}^{n}\epsilon_i \\ &\text{subject to} && y_i((\mathbf{w}\cdot\mathbf{X_i}) + b) \geq 1 - \epsilon_i, \quad i = 1, ..., n \end{aligned} \tag{5.9}$$

Here, the parameter C has to be selected carefully, as a small C leads to excessive relaxation of the constraint very much, causing the margin to be very large and vice versa. If $0 < \epsilon < 1$, dots are located between the margin and on the correct side of the hyperplane. But, $\epsilon > 1$ causes a misclassification, i.e. some dots can be located on the wrong side of the hyperplane. As a result,

ϵ can be substituted with $\epsilon = max(0, 1 - y_i f(\mathbf{x}))$. Now, equation 5.8 can be written as:

$$\text{maximize:} \quad \frac{2}{\|\mathbf{w}\|^2} + C \sum_{i}^{n} \max(0, 1 - y_i f(\mathbf{x})) \tag{5.10}$$

This optimization problem is then unconstrained, convex and has a unique minimum [15]. Therefore, this optimization problem can be carried out by any gradient-based algorithm. In conclusion, it should be noticed, that box constraint parameter C plays an important role in finding a large margin with low amount of misclassification. This parameter has to be adjusted such that less misclassification is ensured.

So far, we clarified the idea of classification with a straight line, flat plane or an N-dimensional hyperplane. However, there are cases, where a non-linear regions can separate the classes more efficiently. Such cases occur when data is not distributed linearly, figure 5.12. In such cases, the non-linear support vector machines must be applied.

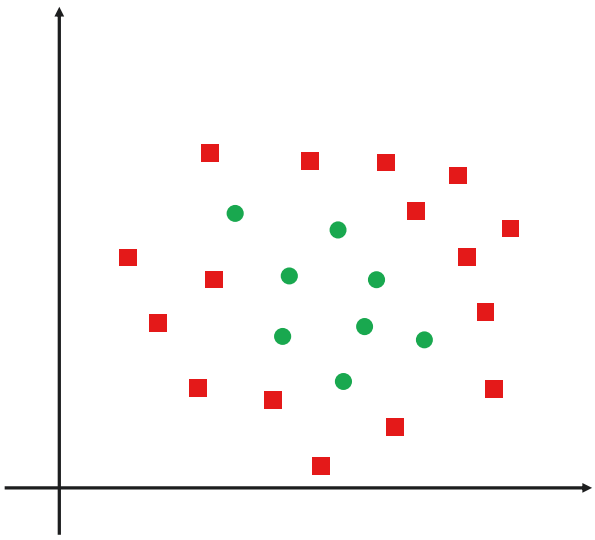

Figure 5.12: Non-linear distributed data

Non-linear Support Vector Machines

When the data cannot be separated linearly, it is mapped into higher dimensional spaces by applying a kernel function where the mapped data can be classified linearly. This is called Kernel trick. Some kernel functions are listed below:

- Linear: $K(\mathbf{x}_i, \mathbf{x}_j) = \mathbf{x}_i \mathbf{x}_j$
- Polynomial: $K(\mathbf{x}_i, \mathbf{x}_j) = 1 + (\mathbf{x}_i \mathbf{x}_j)^p$ for any $p \geq 0$
- Gaussian: $K(\mathbf{x}_i, \mathbf{x}_j) = exp\left(-\frac{\|\mathbf{x}_i - \mathbf{x}_j\|^2}{2\gamma^2}\right)$

There are several studies which have investigated each of above-mentioned kernel functions with respect to the size of margins [10, 50]. In this work, the Gaussian function is applied, as it normally produces bigger margins [10]. In this case, the parameter γ has to be adjusted such that the misclassification is still kept small.

Briefly, the non-linear data is mapped with Gaussian kernel function into the higher dimensional spaces and a linear classifier is found for this space based on equation 5.10. As a result, we need enough data, the adjusted C, and γ parameters to obtain the trained SVM model, figure 5.13.

Figure 5.13: SVM-Functionality

Model Quality

The goal of classification is to separate data into two definite classes with less misclassification. But, getting less misclassification sometimes leads to the overfitting of this meta-model. Quite contrary to the neural networks, which need two groups of data, namely training and test data, it is necessary to train SVM with all available data. Otherwise the exact classification may not be reached. Accordingly, a cross validation is employed for the calculation of the misclassification and avoiding any overfitting. The applied cross validation is the *K-Fold* [69].

The availabe data is split into K groups. One group is employed to test the model quality. The SVM is then trained with K-1 groups of the data and the associated misclassification is computed. This procedure is then done K-times. Accordingly, the meta-model is finally trained with all available data and the model quality is then the average of all misclassifications obtained from each iteration. All the calculated misclassifications depend on the parameters C and γ. They have to be adjusted such that the misclassification of each iteration becomes as small as possible and a good model quality is then reached. However, adjusting these two parameters manually for high dimensional spaces is very difficult and time-consuming.

Consequently, we apply optimization methods such as genetic algorithm or partial swarm algorithm to find the most optimal C and γ, which hand in a minimum misclassification. In this dissertation, the genetic algorithm and the machine learning tool box in Matlab [27, 17] are employed to obtain a trained support vector machine with a good model quality. C and γ are disposed to the range of $[10^{-5}10^{5}]$ in our algorithm in order to have a better distributed population in the whole design space. Like ANNs, we also generate one specific trained SVM for each of the driving dynamics performance measures. The goal is to have a trained SVM for each CV with a misclassification less than 15%.

The combination of ANN and SVM for the two variables in figure 5.10 can be seen in figure 5.14. As shown, this combination leads to no interpolation failure.

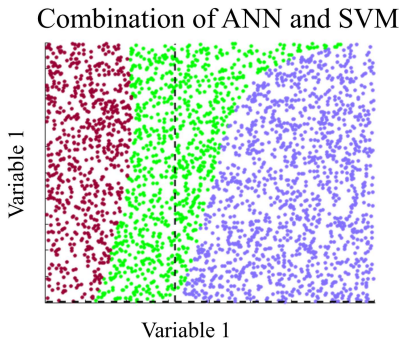

Figure 5.14: The combination of SVM and ANN for the design space of two design variables

5.3 Top-down mapping

As mentioned at the beginning of this chapter, the V-Model is an effective way to break down qualitative requirements of a large-scale system into qualitative subsystem requirements. But, the question is how we can break down the quantitative requirements formulated on a large-scale system like a vehicle with a control system and an actuator into the quantitative requirements for components such as the control system and the actuator, especially with respect to uncertainties. Such a quantitative method must be able to deal with uncertainties. In our case, there are two types of uncertainties:

- **Lack of information about the derivatives of a vehicle**: In the early stage of the vehicle development, we know that we do not deal with only one vehicle but rather different derivatives. They are distinguished mainly by their mass, moment of inertia, rear axle ratio, and center of gravity hight.
- **Discarded subjective driving dynamics performance measures**: So far we have just introduced the objective driving dynamics performance measures. But, in the late stages of the vehicle development, each vehicle must be driven by an experienced driver, tuned and assessed subjectively. As a consequence, there are still subjective perceptions which cannot be formulated as objective driving dynamics performance measures. For example, parametrization of the logic of a control system virtually based on only the objective driving dynamics performance measures may not be able to deal with the subjective driving experience. Most of these subjective challenges are referred to as the steering feeling, which cannot be formulated objectively. In other words, a virtual parametrization of the control system can satisfy all the objective driving dynamics performance measures but cannot still deliver a good steering feeling, assessed subjectively.

Even if we would have no uncertainty in the design procedure, it would be still not desirable to find one optimal solution regarding all considered requirements, because the realization of only one optimal design of a component may be impossible or highly expensive if possible.

The approach to keep uncertainties under control and decompose the requirements quantitatively is a so-called solution space [77], which finds a target region of all good designs for design variables, which fulfill all objective driving dynamics performance measures (CVs). This method is also applicable to arbitrary non-linear and high-dimensional problems and does not demand specific

uncertainty model or probability distribution. Target intervals will be sought to realize independent target regions for design variables. In order to increase the design flexibility, the product of the intervals should be maximized.

What will be clarified in more details in this section, is this method and the improvements made so that it can be applied to the control system and actuator designs.

5.3.1 Solution spaces

The design variables available for the design procedure of control system logics and actuators are represented by the vector $\mathbf{x} = [\mathbf{x}_{log},\ \mathbf{x}_{act}]$, where $\mathbf{x}_{log} = [x_{log_1}, x_{log_2}, \ldots, x_{log_k}]$ and $\mathbf{x}_{act} = [x_{act_1}, x_{act_2}, \ldots, x_{act_j}]$ represent the design variables of the control system logic and the actuator, respectively. $p = k + j$ is the number of the whole design variables. The design space Ω_{ds} is defined by a set of all possible design variables as follows:

$$\Omega_{ds} = \{\mathbf{x} | 0 \leq x_i \leq 1; i = 1, ...p\} \tag{5.11}$$

where x_i represents the normalized value of a design variable. $\underline{f}(\mathbf{x})$ and $\underline{f}(\mathbf{c})$ express the vectors of objective driving dynamics performance measures and their associated threshold values, respectively. It should be considered that the analytical form of the function f is usually not known and it can be calculated numerically or by any black-box function.

By setting the threshold on each objective driving dynamics performance measures as follows:

$$f_i(\mathbf{x}) \leq f_{c,i} \tag{5.12}$$

The design space is restricted and divided into two regions, namely bad and good regions. A good region includes only possible design samples satisfying equation 5.12 and the bad region is depicted in figure 5.15.

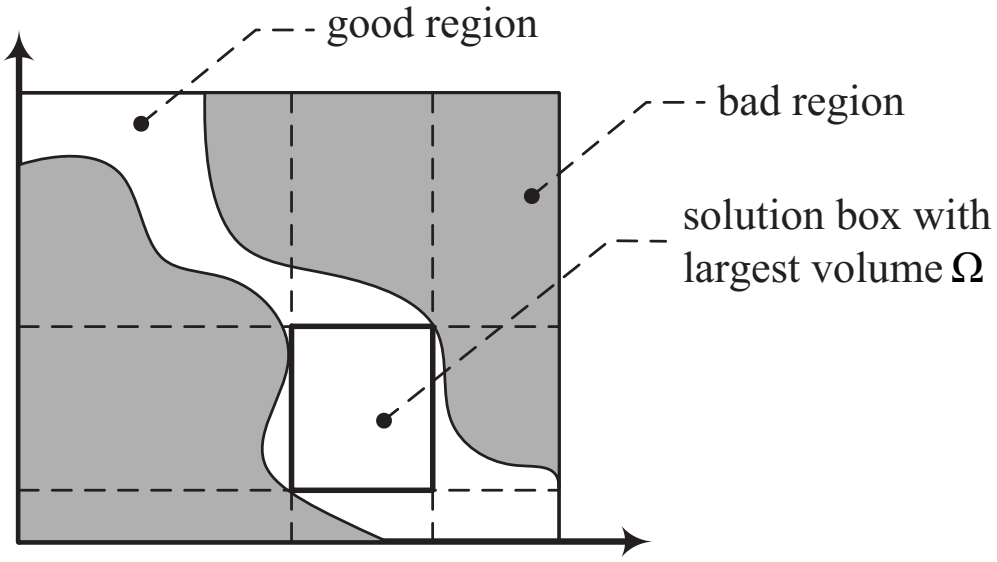

Figure 5.15: Representation of good and bad region in the design space

Target intervals will be sought to realize independent target regions for design variables and the product of the intervals will be maximized to find the largest box in the good region, which increases the design flexibility. In this way, we obtain an independent interval for each design variable, which makes it possible, that the realization of each design variable in such an interval does not depend on the solution interval of other design variables. As a result, the solution box calculated from the maximized intervals has the form:

$$\Omega = I_{act_1} \times I_{act_2} \times \ldots I_{act_j} \times I_{log_1} \times \ldots \times I_{log_k} \tag{5.13}$$

Where $I_{act_j} = \left[x^l_{act,j}, x^u_{act,j}\right]$ denotes an interval for the j-th variable of an actuator and $I_{log_i} = \left[x^l_{log,k}, x^u_{log,k}\right]$ for the k-th variable of the control system logic. x^l and x^u show the lower and the upper bound of each interval. The optimization problem can now be defined as follows:

$$\begin{aligned} &\max_{\Omega \subseteq \Omega_{ds}} \ (\mu(\Omega)) \\ &\text{subject to} \qquad f_i(x) \leq f_{c,i}, \quad i = 1, ..., n \end{aligned} \tag{5.14}$$

n is the number of objective driving dynamics performance measures. The volume of the good region to the entire volume of a determined box is called

fraction of good designs(fgd). A *solution box* is a box with a specific fraction of good designs, figure 5.15.

As it can be seen from figure 5.15, there are many solution boxes in a solution space. However, the largest solution box has a unique volume and is of an optimizing problem, equation 5.14. The algorithm to solve this optimization problem has been introduced in [77]. The optimization is done when the fgd of the solution box reaches a certain threshold.

The solution box of a high dimensional design space is identified by the representation of two dimensional plots with the projection of all other design variables on each two dimensional plot. This is called *interactive design space projection and modification* [78].

Interactive design space projection and modification

It is impossible to depict the solution space for more than three dimensions. However, there is a possibility to demonstrate such a solution space in form of two dimensional projections by sectional views. As soon as all design variables except two are fixed to a chosen value, the two variable dimensions can be plotted by a section through the high dimensional design space. Figure 5.16 shows a four dimensional design space. The depiction of the plot on the right side is carried out by fixing the variable 3 and 4 to the values 1.2 and 1.12, respectively. This is also done for the plot on the left side by setting the values of the variable 1 and 2 to 1970 and 0.53, respectively. Consequently, the plots can be seen as cuts through two dimensions. Each dot shows a certain design configuration. Green dots stand for good designs and all other colorful dots represent bad designs which violate a certain constraint of a driving dynamics performance measure.

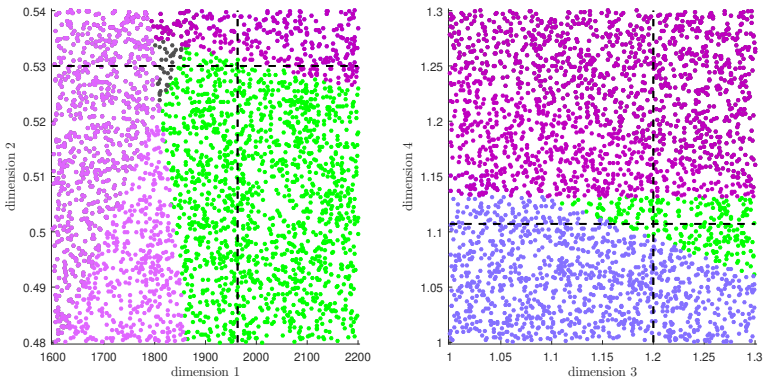

Figure 5.16: Two dimensional sectional views

Now if the variable 2 has a random value in a given interval, the plot of the variable-3-4 becomes blurry which is due to the projection of good and bad designs, lying beside each other, in the interval of the variable 2 on the sectional view of variable 3-4. Figure 5.17 clarifies this fact.

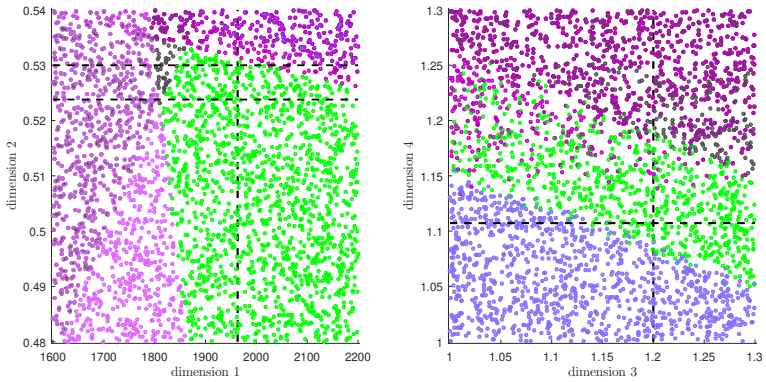

Figure 5.17: Collapsed two dimensional sectional views

Figure 5.18 shows a three dimensional example. The form of the solution space is depicted in dark gray and the largest solution box in a light gray. The projection of this box along the x_2 and x_3 dimensions results in the yellow rectangle and the blue rectangle, respectively.

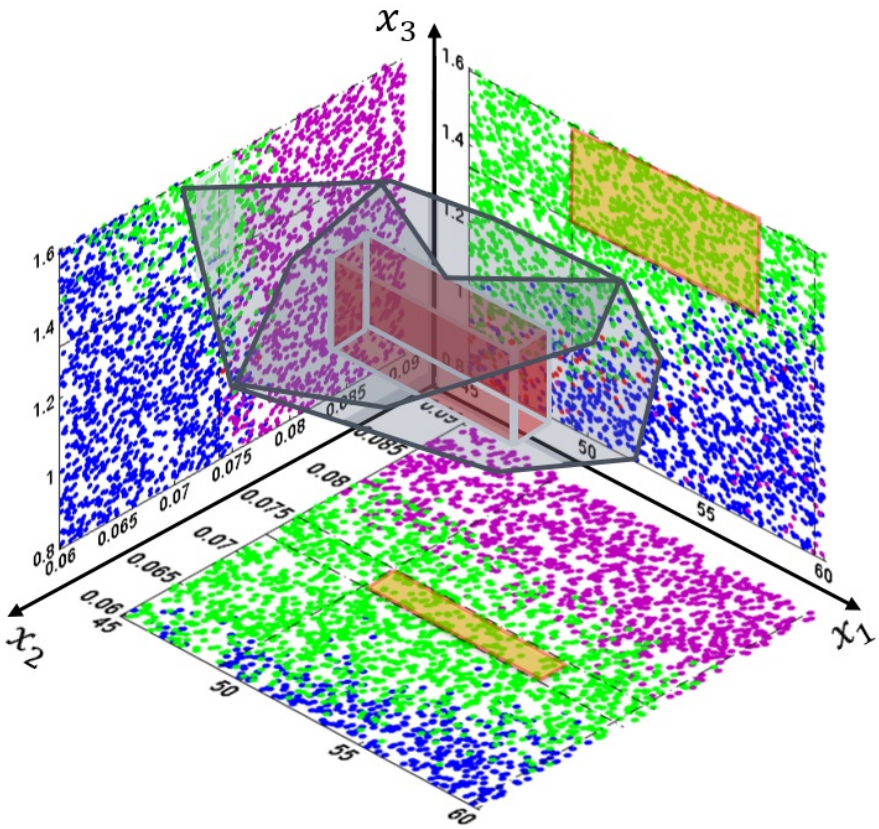

Figure 5.18: Solution-Box

5.4 Computing requirements on verification variables

After computing the solution box and calculating the solution intervals of design variables of control system logics and actuators, figure 5.19, the solution intervals of control system logics can be used directly for the parametrization of the control system. However, the requirements formulated on the design variables of the actuator should be transformed into the requirements of verification test variables, which are mentioned directly in a product requirement document(PRD). When the design variables of actuators are those of a functional model (empirical or semi-physical model).

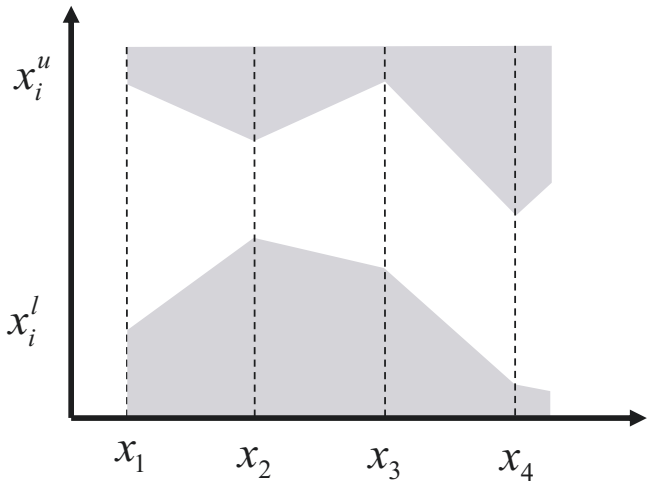

Figure 5.19: Solution intervals

Verification tests are the test-rig ones which have to be done on a physical product to prove whether it satisfies the defined requirements. As a result, three important verification tests with their associated verification variables for testing an actuator are introduced here:

1. Performance test.
2. Step response test.
3. Sine response test.

Performance test

This test should be done to determine the velocity limitation of an actuator regarding a counter force or torque. The input of this test is a step input with a high gradient toward high counter-forces or torques. Accordingly, the velocity of the actuator should be measured in the course of time with the interval of one second. In this way, the product can be tested. The characteristic of this test is the Force-Velocity characteristic curve of the actuator, depicted by the measurement points at each sample time, figure 5.20.

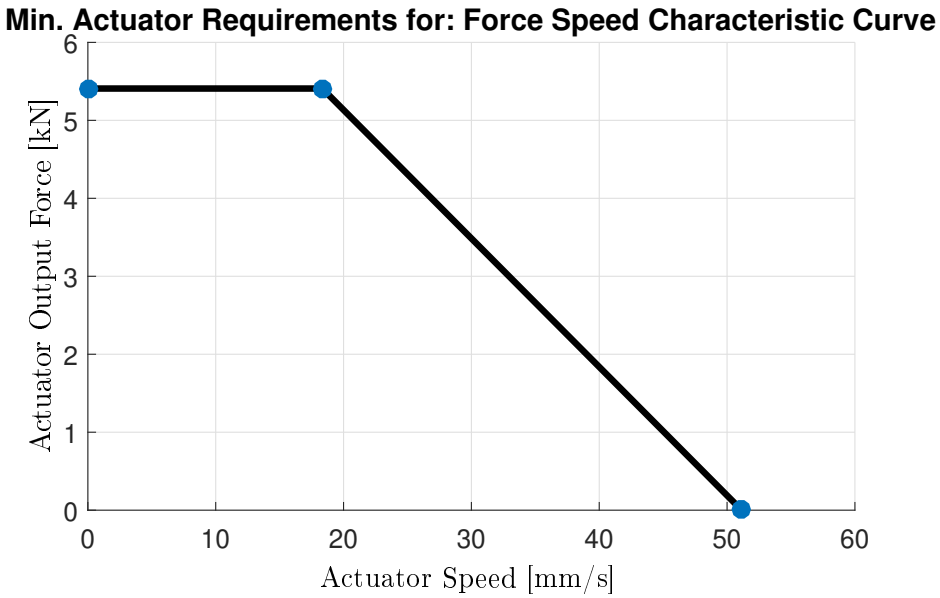

Figure 5.20: Force-Velocity characteristic curve of the performance test

Step response test

By a step response, some important characteristic parameters of an actuator in the time domain can be identified. The most important ones are:

- Overshoot
- Rising time (T_{ris})
- Stabilization time (T_{st})
- Static error (SE)

All these variables are shown in figure 5.21. For a transfer function of equation 4.1, all above-mentioned parameters can be calculated numerically. The overshoot depends only on the damping ratio of the second-order transfer function as follows [37]:

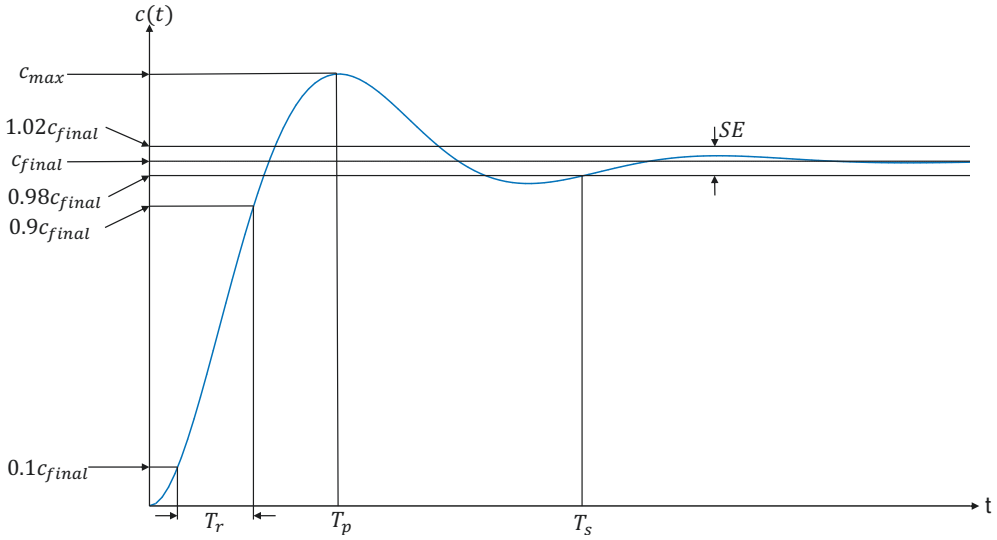

Figure 5.21: Step response and its characteristic parameters

$$\text{Overshoot}[\%] = \begin{cases} 100 \cdot exp\left(\dfrac{-D\,\pi}{\sqrt{1-D^2}}\right) & \text{for } D < 1 \\ 0 & \text{for } D \geq 1 \end{cases} \tag{5.15}$$

The rising time and stabilization time can also be calculated from the damping ratio and time constant of a second-order transfer function as follows [24]:

$$T_{st,5\%} = \begin{cases} -0.5 \log\left(\frac{1-D^2}{400}\right) \cdot \left(\frac{T_w}{D}\right) & \text{for } D < 0.7 \\ (6.6D - 1.6) \cdot T_w & \text{for } D \geq 0.7 \end{cases} \tag{5.16}$$

$$T_{ris,10-90\%} = \begin{cases} (1.2 - 0.45D + 2.6D^2) \cdot T_w & \text{for } D < 1.2 \\ (4.7 * D - 1.2) \cdot T_w & \text{for } D \geq 1.2 \end{cases} \tag{5.17}$$

Figure 5.22 shows these estimation functions. This figure has been depicted for a defined amplitude.

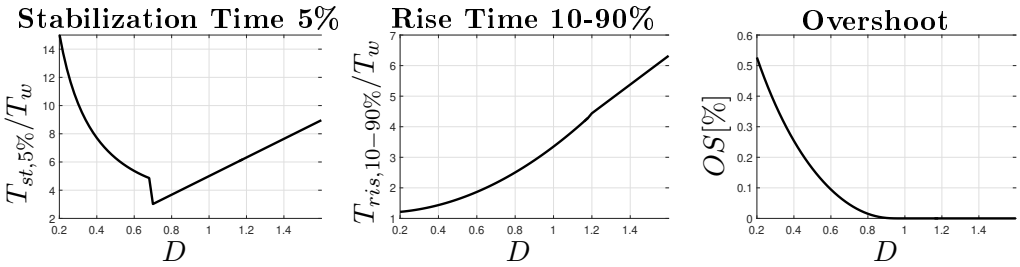

Figure 5.22: Behavior of each step response characteristic parameter with respect to the damping ratio

Sinus response test

According to this test, the behavior of an actuator in the frequency domain can be identified. The input for such a test is a sinusoidal signal with an increasing frequency and a defined amplitude.
The Bode diagram is the most important characteristic of this test, figure 5.23. The damping ratio and the time constant are the significant parameters changing the bode diagram of the second-order transfer function. The effect of the damping ratio can be summarized as follows: if the damping ratio of a second-order transfer function is less than 0.707, a resonance occurs at the natural frequency of the system. The natural frequency is $\omega_0 = \frac{1}{T_w}$. Inversely, if the damping ratio is larger than 0.707, no resonance occurs. The effect of the time constant (T_w) is on the place where the bode diagram falls off. By increasing T_w, the falling happens in the low frequencies.

Extension of the methodology

According to the V-model, figure 5.1, the requirements of a large-scale system can be broken down into the requirements formulated on the design variables of components (System Design). With the introduction of the verification tests in the last section, the dependency graph will be extended. In the extended dependency graph, a new level is added, the so-called component design. Accordingly, the so-called *Verification Variables* level, where verification variables of each verification test are indicated, are defined in the same level of the *Subsystem* level in the original V-model, figure 5.24. Below this, the physical *Components Details* are considered, which should be specified by the manufacturer. In this way, we formulate the requirements on the verification variables from the requirements of the large-scale system. The way in which the actuator is constructed physically will be surrendered to the manufacturer. But the

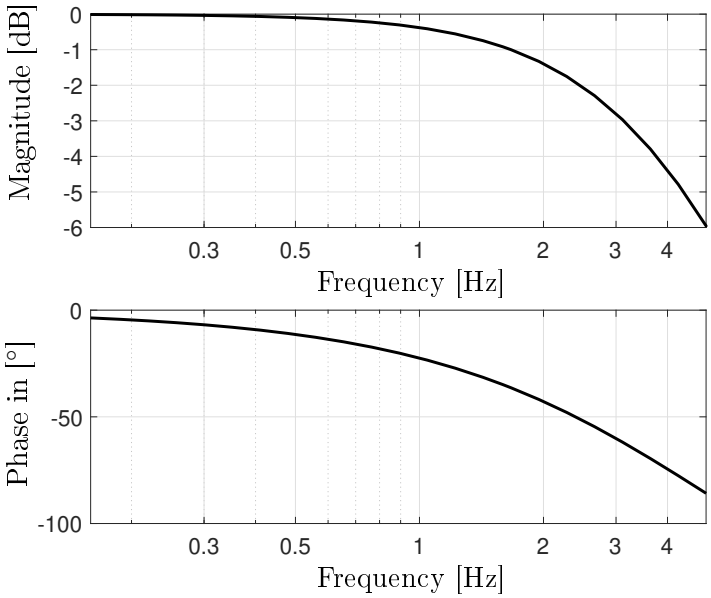

Figure 5.23: Bode diagram of a transfer function with a damping ratio larger than 0.707

manufacturer cannot deliver any kind of physical actuators, rather the realized actuator should be in the form of the predecessors.

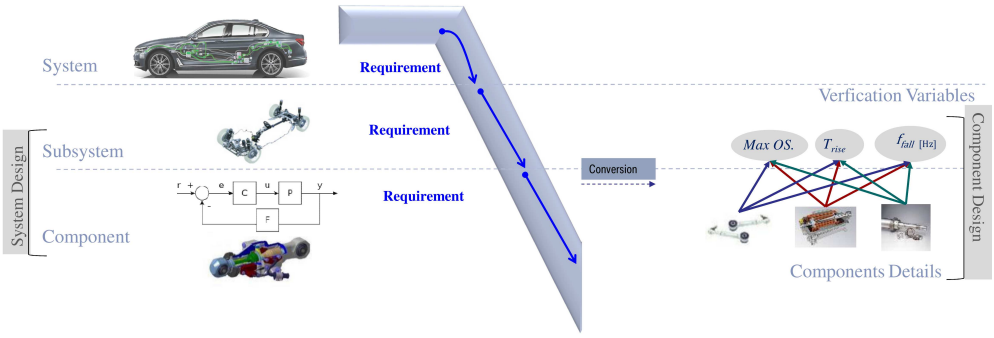

Figure 5.24: Extended V-Model for the design of actuators

Summary

In this chapter, we presented the robust design method for designing actuators and control systems, which can control the complexities in the development process and find optimized intervals for the design variables, rather than only one optimal set of the design variables. We have shown that the method is based on the so-called V-model in the system engineering. The method also includes three enablers, which are dependency graph, Bottom-Up mapping and Top-Down mapping. The dependency graph manages the know-how in the design procedure and is a graph in which the measurable system, subsystem, and component properties are depicted as vertices. Their dependencies or interactions were shown with an edge, whose direction shows which subsystems' and components' properties interact with each other and influence the measurable system properties. The Bottom-Up mapping is the quantitative evaluation of the influence of the inputs on the outputs. For this purpose, we needed a model which maps the inputs to the outputs. This model was the actuator and the control system model developed in the last two chapters. We explained the necessity of lots of simulations on this model, which provide information for the Top-Down mapping. As a consequence, we have clarified the idea of the Design of Experiments (DoEs) and how we can find the best method of DoEs based on the discrepancy factor. We also used the artificial neural networks and support vector machines as meta-models to model our original actuator and control system model. This was done to accelerate the optimization procedure. This optimization problem was to find the largest box, so-called solution box, inside of the solution space of the design variables. The solution space integrated different requirements from diverse disciplines. The edges of the solution box served as independent target regions for component properties. The solution box also enhanced the probability of finding a valid design in the solution space. We clarified that we have to convert the requirements formulated on the design variables into the requirements which should be formulated on the verification variables. As a consequence, we explained different verification tests and variables for the design variables of an actuator.

6 Application

6.1 Results for robust designing of the rear steering system

In this chapter, we apply the explained method in the previous chapter for formulating requirements on the design variables of the control system, introduced in chapter 4, and the design variables of ARS actuators, introduced in chapter 5. The first step is to determine the dependency graph. In this dependency graph, the relations between design variables of ARS actuator and the control system and the objective driving targets (CVs) are demonstrated. Moreover, the relations between CVs and the assessment indices (AIs) are depicted, figure 6.1.

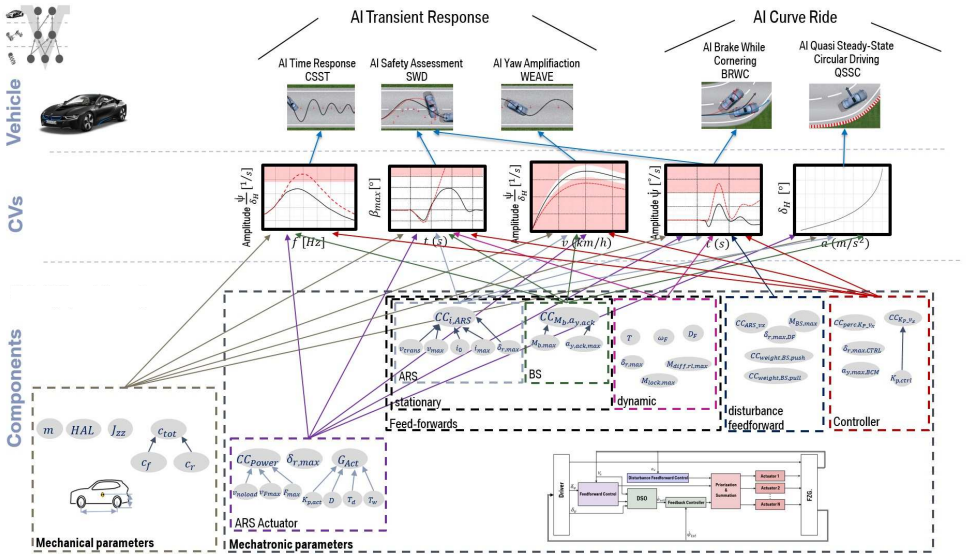

Figure 6.1: Dependency graph for the ARS actuator, the lateral dynamics control system, and the vehicle genes

As can be seen, the design variables of each function of the control system and the ARS actuator and the genes of the vehicle influence the determined CVs.

For example, all design variables of the static feedforward control of ARS can only effect the stationary objective driving dynamics performance measures, namely BRWC and QSSC.

Identification of design variables

In the second step, we have to identify the variables of the control system and the ARS actuator on which the requirements have to be formulated. The relevant parameters are as follows:

Table 6.1: Design variables of the ARS actuator and its associated control system

System	Parameter	Description
Stat. Feedforward	v_{trans} v_{max} $i_{ARS,stat.,min}$ $i_{ARS,stat.,max}$	Characteristic curve for the stationary feedforward (figure 3.2)
Dyn. Feedforward	T_f ω_f D_f	Factors for the desired transfer function $G_{\dot{\psi}\delta_f,des}$ (equation **??**)
Feedback	K_p	Feedback controller proportional gain (equation 3.45)
Actuator	K_p D T_w T_d F_{max} v_{noload} $v_{(F_{max})}$ $\delta_{r,max}$	Actuator LTI transfer function paramters (equation 4.1) Actuator force-speed characteristic curve (figure 6.2) Maximum permitted rear steering wheel angle
Genes	m $rearload$ h J_z	Vehicle mass Vehicle rear load ratio Vehicle CG-height Vehicle Inertia in z axis

It should be considered that the characteristic curve of the actuator has to have a unit form like the one in figure 6.2 for the design regarding the counter-forces in the same as well as opposite direction.

Accordingly, we deal with three different groups of design variables. The first group contains the genes of a vehicle introduced in table 6.1. They have their nominal values which are already predefined. A margin is left for them in order to ensure the robustness of the designed ARS actuator and its associated control system logic with respect to the changes in the vehicle genes which is the case, if we deal with different derivatives. The second group includes the design variables of the ARS actuator and the third group is made of the design variables of the control system logic relevant to the ARS.

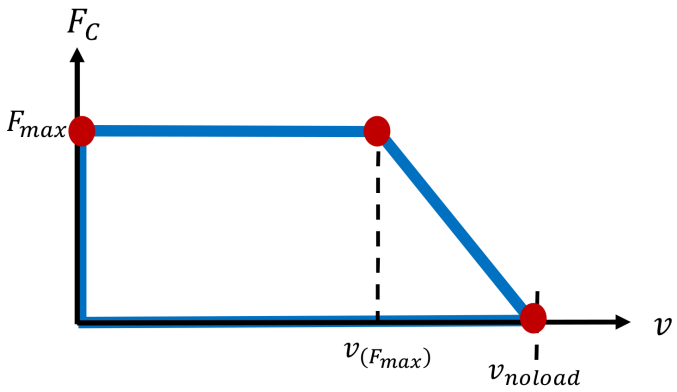

Figure 6.2: QSSC-CV

For all these design variables, we first sample the design space. The sampling method is scramble Halton sequence in this application and the number of sampling points is 4000.

The considered driving dynamics performance measures (CVs) are listed below:

Table 6.2: Considered objective driving dynamics performance measures

Maneuver	**CV**
QSSC	$EG_{H,nl}$ $a_{y,max}$
WEAVE	$(\dot{\psi}/\delta_H)_{stat,70}$ $(\dot{\psi}/\delta_H)_{stat,190}$ $(\dot{\psi}/\delta_H)_{stat,max}$
SWD	β_{max} $F_{z,min}$ SF_{MAX}
CSST	$T_{eq,\dot{\psi}/\delta_H}$ $(H/H_0)_{\dot{\psi}/\delta_H}$ T_{a_y/δ_H}
BRWC	$\Delta\dot{\psi}_{1s}$

For each of these CVs, the simulation of the whole system is executed 4000 times. Then, individual ANN and SVM are trained by each output (CV) and a set of inputs (design variables). Some results of ANN training are shown in figure 6.3 and figure 6.4.

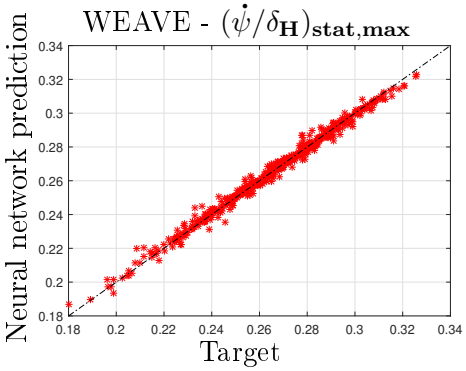

(a) R^2_{test}=0.985 $R^2_{training}$=0.990

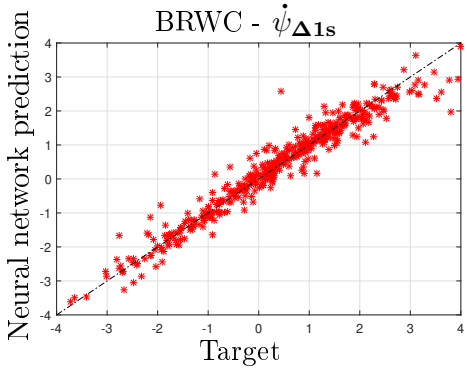

(b) R^2_{test}=0.920 $R^2_{training}$=0.949

Figure 6.3: Regression plots for CV $\dot{\psi}_{\Delta 1s}$ and $(\dot{\psi}/\delta_H)_{stat,max}$

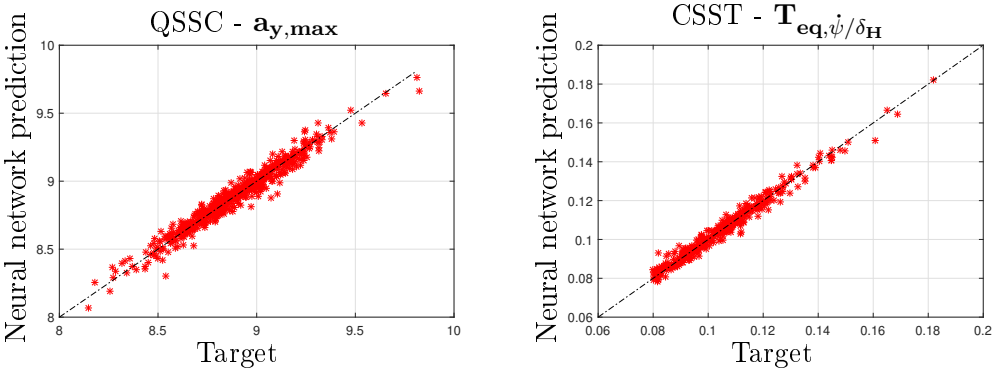

(a) R^2_{test}=0.940 $R^2_{training}$=0.956 (b) R^2_{test}=0.960 $R^2_{training}$=0.975

Figure 6.4: Regression plots for CV $a_{y,max}$ and $T_{eq,\dot{\psi}/\delta_H}$

As we can see from figure 6.3 and figure 6.4, the model quality of the training data ($R^2_{training}$) is larger than the the model quality of the test data (R^2_{test}), which means, there is no overfitting. The model quality of all computed response surfaces for all CVs is more than 0.9, which means, the requirement identified in the last chapter regarding the model quality is met. The misclassification of each SVM for each CV is listed below:

Table 6.3: Misclassification of all trained SVM for each CV

CV	**Constraints of CVs**
$EG_{H,nl}$	1.1
$a_{y,max}$	1.1
$(\dot{\psi}/\delta_H)_{stat,70}$	1.1
$(\dot{\psi}/\delta_H)_{stat,190}$	8
$(\dot{\psi}/\delta_H)_{stat,max}$	4.2
β_{max}	12.8
$F_{z,min}$	13.7
$T_{eq,\dot{\psi}/\delta_H}$	15
$(H/H_0)_{\dot{\psi}/\delta_H}$	11.5
T_{a_y/δ_H}	12
$\Delta\dot{\psi}_{1s}$	12.1

All the misclassifications are less than 15; hence the requirement regarding the misclassification introduced in the last chapter is satisfied.

In the third step, we have to set constraints on the CVs. By setting lower and

upper bounds on each CV, the solution space will be formed. As mentioned before, the largest volume of the solution box is unique. But there could be more than one box in the solution space which has the largest volume. For instance, let us look at the solution space of two design variables, the actuator transport delay T_d, and the natural frequency factor of the dynamic feedforward control w_f, figure 6.5.

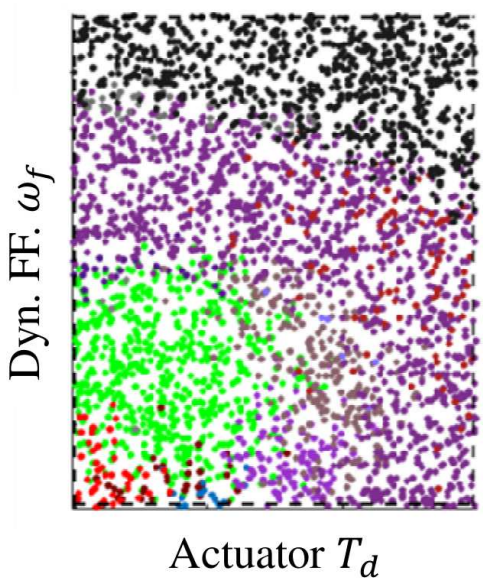

Figure 6.5: Solution space of the actuator's transport delay and natural frequency factor of the dynamic feedforward control

Based on the introduced optimization algorithm in the last chapter, the algorithm seeks a solution box with the maximum size and does not consider the meaning of design variables. For instance, the solution box illustrated in figure 6.6 restricts the lower bound of the transport delay interval. It means, the actuator transport delay must not begin from zero, which implies slow performance of the actuator regarding its input. But on the other hand, the flexibility for the parameterization of the natural frequency factor has been improved by extending its permissible interval with respect to this solution box. However, such a solution box is undesirable, as we require a high-performance actuator preferably with no delay and of course more flexibility for designing an actuator.

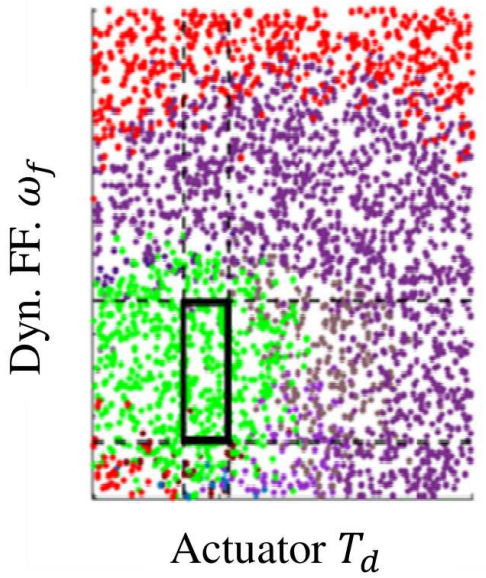

Figure 6.6: Solution box with the largest interval for the natural frequency factor of the dynamic feedforward control

Balancing design variables of the rear steering actuator and the control system logic

Therefore, the algorithm has to be forced to avoid such undesirable computation effects. As a result, we have to balance the actuator and the control system logic design variables before starting the optimization procedure. Accordingly, we fix the lower bound of the actuator transport delay T_d to zero in order not to allow the optimization algorithm to find a box which restricts the actuator performance, i.e. an interval for the transport delay is calculated which does not start from zero. Based on the same reason, we also fix the lower bound of the time constant T_w of the actuator transfer function. The lower bound of the damping ratio D has also to be fixed to 0.707 in order to prevent a resonance magnification [46]. In order to prevent limiting the maximal actuator power, the upper bounds of parameters v_{noload} and F_{max} have also to be fixed to their defined upper values.

Consequently, all constraints demanded for finding the largest box can be summarized mathematically as follows:

$$\max_{\Omega \subseteq \Omega_{ds}} \quad \mu(\Omega)$$

$$\text{subject to} \quad \begin{cases} f_i(\mathbf{x}) \leq f_{c,i}, & i = 1, ..., n_1 \\ g_j(\mathbf{x}) = 1, & j = 1, ..., n_2 \\ h_k(\mathbf{x}) \leq h_{c,k}, & k = 1, ..., n_3 \end{cases} \quad \text{for all } \mathbf{x} \subseteq \Omega \tag{6.1}$$

where f_i is a predicted function of the i-th objective driving dynamics performance measures by ANN, g_j is a classification of the j-th objective driving dynamics performance measures and h_k represents additional boundary constraints formulated on the k-th design variables.

Now, by setting all the constraints and executing the optimization, the largest solution box is found for $ffd \geq 95\%$. Figure 6.7 shows the projection of the computed box for some design values based on the interactive design space projection and modification. The volume of the computed box is $7.5e^{-10}\%$ of the entire design space volume. At the first glance, it seems to be very small, but it still gives us flexibility in the procedure of the actuator design and the adjustment of the control system parameters. In addition, such a small volume proves that finding the solution box manually is almost impossible. The intervals of the design variables (normalized), obtained from the solution box, are depicted in figure 6.8.

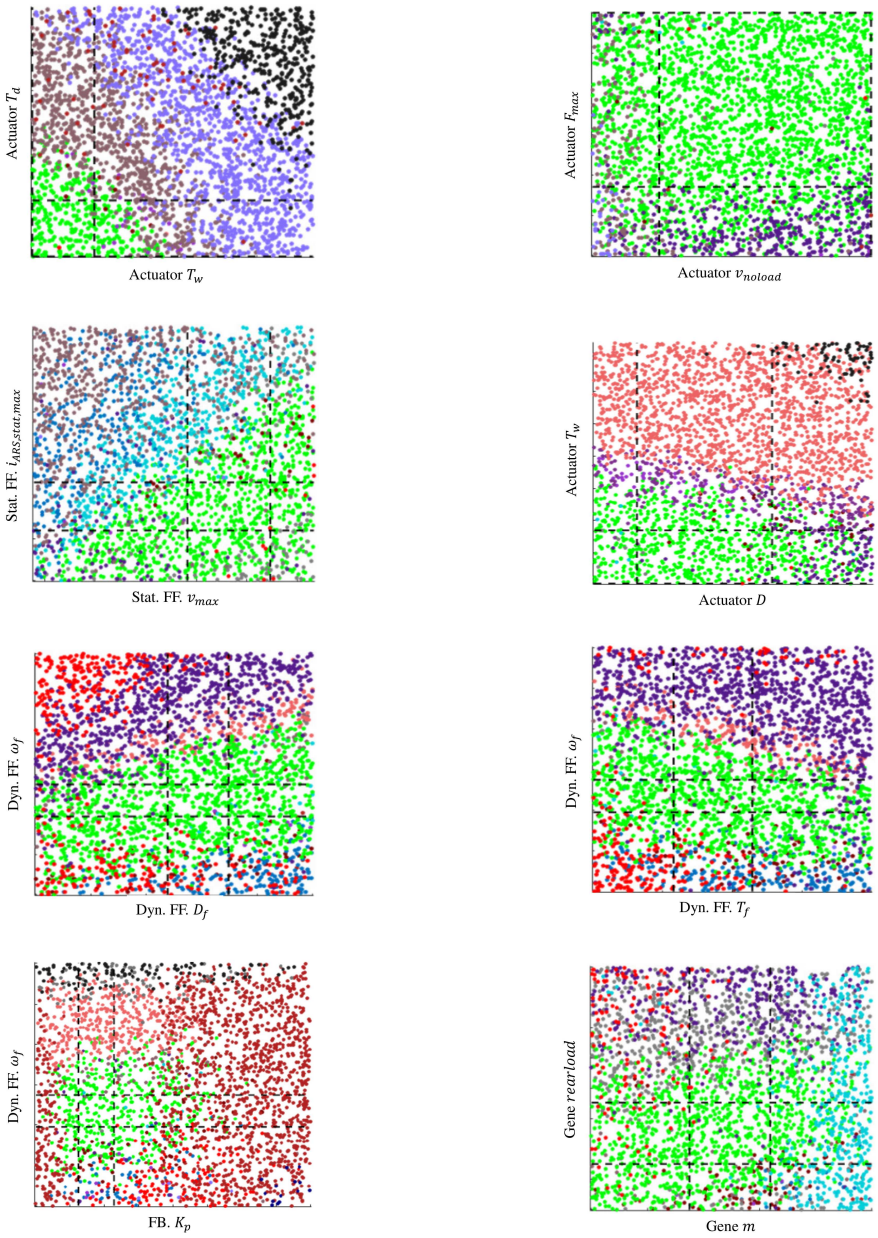

Figure 6.7: Projection of the solution box for some considered design variables

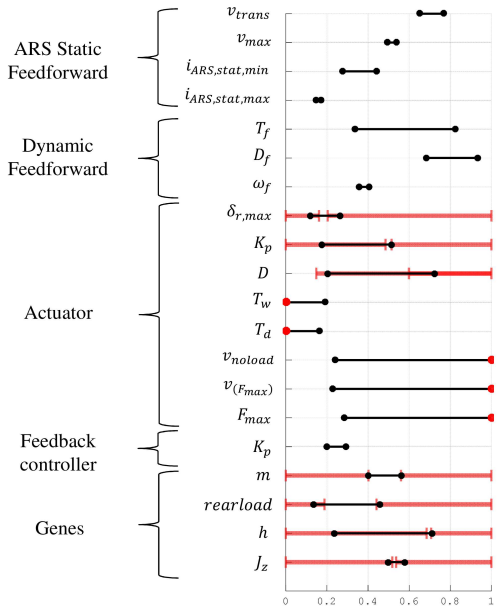

Figure 6.8: ARS Solution intervals (normalized)

The parameters of the dynamic feedforward control and the feedback controller can be adjusted now with respect to the determined intervals. The characteristic curve of the ARS static feedforward control can also be laying in the yellow area of figure 6.9.

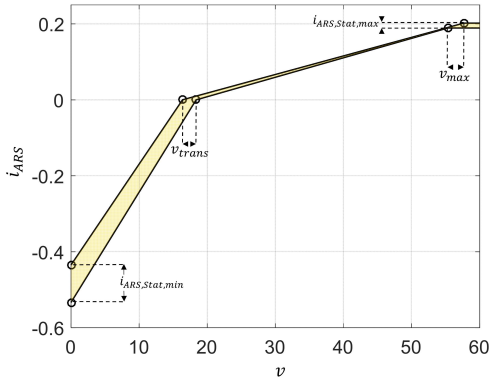

Figure 6.9: Solution space for the characteristic curve of the ARS static feedforward control

Computing requirements on verification test variables of ARS actuator

As was explained in the previous chapter, the solution intervals of the actuator design variables should be converted into requirements on the verification test variables of the actuator. These requirements can be then specified in the product requirement document (PRD) of the actuator, which has to be satisfied by the supplier. As mentioned before, these requirements are formulated regarding the verification tests. The verification tests have to be carried out on the test-rig depicted in figure 6.10. This has to be done for a selected maximum rear steering angle from its solution intervals. The following requirements will be calculated for $\delta_{r,max} = 2.7°$, the maximum of the rear steering angle interval.

Figure 6.10: Test-rig setup of ARS

Requirements of the ARS actuator with respect to performance test

It is definitely possible to compute solution intervals for the verification test variables from the solution intervals of the design variables as well. However, it

is enough to define the worst-case of the actuator response to the verification tests with respect to the calculated solution intervals. Before calculating the worst-case of the actuator force-velocity characteristic curve, it has to be mentioned that the upper bound of this design variable (F_{max}, v_{noload}) was fixed to a constant value during the optimization process. This constant value should also be given to suppliers, as they may not construct an actuator with the performance more than this constant value. Jumping back to the calculation of the requirements on the verification test variables, the worst-case of the actuator force-velocity characteristic curve occurs by the lower bounds of the solution intervals of the F_{max}, v_{noload} and $v_{(F_{max})}$. Figure 6.11 depicts the minimum ARS actuator force-speed characteristic curve. The red area is the prohibited area. It means, a supplier must construct an actuator whose force-velocity characteristic curve is located above this area.

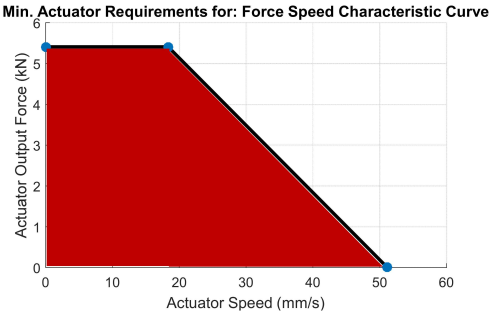

Figure 6.11: Minimum ARS actuator force-velocity characteristic curve

Requirements of the ARS actuator with respect to step response test

Generally, it is desirable to have less overshoot, less rising time, less stabilization time, and less time delay (quick response to the step input). The fact is, every mechanical component, e.g. actuator, definitely has some overshoot, rising time, stabilization time and time delay because of it's physical construction limits. As a consequence, the worst-case of the actuator response to the step input with respect to the calculated solution intervals leads to the maximum overshoot, maximum time delay, maximum stabilization time, maximum rising time, and maximum stationary error. All these worst-cases subsequently satisfy the upper and lower bounds of the design variables solution intervals.

Inserting the lower bound of the damping ratio interval D into equation 5.15 leads to the maximum overshoot. In this manner, it guarantees the satisfaction of the lower bound of the solution interval of the damping ratio, D.

The stabilization time is dependent on the damping ratio and the time constant regarding equation 5.16. Accordingly, the maximum stabilization time is calculated from the lower bound of the determined interval of the damping ratio, D, and the upper bound of the time constant, T_w, solution interval; hence, the maximum stabilization time guarantees the realization of the upper bound of the time constant solution interval.

With respect to equation 5.17, the worst-case of the rising time occurs by the upper bounds of the damping ratio and the time constant interval. Consequently, the maximum rising time realizes the upper bound of the solution intervals of D and T_w.

Moreover, it is desirable to have a stationary error as small as possible. As a result, the maximum possible permitted stationary error has to be given to suppliers. This arises out of the minimum between the ratios of the upper and lower bound of the solution interval of the stationary gain K_p and 1.

Finally, the maximum time delay is measured by the upper bound of the determined intervals of T_d. Here, it should again be mentioned that the lower bound of the T_d was fixed during the optimization.

It should also be noticed that calculating all the worst-case requirements has been carried out regarding worst-case of the force-velocity characteristic curve. In other words, after inserting all these upper and lower bounds of the determined intervals into the transfer function of the ARS actuator and setting the step as input, the worst-case of the force-velocity should be built as the rate-limiter after the output of the transfer function, shown in figure 4.17. Then, all the requirements are formulated for the output as follows:

Table 6.4: ARS actuator step response requirements

Force speed curve parameters	**Value**
Max. Time delay	$25ms$
Max. Overshoot	0.0%
Max. Stabilization Time	$405ms$
Max. Rising Time	$319ms$
Max. Stationary Error	0.3%

Requirements of the ARS actuator with respect to sine test

Here, the test is defined with an increasing frequency from 0.1 to 5 Hz. The amplitude is considered as 1°. As mentioned in the previous chapter, the requirements should be formulated on the bode diagram. It is desirable that the

decay of the magnitude and the phase shift takes place in higher frequency, but not in any high frequency. In this manner, the actuator performs well in lower frequencies and the output of the actuator has no phase shift and amplitude decay in low frequencies. As a consequence, the requirements of this test are defined for the upper and lower bound of the bode diagram. The better the phase response, the better the performance of the actuator in the frequency domain is. Therefore, the phase response of the actuator may not be worse than the determined worst-case. It means, the frequency response of the ARS actuator should be equal or better than this worst response. The decay of the magnitude and the phase shift of the bode diagram of a second-order transfer function occurs at the natural frequency of the system [45]. The natural frequency is equal to $\omega_0 = \frac{1}{T_w}$. In other words, the smaller the natural frequency (the larger the time constant) is, the sooner the decrease of the amplitude and phase shift takes place. As a consequence, the worst-case of the bode-diagram takes place on the upper bound of the optimized time constant interval. Concerning the damping ratio D, the larger the damping ratio is, the earlier the magnitude response decreases. Subsequently, the worst-case of the bode diagram occurs by the upper bound of the optimized damping ratio interval; hence, the worst-case of the bode-diagram realizes the upper bounds of the D and T_w solution intervals. However, as mentioned before, the decay of magnitude and phase shift may not occur at ordinary high frequency. So, the lower bounds of D and T_w result in the upper bound of the bode-diagram. Accordingly, the permitted bode-diagram is between the two red areas depicted figure 6.12.

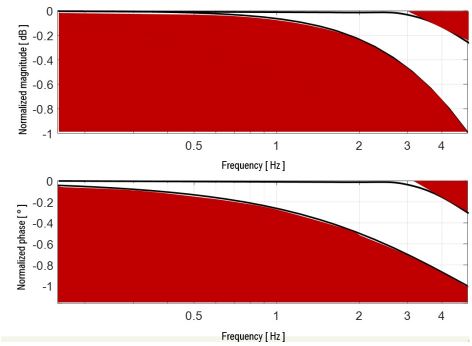

Figure 6.12: Frequency response requirement for the ARS actuator

Summary

In this chapter, we applied the explained method in the previous chapter on the design variables of the ARS actuator and its associated control system. We have identified the design variables and the driving dynamics performance measures (CVs). We depicted the dependency graph between these design variables and the CVs. We also showed which limits the optimization of the actuator's design variables have to overcome them, we added another constraint to the goal function of the optimization problem. We then found the solution intervals for the design variables of the control systems. We have transformed the computed solution intervals of the actuator into the solution intervals of the verification variables. We also explained that it suffices to formulate the worst requirements on the verification variables in the PRD. As a result, we clarified how to calculate the worst requirements from the solution intervals for the verification variables.

7 Conclusion and future work

The customer requirements regarding the vehicle dynamics increase very quickly. The vehicle manufacturer should also be able to react quickly to the varying requirements and adapt the developments to them. One way to develop the vehicle dynamics with respect to the new requirements is to build different components physically, set them up in a prototype vehicle, and drive it. In this way, the development takes a very long time, since if the prototype vehicle does not drive as it should, other components should be built and set up. This kind of iterative development is not suitable anymore for an agile reaction to the varying customer requirements; hence, it is necessary to digitalize the vehicle dynamics development as much as possible. The simulation models of different components accelerate the development process significantly. Consequently, one of the aims of this dissertation was to design simulation models of the control system and actuator for the preliminary design of the vehicle dynamics in the early stages of the vehicle dynamics development. As the lateral dynamics is of high importance with respect to the ride and safety, we concentrated on the simulation model development of the control systems and actuators for the vehicle lateral dynamics. The proposed control system was made up of different units, namely static and dynamic feedforward control, disturbance feedforward control, driving situation identifier (DSI), feedback controller, and the priorization and allocation unit. The static feedforward control was designed for each actuator individually. However, the dynamic feedforward control, the disturbance feedforward control, and the feedback controller were centralized and designed independently of available actuators. Each of them generates a yaw moment based on its inputs and functions. The priorization and allocation unit then attempts to distribute and allocate all the generated yaw moments on different actuators based on the explained daisy chain method and with respect to the driving situation recognized by the DSI. In order to react quickly to the varying requirements of customers, it is necessary to be able to translate these requirements into the vehicle dynamics requirements. For this purpose, we introduced various domains of the vehicle lateral dynamics and their assessment indices (AIs). These AIs are closely connected to the customer requirements. For each Al, we presented the objective driving dynamics performance measures (CVs). In other words, once the customer requirements change, the AIs will change and

hence the CVs. We showed, the CVs are affected directly by components, for example, assembled in the chassis. With these simulation models and defined CVs, we demonstrated, how the performance of the vehicle will be enhanced by applying the mechatronic system, i.e. the control systems and the actuators, in the chassis. As mentioned before, this dissertation does not definitely deal with one vehicle, but with different derivatives of a vehicle. In addition, physical components such as actuators are not designed and constructed for each vehicle individually. Rather, actuators must be designed so robustly that they can deal with all derivatives. Besides, actuators and control systems affect each other, both influence the CVs and are designed by different teams. Each team tries to reach the defined requirements on the CVs by developing its own component separately. In this way, there is a risk that the vehicle does not achieve the defined requirements due to the goal conflicts caused by the components, since each component was designed separately. Moreover, designing optimized components with respect to the defined requirements on the CVS might lead to the fact that the construction of them is either impossible or highly expensive.

So, using a simulation model and CVs for the development process is an effective way for the development and reduces the development time significantly but not enough to control the above-mentioned complexities during the digital development of the vehicle dynamics in the preliminary stages of the development. Accordingly, we presented the robust design of actuators and control systems method, which can control the complexities in the development process and find optimized intervals, rather than only one optimal set of design variables of actuators and control systems with respect to the requirements formulated on the CVs. The proposed method was based on the V-Model and had three enablers, namely, the dependency graph, the evaluation step (Bottom-Up mapping) and the design step (Top-Down mapping). We explained how the dependency graph manages the know-how during the development process. It clarifies, what the design variables and performance measures are and how the design variables should be verified.

The evaluation step addressed the question how to quantify the performance of the large scale system, i.e. the vehicle dynamics, with the control system and the actuator in this dissertation. In this step, we introduced the idea of the Design of Experiments (DoEs), necessary for the large number of simulations. Furthermore, we explained, that it is highly time-consuming to optimize our whole system for the large number of simulations. Accordingly, we proposed the idea of the mathematical surrogate models, such as artificial neural networks (ANNs) and support vector machine (SVM), which approximate highly nonlinear systems and are much less time-consuming for the optimization problem.

In the design step, we illustrated how to break down the requirements of the

CVs into the requirements of the design variables quantitatively. We explained the design space and the solution space of the design variables. The solution box was then proposed, which decouples the requirements of design variables of the control system from the actuators. There, we formulated the optimization problem statement, which finds the largest solution box in the n-dimensional solution space. The interactive design space projection and modification was also cleared up. It demonstrates an n-dimensional solution space in form of two dimensional projections by sectional views. In this method, we also showed, which verification tests and variables are necessary for verifying the design variables of the actuator functional model. Additionally, we explained how to transform the requirements formulated on the design variables of the actuator functional model into the requirements of the verification variables.

Finally, we applied the robust design of actuators and control systems method on the design of the active rear steering (ARS) actuator and the control system. There, we identified the design variables of the ARS actuator and the control system and defined CVs which have to be considered. Afterwards, we drew the dependency graph for these design variables and CVs and computed the ANNs and SVM models from the simulation results of the vehicle model with the actuator and control system model. Also, we showed that the optimization problem does not conceive any balance between actuator and control system parameters. Therefore, we clarified the balancing method between the design variables of the ARS actuator and its associated control system and changed the optimization problem statement respectively. We calculated then the solution intervals for these design variables based on the requirements of the defined CVs. In addition, we pointed out, why it is enough to just identify the worst requirements on the verification variables of the ARS actuators. In the end, we depicted the solution box and the solution intervals of the ARS actuator and its associated control system design variables. We also demonstrated the requirements on the verification variables of the ARS actuator.

Future Work

We propose the following research areas to enhance and expand the models and the methods proposed in this dissertation.

1. *Driving Maneuvers and the objective driving performances:* Since the control concepts have been proposed for the lateral dynamics, we have introduced the driving maneuvers and the objective driving dynamics performance measures regarding the lateral dynamics. They can also be expanded to the longitudinal and vertical dynamics. It means, for the

vertical and the longitudinal dynamics, we can also objectify the behavior of a vehicle from different subjective driving experiences done by the test drivers on the side and find out some objective driving performance measures for these two areas of vehicle dynamics.

2. *Vehicle dynamics control system and actuators:* As we clarified, simulation models of the control system and actuators are necessary for the digital development of the vehicle dynamics. The mechatronic chassis system presented in this dissertation offers a structure for the development of other vehicle dynamics control systems with high compatibility and reproducibility. In other words, the simulation models of the vertical and longitudinal vehicle dynamics control systems can also be developed and incorporated into the proposed lateral vehicle dynamics control system. In this way, we can also investigate the behavior of the vehicle with respect to the driver input in the preliminarily phase of the vehicle dynamics development, if all control systems are available in the vehicle. Accordingly, it can be figured out in which situations and driving maneuvers which control system has the most impact on the behavior of the vehicle. The proposed method in this dissertation for modeling an actuator can be used for modeling almost all actuators in the chassis. Therefore, the actuators relevant to the vertical and longitudinal vehicle dynamics can also be modeled functionally based on this method. These models can also be incorporated into the proposed mechatronic chassis system structure presented in this dissertation.

3. *Robust design of actuators and control systems:* The generic method of the development by means of the solution spaces is not only proper for the development of actuators and control systems together, but also it can only be applied for the parametrization of the control systems with respect to the objective driving dynamics performance measures. It means, if the actuators are available and there is no need to develop actuators, the generic method can be used for parametrization of the available control systems in the vehicle. In this way, we reduce the time of the development significantly. Because there are cases, where the vehicle and the actuators are developed but the control systems have not been parametrized yet. If a test driver begins without having a good initial set of parametrization, it would take weeks to find such a a good set. However, applying this method can deliver the test driver a good initial set of parametrization.

4. *Expansion of the robust design of actautors and control systems:* So far we have clarified that the box-shaped solution spaces are the Cartesian

product of the permissible intervals for the design variables of the control system and the actuator. Sometimes, the size of these intervals for important design variables is not large enough to cope with all uncertainty and to ensure the feasibility. For example, the permissible intervals of the actuator's design variables must be feasible and able to cope with the uncertainty in the design procedure. However, the design variables of the control system can be adjusted arbitrarily and in a manner to satisfy the requirements on the objective driving dynamics performance measures; hence, a new approach is needed, where the design variables are divided into two groups, early- and late-decision variables. Accordingly, the interval of the early-decision design variables such as the actuator's variables can be expanded, since the late-decision variables such as control systems' variables are associated with intervals where we can adjust them to any specific value. The expansion of the intervals of the actuator's design variables leads to more flexibility and feasibility in the design procedure.

Bibliography

[1] *Roadvehicles - braking in a turn - open-loop test method.* Technical Report ISO 7975, International Organization for Standardization, 1985.

[2] *Roadvehicles - test method for the quantification ofon-centre handling, part 1: Weave test.* Technical Report ISO 13674 - 1, International Organization for Standardization, 2002.

[3] *Sine with dwell.* Technical Report FMVSS 126, The United States National Highway Traffic Safety Administration, 2008.

[4] *Passenger cars - steady-state circular driving behaviour - open-loop test methods.* Technical Report ISO 4136, International Organization for Standardization, 2012.

[5] Ahmed, Nasir and Kamisetty Ramamohan Rao: *Fast fourier transform.* In *Orthogonal Transforms for Digital Signal Processing*, pages 54–84. Springer, 1975.

[6] Alberer, Daniel, Hakan Hjalmarsson, and Luigi Del Re: *Identification for automotive systems*, volume 418. Springer Science & Business Media, 2011.

[7] Åström, Karl Johan and Tore Hägglund: *PID controllers: theory, design, and tuning*, volume 2. Isa Research Triangle Park, NC, 1995.

[8] Bardawil, Carine, Reine Talj, Clovis Francis, Ali Charara, and Moustapha Doumiati: *Integrated control for vehicle lateral dynamics improvements using second order sliding mode.* In *Control Applications (CCA), 2014 IEEE Conference on*, pages 322–327. IEEE, 2014.

[9] Beiker, Sven and Manfred Mitschke: *Verbesserungsmöglichkeiten des fahrverhaltens von pkw durch zusammenwirkende regelsysteme.* ATZ-Automobiltechnische Zeitschrift, 103(1):38–43, 2001.

[10] Boser, Bernhard E, Isabelle M Guyon, and Vladimir N Vapnik: *A training algorithm for optimal margin classifiers.* In *Proceedings of the fifth annual workshop on Computational learning theory*, pages 144–152. ACM, 1992.

[11] Bradawil, Carine, Reine Talj, Clovis Francis, Ali Charara, and Moustapha Doumiati: *Integrated control for vehicle lateral dynamics improvements using second order sliding mode*. 2014 IEEE Conference on Control Applications (CCA), pages 322–327, October 2014.

[12] Breuer, Bert and Karlheinz H Bill: *Bremsenhandbuch: Grundlagen, Komponenten, Systeme, Fahrdynamik*. Springer-Verlag, 2006.

[13] Bünte, Tilman: *Die anwendung des parameterraumverfahrens auf ortskurvenkriterien (the application of the parameter space method to frequency loci criteria)*. at-Automatisierungstechnik Methoden und Anwendungen der Steuerungs-, Regelungs-und Informationstechnik, 49(12/2001):547, 2001.

[14] Bünte, Tilman, Dirk Odenthal, Bilin Aksun-Güvenç, and Levent Güvenç: *Robust vehicle steering control design based on the disturbance observer*. Annual reviews in control, 26(1):139–149, 2002.

[15] Burges, Christopher JC: *A tutorial on support vector machines for pattern recognition*. Data mining and knowledge discovery, 2(2):121–167, 1998.

[16] Busch, Jochen and Dieter Bestle: *Optimization of a new steering strategy to improve the driving behavior of cars*. 2011.

[17] Chipperfield, Andrew, Peter Fleming, Hartmut Pohlheim, and Carlos Fonseca: *Genetic algorithm toolbox for use with matlab*. 1994.

[18] Decker, Medon: *Zur beurteilung der querdynamik von personenkraftwagen*. Diss., TU München, 2009.

[19] Dettlaff, Kilian, Jochen Wiedemann, Uli Schaaf, Ingo Scharfenbaum, and Andreas Wagner: *The influence of the modeling depth of active chassis systems with respect to the development stage and their interaction with driving characteristics*. 6th International Munich Chassis Symposium 2015, pages 103–121, 2015.

[20] Diermeyer, Frank: *Methode zur Abstimmung von Fahrdynamikregelsystemen hinsichtlich Überschlagsicherheit und Agilität*. PhD thesis, Dissertation, TU München, 2008.

[21] Donges, E, R Auffhammer, P Fehrer, and T Seidenfuß: *Funktion und sicherheitskonzept der aktiven hinterachskinematik von bmw*. Automobiltechnische Zeitschrift, 92(10), 1990.

[22] Eichstetter, Markus: *Solution spaces for damper design in vehicle dynamics*. In *5th International Munich Chassis Symposium 2014*, pages 107–132. Springer, 2014.

[23] Eslamian, M, G Alizadeh, and M Mirzaei: *Optimization-based non-linear yaw moment control law for stabilizing vehicle lateral dynamics*. Proceedings of the Institution of Mechanical Engineers, Part D: Journal of Automobile Engineering, 221(12):1513–1523, 2007.

[24] Franklin, Gene F, J David Powell, Abbas Emami-Naeini, and J David Powell: *Feedback control of dynamic systems*, volume 3. Addison-Wesley Reading, MA, 1994.

[25] Gevers, Michel: *Towards a joint design of identification and control?*

[26] Greger, Matthias: *Auswirkungen einer variablen Momentenverteilung auf die Fahrdynamik*. PhD thesis, Dissertation, TU München, 2006.

[27] Gunn, Steve R *et al.*: *Support vector machines for classification and regression*. ISIS technical report, 14:85–86, 1998.

[28] Haskins, Cecilia, Kevin Forsberg, Michael Krueger, D Walden, and D Hamelin: *Systems engineering handbook*. In *INCOSE,*, 2006.

[29] He, Junjie, David A Crolla, Martin C Levesley, and Warren J Manning: *Integrated active steering and variable torque distribution control for improving vehicle handling and stability*. Technical report, SAE Technical Paper, 2004.

[30] Heissing, Bernd, Metin Ersoy, and Stefan Gies: *Fahrwerkhandbuch*. Vieweg+ Teubner Verlag, Wiesbaden, 2007.

[31] Iooss, Bertrand, Loïc Boussouf, Vincent Feuillard, and Amandine Marrel: *Numerical studies of the metamodel fitting and validation processes*. arXiv preprint arXiv:1001.1049, 2010.

[32] Isermann, Rolf: *Fahrdynamik-Regelung: Modellbildung, Fahrerassistenzsysteme, Mechatronik*. Vieweg+ teubner Verlag, 2006.

[33] Jain, Anil K, Jianchang Mao, and K Moidin Mohiuddin: *Artificial neural networks: A tutorial*. Computer, 29(3):31–44, 1996.

[34] Kaiser, Gerd, Frédéric Holzmann, Benoît Chretien, Matthias Korte, and Herbert Werner: *Torque vectoring with a feedback and feed forward*

controller-applied to a through the road hybrid electric vehicle. In *Intelligent Vehicles Symposium (IV), 2011 IEEE*, pages 448–453. IEEE, 2011.

[35] Kleijnen, Jack PC and Robert G Sargent: *A methodology for fitting and validating metamodels in simulation.* European Journal of Operational Research, 120(1):14–29, 2000.

[36] Knudsen, Morten H: *Experimental modeling of dynamic systems: an educational approach.* IEEE Transactions on Education, 49:29–38, 2006.

[37] Kuo, Benjamin C: *Automatic control systems.* Prentice Hall PTR, 1987.

[38] Kvasnicka, P, G Prokop, M Dorle, A Rettinger, and H Stahl: *Durchgangige simulationsumgebung zur entwicklung und absicherung von fahrdynamischen regelsystemen.* VDI BERICHTE, 1967(1):387, 2006.

[39] Ljung, Lennart: *Estimation focus in system identification: Prefiltering, noise models, and prediction.* pages 2810–2815. IEEE.

[40] Ljung, Lennart: *Identification for control: Simple process models.* pages 4652–4657. IEEE.

[41] Ljung, Lennart: *System identification toolbox for use with matlab.*

[42] Ljung, Lennart: *System identification.* Springer, 1998.

[43] Maeder, Dominik: *Simulationsbasierte Grundauslegung der Fahrzeug-Querdynamik unter Berücksichtigung von Erfahrungswissen in der Fahrdynamikentwicklung.* Verlag Dr. Hut, 2012.

[44] Markowitz, Harry: *The optimization of a quadratic function subject to linear constraints.* Naval Research Logistics (NRL), 3(1-2):111–133, 1956.

[45] Michels, K., F. Klawonn, R. Kruse, and A. Nürnberger: *Fuzzy Control: Fundamentals, Stability and Design of Fuzzy Controllers.* Studies in Fuzziness and Soft Computing. Springer Berlin Heidelberg, 2007, ISBN 9783540317661. `https://books.google.de/books?id=Go67BQAAQBAJ`.

[46] Michels, Kai: *Regelungstechnik.* 2012.

[47] Michels, Kai: *Regelungstechnik, vorlesungsmanuskript.* 2012.

[48] Mitschke, Manfred and Henning Wallentowitz: *Dynamik der kraftfahrzeuge*, volume 4. Springer, 1972.

[49] Mokhiamar, Ossama and Masato Abe: *Simultaneous optimal distribution of lateral and longitudinal tire forces for the model following control.* Journal of dynamic systems, measurement, and control, 126(4):753–763, 2004.

[50] Muller, K R, Sebastian Mika, Gunnar Ratsch, Koji Tsuda, and Bernhard Scholkopf: *An introduction to kernel-based learning algorithms.* IEEE transactions on neural networks, 12(2):181–201, 2001.

[51] Obermüller, Anton: *Modellbasierte Fahrzustandsschätzung zur Ansteuerung einer aktiven Hinterachskinematik.* Cuvillier, 2012.

[52] Odenthal, Dirk and Roland Lohninger: *Verfahren zur erhoehung der fahrstabilitaet eines kraftfahrzeug.* Patentus, WO 2006/007908, 2006.

[53] Orend, Ralf: *Modelling and control of a vehicle with single-wheel chassis actuators.* IFAC Proceedings Volumes, 38(1):79–84, 2005.

[54] Pacejka, Hans: *Tire and vehicle dynamics.* Elsevier, 2005.

[55] Pellegrini, Enrico: *Model-Based Damper Control for Semi-Active Suspension Systems.* Verlag Dr. Hut, 2012.

[56] Pfeffer, Peter and Manfred Harrer: *Lenkungshandbuch.* Wiesbaden: Vieweg+ Teubner Verlag| Springer Fachmedien Wiesbaden GmbH, 2011.

[57] Rake, H: *Step response and frequency response methods.* Automatica, 16(5):519–526, 1980.

[58] Rau, Magnus: *Koordination aktiver fahrwerk-regelsysteme zur beeinflussung der querdynamik mittels verspannungslenkung.* 2007.

[59] Redeker, Christian: *Robuste auslegung von achseigenschaften in der frühen entwicklungsphase.* Master Thesis, Paderborn University, 2014.

[60] Reitze, Clemens: *Closed loop entwicklungsplattform für mechatronische fahrdynamikregelsysteme.* 2004.

[61] Rizzoni, Giorgio: *Principles and applications of electrical engineering.* McGraw-Hill Science/Engineering/Math, 2005.

[62] Rogers, Simon and Mark Girolami: *A first course in machine learning.* CRC Press, 2016.

[63] Röski, Karsten: *Eine Methode zur simulationsbasierten Grundauslegung von PKW-Fahrwerken mit Vertiefung der Betrachtungen zum Fahrkomfort.* Verlag Dr. Hut, 2012.

[64] Scharfenbaum, Ingo: *Funktionale Grundauslegung von Fahrwerkregelsystemen in der frühen Entwicklungsphase.* Cuvillier Verlag, 2016.

[65] Scharfenbaum, Ingo, Alessio Fratini, and Gunther Prokop: *A novel method for the development of an idealised active roll stabilisation system model.* In *Systems, Man, and Cybernetics (SMC), 2013 IEEE International Conference on*, pages 4499–4504. IEEE, 2013.

[66] Schramm, Dieter, Manfred Hiller, and Roberto Bardini: *Modellbildung und Simulation der Dynamik von Kraftfahrzeugen*, volume 124. Springer, 2010.

[67] Schumacher, Walter: *Erweiterte methoden der regelungstechnik.* 2015.

[68] Schuster, M, D Herold, M Wallbrecher, and T Thalhammer: *The new steering system of bmw–the integral active steering. synthesis of agility and sovereignty.* Proceedings of FISITA World automotive congress, Munich, 2008.

[69] Siebertz, Karl, David Van Bebber, and Thomas Hochkirchen: *Statistische Versuchsplanung: design of experiments (DoE).* Springer-Verlag, 2010.

[70] Smakman, H, P Köhn, H Vieler, M Krenn, and D Odenthal: *Integrated chassis management–ein ansatz zur strukturierung der fahrdynamikregelsysteme. 17.* In *Aachener Kolloquium*, volume 6, 2008.

[71] Van Den Hof, Paul MJ and Ruud JP Schrama: *Identification and control-closed loop issues.* IFAC Proceedings Volumes, 27(8):311–323, 1994.

[72] Wagner, Sebastian: *Parameter analysis of a lateral control system for simulation of highly automated driving.* Master thesis, Technical University of Munich, 2016.

[73] Wallbrecher, M, M Schuster, and P Herold: *Das neue lenksystem von bmw–die integral aktivlenkung.* Eine Synthese aus Agilität und Souveränität, 17, 2008.

[74] Wimmer, Christian: *Entwurf und analyse von algorithmen fuer einen integrierten allrad-querdynamikregler.* Master Thesis, Technical University of Munich, 2008.

[75] Wimmler, Dipl Ing FH Jens, Ing Dieter Schramm, and Markus Zimmermann: *Concurrent design of vehicle tires and axles.* In *6th International Munich Chassis Symposium 2015*, pages 839–851. Springer, 2015.

[76] Yu, Fan, Dao Fei Li, and DA Crolla: *Integrated vehicle dynamics control, state-of-the art review.* In *Vehicle Power and Propulsion Conference, 2008. VPPC'08. IEEE*, pages 1–6. IEEE, 2008.

[77] Zimmermann, Markus and Johannes Edler Hoessle: *Computing solution spaces for robust design.* International Journal for Numerical Methods in Engineering, 94(3):290–307, 2013.

[78] Zimmermann, Markus, Simon Königs, Constantin Niemeyer, Johannes Fender, Christian Zeherbauer, Renzo Vitale, and Martin Wahle: *On the design of large systems subject to uncertainty.* Journal of Engineering Design, 28(4):233–254, 2017.